Stony Brook University

The Role of the Hemopexin Domain of Matrix Metalloproteinases in Cell Migration

A Dissertation Presented

by

Antoine Hugues-Olivier Dufour

to

The Graduate School

in Partial Fulfillment of the

Requirement of the Degree of

Doctor of Philosophy

in

Chemistry
(Chemical Biology)

Stony Brook University

December 2010

Stony Brook University

The Graduate School

Antoine Hugues-Olivier Dufour

We, the dissertation committee for the above candidate for the

Doctor of Philosophy Degree,

Hereby recommend acceptance for this dissertation.

Professor Nicole S. Sampson, Advisor
Department of Chemistry

Professor Jian Cao, Co-Advisor
Department of Medicine

Professor Erwin London, Chair
Department of Biochemistry and Cell Biology

Professor Elizabeth Boon, Third member
Department of Chemistry

Professor Howard Crawford, Outside Member
Department of Pharmacological Sciences

This Thesis is accepted by the Graduate School

Lawrence Martin

Dean of the Graduate School

Abstract of the Dissertation

The Role of the Hemopexin Domain of Matrix Metalloproteinases in Cell Migration

By

Antoine Hugues-Olivier Dufour

Doctor of Philosophy

In

Chemistry
(Chemical Biology)

Stony Brook University

2010

The biological functions of matrix metalloproteinases (MMPs) extend beyond extracellular matrix degradation. Non-proteolytic activities of MMPs are just beginning to become understood. The role of proMMPs in cell migration was herein evaluated using transfected COS-1 cells with various proMMP cDNAs employed in a Transwell chamber migration assay. Latent MMP-2 and MMP-9 enhanced cell migration to a greater extent than latent MMP-1, -3, -11 and -28.

To examine if proteolytic activity is required for MMP-enhanced cell migration, three experimental approaches including a fluorogenic substrate degradation assay, transfection of cells with catalytically inactive mutant of MMP cDNAs, and addition of MMP inhibitors were utilized. The mechanism underlying the non-proteolytic enhancement of cell migration by MMPs was evaluated by the structure-function relationship of MMP-9 on cell motility. A domain swapping approach was utilized to demonstrate the role of the hemopexin (PEX) domain of proMMP-9 in cell migration when examined by a Transwell chamber assay and by a phagokinetic assay. TIMP-1, which interacts with the PEX domain of proMMP-9, inhibited cell migration whereas TIMP-2 had no effect.

Furthermore, using a biochemical approach, it was demonstrated that dimerization of MMP-9 through the PEX domain appears necessary for MMP-9-enhanced cell migration. Following a series of substitution mutations within the MMP-9 PEX domain, blade IV was shown to be critical for homodimerization, whereas blade I was required for heterodimerization with CD44. Both blade I and IV mutants showed diminished enhancement of cell migration compared to wild type MMP-9 transfected cells. Peptides mimicking motifs of the outermost strands of the first and fourth blades of the MMP-9 PEX domain were designed; these peptides efficiently blocked MMP-9 dimerization and inhibited motility of COS-1 cells overexpressing MMP-9, HT-1080 and MDA-MB-435 cells. Using a shRNA approach, CD44 was found to be a critical molecule in MMP-9-mediated cell migration. An axis involving an MMP-9-CD44-EGFR signaling pathway in cell migration was identified using an antibody array and specific receptor tyrosine kinase inhibitors.

In conclusion, the mechanism by which proMMP-9 can enhance cell migration was dissected. Biochemical studies led to the development of structure-based inhibitory peptides, and small molecules targeting MMP-9-mediated cell migration.

Table of Contents

Chapter 1- Introduction

Chapter 2 - Role of the Hemopexin Domain of Matrix Metalloproteinases in Cell Migration

Chapter 3 - Roles of Matrix Metalloproteinase-9 (MMP-9) dimers in Cell migration: Design of Inhibitory Peptides

Chapter 4 - Discovery of Novel Inhibitors Binding the Hemopexin domain of Matrix Metalloproteinase-9 using *In Silico* Modeling

List of Figures

Chapter 4

List of Tables

List of Abbreviations

APMA	4-aminophenylmercuric acetate
BSA	Bovine Serum Albumin
CAM	chick chorioallantoic membrane
CL	Cell Lysate
CM	Conditioned Media
COIP	Co-Immunoprecipitation
DMSO	Dimethyl Sulfoxide
EGFR	Epidermal Growth Factor Receptor
FCS	Fetal Calf Serum
FDA	Food and Drug Administration
FITC	Fluorescein Isothiocyanate
FRET	Fluorescence Energy Transfer
IP	Immunoprecipitation
kDa	Kilodalton
MMP	Matrix Metalloproteinase
MT-MMP	Membrane Type-Matrix Metalloproteinase
NMR	Nuclear Magnetic Resonance
PBS	Phosphate Buffer Saline
PCR	Polymerase Chain Reaction
PDB	Protein Data Bank

PEX	Hemopexin-like domain
PI	Propidium Iodide
RECK	Rerversion-Inducing Cysteine-rich protein with Kazal motifs
RMSD	Root Mean Square Deviation
ROS	Reactive Oxygen Species
RTK	Receptor Tyrosine Kinase
SAR	Structure-Activity Relationship
SDF-1	Stromal-cell-Derived Factor 1
SDS	Sodium Dodecyl Sulfate
TGF	Transforming Growth Factor
TIMP	Tissue Inhibitor of Metalloproteinase
TNF	Tumor Necrosis Factor
TRAIL	TNF-Related Apoptosis-Inducing Ligand
VEGF	Vascular Endothelial Growth Factor
WASP	Wiskott-Aldrich syndrome protein
WB	Western Blot

Chapter 1- Introduction

1.1 Background

Proteolysis is the degradation of proteins accomplished by enzymes termed proteases and occurs during a multitude of biological processes including DNA replication, transcription, translation, cell proliferation, angiogenesis, neurogenesis, cell migration and invasion, embryogenesis, apoptosis, etc. (1). In the first issue of *The Journal of Biological Chemistry* in 1905, P. A. Levene published a paper entitled: ”The Cleavage Products of Proteoses (2).” This was one of the first published reports on this class of enzymes and since the beginning of the 20th century, our view of proteases has greatly expanded. Proteases are enzymes that hydrolyze peptide bonds that link amino acids together in the polypeptide chain that constitute a protein. They can be either exopeptidases, cleaving a substrate’s terminal peptide bond or endopeptidases, cleaving an internal peptide bond. Based on the different mechanisms of catalysis, mammalian endopeptidases are divided into five groups: aspartic, cysteine, serine, threonine and metalloproteases. The different classes are further grouped into families, based on amino acid sequence comparison, and into clans, based on similarities of their three-dimensional structure (1). MEROPS (merops.sanger.asc.uk), a database of proteases and inhibitors, contains over 1000 entries for human proteases and homologs; in this database, there are multiple pseudogenes and protease-related sequences derived from endogenous retroviral elements. In the Degradome Database, protease pseudogenes or retrovirus-derived sequences are excluded and the total number of human proteases and homologs is 569, which are classified into 68 families (3). In this database, the Metalloprotease superfamily contains 194 members followed by the serine protease (176 members), cysteine protease (150 members), threonine protease (28 members), and aspartic protease superfamilies (21 members). Within the metalloproteases, the metzincin family includes astacins, adamalysins

(ADAMs and ADAMTSs), serralysins, snapalysins, leishmanolysins and matrixins (aka: MMPs).

Recent emphasis has been placed on the fact that proteases act in the context of complex cascades, circuits, networks and pathways thereby creating a multifaceted universe of protein-protein interactions termed the “protease web”. This complex proteolytic universe is currently being investigated by multiple laboratories and pharmaceutical companies to better understand the extent of their impact on biological processes.

1.2 Matrix Metalloproteinases Structure and Chemistry

The matrix metalloproteinase (MMP) family consists of twenty-four members in humans and they all require Zn^{2+} in their active site for proteolytic activity (Fig. 1.1) (4, 5). These enzymes have initially been given a descriptive name based on a preferred substrate and a MMP numbering system based on order of discovery (Table 1.1). The basic structure of MMPs consists of five typical domains: 1) a N-terminal signal peptide (or “pre” domain) which directs MMPs to the secretory pathway; 2) a ~80-90 residue prodomain that confers latency to the enzymes (zymogen); 3) a zinc containing catalytic domain which is compact, spherical, and ~165 residues in length; 4) a 15-65 flexible residue linker (hinge) region which links the catalytic and the PEX domains; and 5) a ~200 residue hemopexin-like (PEX) domain with a three-dimensional disc-like β-propeller structure, which mediates interactions with substrates and confers specificity of the enzymes. Besides these five typical domains of secretory MMPs, membrane anchored MMPs (MT-MMPs) contain additional hydrophobic transmembrane and a short cytoplasmic domains at the C-terminus.

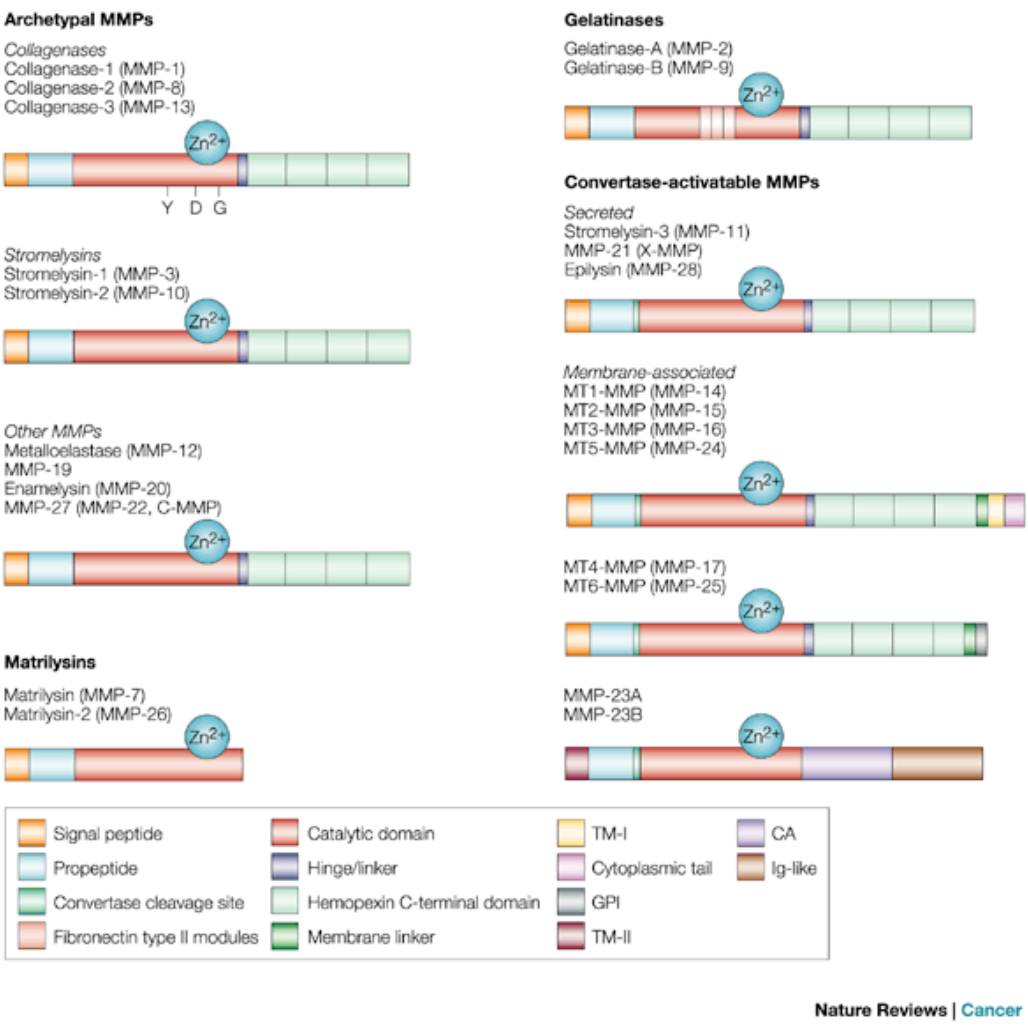

Figure 1.1: **24 members of the MMP family.** Domain structure of the MMPs classified into four different groups based on their domain organization. Pre, signal sequence; Pro, propeptide with a free zinc-ligating thiol (SH) group; F, furin-susceptible site; Zn, zinc-binding site; II, collagen-binding fibronectin type II inserts; H, hinge region; TM, transmembrane domain; C, cytoplasmic tail; GPI, glycophosphatidyl inositol-anchoring domain; C/P, cysteine/proline. The hemopexin/vitronectin-like domain contains four repeats with the first and last linked by a disulfide bond. Adapted from Overall and Lopez-Otin (6).

There are two motifs that are highly conserved in all MMPs. The PRCGXPD (where P is proline, R is Arginine, C is cysteine, G is glycine, X is a variable

amino acid and D is aspartic acid) motif is located in the prodomain. The cysteine residue coordinates the zinc atom at the active site, conferring latency to the proenzyme form (7). The catalytic domain has an extended zinc-binding motif, HEBXHXBGXHS (where H is histidine, E is glutamic acid, B is a bulky hydrophobic amino acid, G is glycine, X is variable amino acid and S is serine), which contains three zinc-binding histidines and a glutamate that activates a zinc-bound H_2O molecule providing the nucleophile that cleaves peptide bonds (8). Importantly, mutation of any of the histidines or the glutamate ablates catalytic activity (9).

In the PEX domain, each propeller blade is constituted of four anti-parallel β-strands and one α-helix held together by two conserved cysteine residues. The PEX domain of some MMP family members, e.g. MMP-9, and MT1-MMP, was found to form homodimers and/or heterodimers, which are required for function (10, 11). The PEX domain of MMP-1, -8 and -13 is also required for collagenase activity; a mutant is which the PEX domain is deleted fails to cleave native triple helix collagen but maintains proteolytic integrity with other substrates (7).

To examine the structure and chemistry of MMPs, several crystal structures (MMP-1, -2, -3, -7, -8, -9, -11, -12, -13 and -14) of different domains have been solved providing important information about their three-dimensional structures (12). The structures of the prodomains of MMP-2, -3 and -9 display three α-helices and connecting loops. The first loop between the helix 1 and 2 is a protease-sensitive “bait region”, whereas a region after helix 3 lies in the catalytic domain substrate-binding pocket keeping the zymogen inactive (12).

1.3 MMP’s Activation and Biology

MMPs are first synthesized as pre-proenzymes and once the signal peptide is removed during translation, MMPs are secreted as an inactive zymogen (proMMP). Their latency is maintained by a sulfhydryl group from a cysteine

residue embedded in the conserved PRCGXPD sequence within the prodomain inhibiting the catalytic Zn^{2+} ion. Removal of the prodomain enables access of the catalytic solvent molecule and substrate molecules to the active site cleft. The "cysteine switch" mechanism occurs when the cysteine residue coordinates the catalytic zinc ion and blocks the accessibility of an essential H_2O molecule to the active site (Fig. 1.2) (13, 14). Once the thiol group is displaced, a water molecule takes its place and can further attack peptide bonds of MMP targets.

Activation can occur upon disruption of the prodomain interaction with the catalytic site by conformational changes, oxidants, or proteolytic removal of the prodomain by other active MMPs. Serine proteases (e.g. plasmin, furin) can also mediate extracellular proteolytic activation of MMPs, which implies an interdependence of these two enzymes groups in extracellular matrix (ECM) degradation and remodeling (4). While most MMPs are activated extracellularly, some MMPs have a furin recognition motif (KX(R/K)R) and can be activated intracellularly by furin: examples include MMP-11 (15), MT-MMPs (16, 17), MMP-23 (18) and MMP-28 (19, 20). Other than proteolytic activation, there are several other non-proteolytic ways of activating MMPs *in vitro*: 1) chemical agents such as thiol-modifying agents ($HgCl_2$, 4-aminophenylmercuric acetate (APMA) and *N*-ethylmaleimide), 2) oxidized glutathione, 3) SDS, 4) chaotropic agents, 5) reactive oxygen species (ROS), 6) low pH and 7) heat treatment (12).

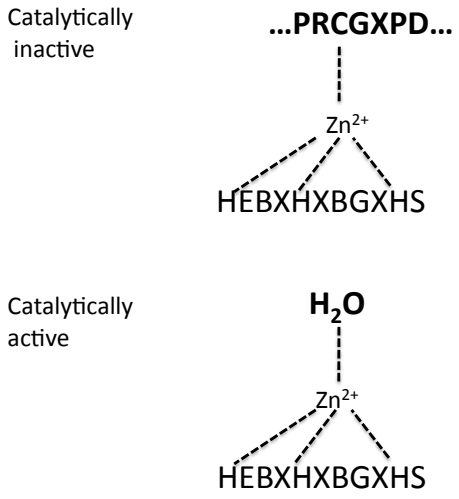

Figure 1.2: **Schematic representation of the "cysteine switch."** The thiol group from the cysteine side chain in the conserved PRCGXPD sequence present in the propeptide coordinates with the catalytic zinc ion in proMMPs. During MMP activation, a H_2O molecule replaces the thiol group resulting in a catalytically active enzyme.

With the exception of MMP-2, which has been widely studied and well characterized, the mechanism for *in vivo* activation of secreted MMPs is not well understood. Activation of secreted proMMP-2 is mediated by a cell-surface complex consisting of a homodimer of MT1-MMP with a single molecule of TIMP-2 (Tissue Inhibitors of MetalloProteinases-2). TIMP-2 binds to the catalytic domain of one of the MT1-MMP molecules of the homodimer and to the PEX domain of proMMP-2, thereby facilitating cleavage and activation of proMMP-2 by the second MT1-MMP molecule of the homodimer (16, 21, 22). The cell surface-bound proMMP-2 is then free of TIMP-2 once activated by MT1-MMP. ProMMP-2 can also be activated by MT2-MMP (independent of TIMP-2) (23), MT3-MMP (24), MT5-MMP (25) and MT6-MMP (26) but interestingly, not by MT4-MMP (27). Zymogen activation is a necessary process for MMPs and it leads to several biological and physiological functions.

To better understand the specific role of each MMP, knockout mice have been studied extensively. In 1995, the first MMP knockout out mouse was generated by deleting MMP-3 (28). Against expectations, these mice did not show phenotypic embryological or reproductive defects, despite the belief that these biological processes required extensive matrix remodeling. Additional knockout mice were generated (MMP-2, -7, -11 and -12) also showing limited phenotypic changes compared to wild types (29-32). MMP-9-deficient mice demonstrated retardation in bone growth plate development but no severe phenotype changes (33). Interestingly, MT1-MMP null mice exhibited several dysfunctional phenotypes ranging from osteopenia, arthritis, dwarfism, craniofacial dysmorphism, fibrotic synovitis due to inadequate collagen turnover, and importantly, these mice did not survive more than 13 weeks *postpartum* (34, 35). Among all the MMP generated knockout mice, the only lethal deletion was that of MT1-MMP, suggesting a critical role for this protease in mouse development. Mostly, knockout mouse data suggested that MMPs might only play a minor role in embryogenesis, although the possibility of redundancy in MMP functions in development might compensate in these single gene knockout situations, thus explaining the small phenotypic changes.

1.4 Natural Inhibitors of MMPs

Once activated, MMPs can cleave a large array of substrates, including chemokines; they can also remodel the extracellular matrix (ECM) environment. It is therefore essential that MMPs are tightly regulated. The Tissue Inhibitors of MetalloProteinases (TIMP-1, -2, -3 and -4) comprise a family of MMP inhibitors that, with few exceptions, inhibit the proteolytic activity of all MMPs in a 1:1 stoichiometric fashion (4, 36). Mammalian TIMPs are composed of two domains: a N-terminal domain of about 125 amino acids and a C-terminal domain of about 65 residues stabilized by three disulfide bonds (37). The TIMPs are relatively small proteins of ~21-34 kDa and are highly glycosylated. It has been demonstrated that both TIMP-1 and TIMP-2 interact with the catalytic domain of MMP-3 using NMR (38) and X-ray crystallography (39). Although these studies

have revealed that the inhibitory activity of the TIMPs reside in the N-terminal part of MMPs, MMP-2 and MMP-9 can bind TIMPs via their C-terminal PEX domains. TIMP-1 can selectively bind the PEX domain of proMMP-9, whereas TIMP-2 binds the PEX domain of proMMP-2; these interactions have been shown to regulate MMP function (40-42).

Individual TIMPs differ little in their ability to inhibit different MMPs (43). One major exception is the inefficiency of TIMP-1 to inhibit MT-MMPs. Total TIMP concentration in tissue and extracellular fluids generally exceed the concentration of MMPs, thereby limiting proteolytic activity to focal pericellular sites. TIMP-1 was initially named EPA for its erythroid-potentiating activity; and later on, TIMP-1, -2 and -3 were demonstrated to act as mitogens in other cell types (44). TIMPs have also been shown to exert growth-promoting activity independent of their MMP inhibitory function (4, 36).

Other endogenous inhibitors of MMPs include β-amyloid precursor protein, α2-macroglobulin (a very potent, high molecular weight inhibitor with high concentrations in blood), tissue factor pathway inhibitor-2, endostatin, the Rerversion-Inducing Cysteine-rich protein with Kazal motifs (RECK), the noncollagenous NC1 domain of type IV collagen, secreted leukocyte protease inhibitor, procollagen C-terminal proteinase enhancer and cystatins (4, 45-49). Even though several inhibitors of MMP activity have been validated, α2-macroglobulin, being an abundant plasma protein of ~725 kDa molecular mass, represents the major inhibitor of MMPs in body fluids, whereas the TIMPs act more locally.

1.5 Pericellular Localization of Proteolytic Activity

Cell-cell and cell-extracellular matrix interactions are a way that cells communicate and provide essential information for several physiological conditions including cell migration, morphogenesis, tissue repair, cell death, cell fate specification and cell-tissue specific function (50). Irreversible proteolytic

cleavage of pericellular proteins by MMPs is an efficient way of regulating extracellular signal transduction. There are several mechanisms for localizing MMPs to the cell surface that have been studied including association of MMPs to cell surface receptors, association with pericellular ECM molecules and the membrane-bound MMPs (MT-MMPs).

Among several cell surface docking receptors of MMPs that have been identified, CD44 has emerged to be an important molecule for its role in regulating cell growth, survival, differentiation and migration; it has therefore been associated with tumor progression and metastasis (51). CD44 is a transmembrane glycoprotein involved in cell-cell and cell-matrix interactions encoded by a single gene but expressed as several isoforms. The structural diversity of the members of the CD44 family is generated by alternative RNA splicing and posttranslational modifications (i.e. glycosylation and binding to glycosaminoglycans) (52). All CD44 isoforms contain an ectodomain that can bind HA (hyaluronan), a transmembrane domain and a cytoplasmic domain. Twenty-one exons encode CD44, of which 7 encode the extracellular domain of the most common form of CD44, termed either hematopoietic or standard form (52). The diversity of CD44 isoforms are generated by up to 11 alternatively spliced exons (v1-v11) into a proximal site of the transmembrane domain (53). The several structural variations in CD44 might be correlated to its functions: spliced variants or posttranslationally modified forms of CD44 can serve as docking molecules for several MMPs. For example, CD44v6 can bind MMP-9 and promote tumor cell invasion and angiogenesis by mediating the activation of latent TGF-β by MMP-9 (54). MMP-7 is able to form a cell surface complex with CD44 in several cell types and impact the regulation of physiological tissue remodeling (55). MT1-MMP can mediate a CD44-dependent tumor cell migration and invasion (56, 57).

Other classes of important cell surface molecules are the integrins: a family of transmembrane glycoproteins that form heterodimer receptors for various

ECM molecules. Every integrin heterodimer is composed of α- and β- subunits; to date, there are 18 known α-subunits and 8 β-subunits forming 24 distinct heterodimers in humans (58). Integrins can serve as docking molecules for several MMPs: activated MMP-2, via its PEX domain, can bind $\alpha_v\beta_3$ integrin on the cell surface of invasive cancer cells and angiogenic blood vessels (59). MMP-1 can interact, via its hinge and PEX domains, with the I domain of α_2 integrin, which induces MMP-1 expression in keratinocytes grown over type I collagen (60).

Pericellular proteolysis, invasion of both stromal (fibroblasts) and tumor cells *in vitro* and *in vivo* have been linked to the expression of membrane attached MMPs (MT1-MMP and MT2-MMP). MT1-MMP, MT2-MMP and MT3-MMP can serve as collagenases to degrade the basement membrane (BM) during cell migration and cell proliferation in a 3D collagen gel matrix (61, 62). MMP-9 has also been demonstrated to be localized to the invadopodia of prostate cancer cells with the Wiskott-Aldrich syndrome protein (WASP) by immunostaining analyses (63). These studies highlight the importance of pericellular localization of MMPs and their impact on human diseases.

1.6 Physiological Roles of MMPs and Participation in Human Disease

For over forty years, the concept that MMPs can degrade the ECM thereby promoting cancer invasion and metastasis has been widely studied. A large number of studies in experimental animal models have demonstrated: 1) modulation of invasion and migration of cancer cells by transfection with expression vectors encoding the cDNA of MMPs; 2) tumor progression correlates with enhanced secretion of MMPs by tumor cells and stromal cells, and 3) reduction of tumor growth and metastasis *in vivo* using TIMPs, synthetic MMP inhibitors, peptidomimetic compounds, antisense oligonucleotides and neutralizing antibodies. The roles of MMPs expand beyond their matrix

degradation properties and there are still several aspects of MMPs' physiological roles that remain unknown and are presently under investigation. These roles include enhancement of cell motility, epithelial-to-mesenchymal transition (EMT), skeletal homeostasis, angiogenic regulation, the modulation of signaling pathways and inflammatory response, cleavage of chemotactic and growth factors, regulation of apoptosis, initiation of neoplastic progression and formation of the metastatic niche (5). Since MMPs have various biological roles, they have been concurrently associated with a large variety of human diseases.

The first discovered human genetic disease linked with MMPs is Sorby's fundus dystrophy, which has been associated with a mutation in the TIMP-3 gene (64). However, most of the early studies on MMPs originally focused on their roles on cell migration by degrading the ECM. Later, it was emphasized that these degrading functions of MMPs are likely of secondary importance to higher order processes that affect signal transduction pathways such as cleavage of cell-cell adhesion or cell-ECM, ectodomain shedding leading to cell motility, invasion and metastasis. For example, MMP-2 and MT1-MMP can cleave the γ2 chain of laminin-5 causing a release of domain III which in turn, enhances mammary epithelial cell migration (65). In MT1-MMP knockout mice, the laminin-5 γ2 chain fragments levels were diminished (66). Disruption of cell-cell contacts and adherens junction components by MMPs can also enhance cell motility. For instance, in mammary and lung epithelial cells, the shedding of E-cadherin on the cell surface caused by MMP-3 and/or MMP-7 enhances cell migration (67, 68).

Compelling experimental data showed that several MMPs (MMP-1, -2, -3, -7, -9, -13 and -14) actively contribute to cancer progression in various stages including tumor growth, invasion, metastasis and angiogenesis (4, 69). In human tumors, the source of MMPs is not only generated by cancer cells but also by surrounding stromal cells and immune cells (4). Importantly, not all MMPs contribute to cancer progression; for instance, in human breast cancers, MMP-8 was shown to be significantly reduced in the cancer cells that acquired the ability

to metastasize in comparison to their non-metastatic counterparts (70). However, the rarity of negative correlations between MMP expression, tumor progression, and differences in their physiological roles need not be overlooked during the development of MMP inhibitors (broad spectrum versus specific inhibitors). Most human cancers are epithelial in origin and the loss of integrity through phenotypic changes of the epithelium is an initiator of cancer invasion and metastasis. The switch of an epithelial cell into a mesenchymal cell requires several alterations in morphology, migration, adhesion and cellular architecture. The loss/decrease of E-cadherin (signature of EMT), cytokeratins and the acquisition of mesenchymal proteins such as vimentin, fibronectin and N-cadherin denote a loss of the epithelial and a transition toward a mesenchymal dedifferentiated phenotype. Overexpression of several MMPs including MMP-1, -2, -3, -7, -9, -13, -28 and MT1-MMP have been associated with EMT (71). The cleavage of E-cadherin by MMPs has also been shown to trigger EMT, leading to a more aggressive invasion program by cancer cells and initiating the metastatic cascade (72).

Certain organs (lung, liver and bone) are more prone to develop micro metastases and, later on, gross metastatic tumors. Metastasis can be affected by the type of primary cancer cell but also requires the formation of a receptive environment, a metastatic niche, which is specifically suited to become the host of distant tumor cells. MMP-9 has been demonstrated to be a critical MMP for the formation of a metastatic niche by either liberating VEGF and promoting angiogenesis (73) or by releasing Kit-ligand, thereby, recruiting stem cells from the bone marrow to the site of metastasis (74). An intriguing body of evidence, and yet not fully understood, suggest that certain primary tumor cells release soluble factors that recruit a specific population of non-malignant hematopoietic cells to mobilize in distant organ tissues, thereby establishing a “premetastatic niche” that lay a foundation for circulating cancer cells (75). This process is permitted by the secretion of growth factors and chemokines that can create a receptive microenvironment for cancer cells, and by the proteolytic matrix turnover (76).

Bone development requires active remodeling of cartilage and bone matrices and vascularization is accomplished via osteoclast-mediated matrix remodeling. Using knockout mice models and biochemical approaches, several MMPs (MMP-2, -9 and MT1-MMP) have been demonstrated to play a role in bone development and skeletal homeostasis (4, 33).

Angiogenesis, the formation of new blood vessels from existing ones, is characterized by new basement membrane deposition and induction of endothelial cell quiescence and is a crucial biological event in both development and tumor progression (77). Matrix degradation and remodeling is therefore crucial in angiogenic regulation. MMPs can contribute to angiogenesis in different ways: 1) by promoting vessel formation by increasing angiogenic factors; 2) generating anti-angiogenic breakdown products, and 3) remodeling the ECM, by enabling endothelial cell migration through adjacent tissues. $CD45^{+}$-myeloid cells have been demonstrated to increase VEGF bioavailability by MMP-9 activity, therefore inducing angiogenesis and regulating tumor cell invasiveness (78). Additional MMPs (MMP-3, -7 and -16) can also affect the vascular patterning of tumors *in vivo* by cleaving VEGF molecules (79). Contrarily, several MMPs (MMP-2, -3, -7, -9 and -12) can also negatively regulate angiogenesis by generating anti-angiogenic peptides like angiostatin (a cleaved product of plasminogen (80)), tumstatin and endostatin, which are cleaved products of collagen IV and XVIII, respectively (81). Therefore, deregulation of MMPs has been linked to several cardiovascular diseases such as atherosclerosis, myocardial infarction, and development and rupture of aneurysms (36). Using two transgenic mouse models of tumor progression (RIP1-Tag2 Insulinoma model (73) and K14-HPV16 skin cancer model (82)), MMP-9 was demonstrated to be an important enzyme in angiogenesis by regulating the bioavailability of the pro-angiogenic factor VEGF. MT1-MMP can degrade the fibrin matrix surrounding newly formed vessels, and therefore, promote angiogenesis by enhancing cell migration, invasion and capillary-tube formation (83, 84).

Collectively, MMPs seem to play a “yin-yang” role in angiogenesis, rather than exclusively stimulating or inhibiting new blood vessel development.

MMPs have been demonstrated to cleave chemokines, a family of chemotactic proteins involved in inflammatory-cell recruitment acting through G-protein-coupled receptors, resulting in modulation of the migration of leukocytes. For instance, in neutrophils, MMP-9 cleaves interleukin-8 (IL-8 or CXCL8), thereby increasing its activity tenfold and affecting the inflammatory response. On the other hand, MMP-9 can also inactivate CXCL7, CXCL4 and CXCL1 (85). Another example is CXCL12 (stromal-cell-derived factor 1 or SDF1), which can be cleaved by several MMPs (MMP-1, -3, -9, -13 and -14).

Rheumatoid arthritis is an autoimmune disorder that is characterized by the inflammation of the joints and degradation of joint cartilage. The collagenases (MMP-1, -8 and -13) have been tightly associated with this pathology by cleaving collagen II, a major structural constituent of cartilage and the remaining fragments are further degraded by MMP-9 (86). MMPs also affect the migration of leukocytes to the site on inflammation, suggesting the potential usage of MMP inhibitors in rheumatoid arthritis. In animal models, among different MMP inhibitors tested, BAY12-9566 inhibited neutrophil infiltration and the swelling of the rats’ paws (87).

Since MMPs have been widely studied in a large number of human pathologies, there has been a high interest in the development of MMP inhibitor to treat human diseases.

1.7 MMP-9 and Cell Migration

Cell migration is a complex biological process implicating a large number of intra- and extracellular proteins interacting and signaling within the cellular environment. The basis of cell migration has been well established but the details

of how this process is regulated in normal physiology and in diverse pathologies is not well understood. The main principle of cell migration is basic; through actin rearrangement of their cytoskeleton, cells acquire a spatial asymmetry allowing them to convert intracellular forces to cell body translocation (88). Migration can either be a random non-directional movement (chemokinesis) or a directed movement towards a signal inducer (chemotaxis). It was originally thought that the main purpose of the protease activity is required for the degradation of the extracellular matrix. It is now apparent that proteases can additionally generate pro-migratory signals by cleavage of latent growth factors and by disruption of cell-cell contacts. More precisely, MMP-9 has been demonstrated to activate VEGF and TGF-β, and therefore increase tumor growth and angiogenesis (73, 89). Although a large number of proteases have been demonstrated to stimulate cell migration, a new line of evidence suggests that the protease activity might not be required to induce cell motility. Some groups have demonstrated that several proMMPs (MMP-1, -2, -3, -7, -9, -11 and -28) can enhance COS-1 cell migration independently of their proteolytic activity (42, 90). Sanceau *et al*. (90) have suggested a migration inducing ability of MMP-9 independent of its catalytic activity. Likewise, using pharmacological inhibition of proteolytic activity, several cell lines continue to migrate utilizing an ameboid-like movement, such as T cells, HT-1080 fibrosarcoma cells, MDA-MB-231 breast carcinoma cells (91, 92). In addition, the cleavage-independent mode of cell migration conducted by MMP-9 has also been observed in a neutrophil transmigration *in vivo* model (93). Collectively, these observations suggest that proMMP-9 might affect cell behavior and increase cell migration in a different manner than active MMP-9. A more thorough understanding of the distinct roles of latent and active MMP-9 can lead to a new line of drugs to inhibit various pathologies caused by this protease.

1.8 Failure of MMP Inhibitors in clinical Trials

Due to the critical importance of MMPs in diverse biological and physiological processes and their involvement in several human diseases, MMPs became a prime target for drug development in the 1990s. A multitude of

approaches were undertaken ranging from pseudopeptides that can mimic MMP substrates to non-peptidic compounds that can coordinate with the catalytic zinc ion. The TIMPs have been considered for treatment of human diseases because of their picomolar affinities to MMPs, however, their lack of selectivity and their multiple biological activities made this strategy unapproachable in the clinic. The first line of compounds primarily focused on a hydroxymate moiety as the zinc-binding group, which later led to the development of a variety of compounds with diverse functional groups. Factors such as potency, selectivity and bioavailability, allowed for the design of more effective drugs. In 1992, British Biotech, first took Batimastat, a broad-spectrum hydroxamic-acid derivative based on the structure of collagen, into a human clinical trial (94). Early administration of batimastat in the pancreatic islet cell carcinogenesis model significantly inhibited angiogenesis, whereas no effect was observed when batimastat was administered in the late stage of the model (95). This is one of many examples that suggested that MMP inhibitors are more efficient in early stages of cancer and not in the more advanced stages. In order to overcome the bioavailibility issues, Batimastat's clinical trials were soon replaced by an orally available compound: Marimastat. However, treatment with Marimastat lead to musculoskeletal problems including stiffening of the joints, pain in the hands, skin discoloration, and inflammation linked to tendonitis (96).

Several groups interested in cancer application designed MMP inhibitors with a selectivity against the gelatinases (MMP-2 and -9), whereas, the groups interested in inhibiting arthritis designed inhibitors targeting the collagenases (MMP-1, -8 and -13). Another hydroxamic-acid derivative, Prinomastat (AG-3340), was designed to be selective for gelatinases but also displayed similar side effects as Marimastat. By contrast, Bayer designed a butanoic-acid analogue (BAY12-9566) that did not cause any musculoskeletal side effects but was clinically ineffective.

Another class of small molecules, the tetracyclines, inhibit antimicrobial activity by interfering with inflammatory cell migration and chemotaxis to the sites of inflammation which is independent of their MMP inhibitory activity (97). Tetracyclines were also shown to inhibit MMP expression and activity; following these findings, several tetracyclines derivatives have entered clinical trials as MMP inhibitors (98). Even though the tetracyclines have not been approved by the FDA for the treatment of cancer, they are used to treat periodontitis. This disease occurs when bacteria located in the gingival tissues release inflammatory cytokines that result in connective-tissue destruction by MMPs, leading to loss of teeth. Periostat (doxycycline hydrate) is the only MMP inhibitor approved in the United States for the treatment of a human disease (periodontitis) by reducing the activity of host-derived collagenases (99), thus, suggesting the possibility of the potential usage of MMP inhibitors in the treatment of human pathologies. MMPs have been examined for several therapeutic targets in various diseases other than cancer, such as corneal ulcers, multiple sclerosis, glomerulonephritis, bacterial meningitis, uveorentinitus, emphysema, aortic aneurysm and atherosclerosis (100, 101).

After the failure of MMP inhibitors to treat cancer in clinical trials, three caveats need to be considered when designing future inhibitors before entering the clinic: 1) focus on preventative therapies in early stage cancers, 2) develop more specific drugs due to extensive homology between MMPs' catalytic domains, and 3) overcome unanticipated long-term drug intolerance. In addition, several MMPs display anti-tumor (MMP-8 and MMP-12) and pro-angiogenic (MMP-9) activity depending on the stage of tumor progression and on the cell types. Despite previous failures of MMP inhibitors in clinical trials, Dyax Corporation designed a highly specific antibody to MT1-MMP (DX-2400) that reacts only with the activated form of the enzyme and not the latent form. This antibody was shown to inhibit tumor invasion, metastasis and angiogenesis and is planned to enter clinical trials (84).

Timelines, costs, patent issues and competition are all important factors affecting decisions made by the pharmaceutical companies. After the failure of several MMP inhibitors in clinical trials, what lessons have we learned? Should we abandon inhibitors of MMPs as a method to treat human diseases? After collecting new sets of data on specific functions of MMPs and understanding their roles beyond ECM degradation, can we design effective MMP inhibitors that can be approved by the FDA? Can we identify and target specific MMPs in human diseases?

Table 1. Human MMP nomenclature and database identifiers

Gene Symbol	Other Name(s)	MEROPS ID	GenBank Locus
MMP-1	Insterstitial/fibroblast collagenase	M10.001	NM_002421
MMP-2	Gelatinase A, 72 kDa gelatinase	M10.003	NM_004530
MMP-3	Stromelysin-1	M10.005	NM_002422
MMP-7	Matrilysin, PUMP-1	M10.008	NM_002423
MMP-8	Neutrophil collagenase	M10.002	NM_002424
MMP-9	Gelatinase B, 92 kDa gelatinase	M10.004	NM_004994
MMP-10	Stromelysin-2	M10.006	NM_002425
MMP-11	Stromelysin-3	M10.007	NM_005940
MMP-12	Macrophage metalloelastase	M10.009	NM_002426
MMP-13	Collagenase-3	M10.013	NM_002427
MMP-14	MT1-MMP	M10.014	NM_004995
MMP-15	MT2-MMP	M10.015	NM_002428
MMP-16	MT3-MMP	M10.016	NM_005941, NM_022564
MMP-17	MT4-MMP	M10.017	NM_016155
MMP-19	n.a.	M10.021	NM_002429, NM_022791, NM_022791
MMP-20	Enamelysin	M10.019	NM_004771
MMP-21	n.a	M10.026	NM_147191
MMP-23A MMP-23B	CA-MMP	M10.037, M10.022	NM_004659, NM_006983
MMP-24	MT5-MMP	M10.023	NM_006690
MMP-25	MT6-MMP	M10.024	NM_022468, NM_022718
MMP-26	Matrilysin-2, endometase	M10.029	NM_021801
MMP-27	n.a.	M10.027	NM_022122
MMP-28	Epilysin	M10.030	NM_024302, NM_032950

Chapter 2- Role of the Hemopexin Domain of Matrix Metalloproteinases in Cell Migration

(The work in this chapter has been published in the *Journal of Cellular Physiology* (2008), **217**(3), pp 643-651 and the co-authors are Nicole S. Sampson, Stanley Zucker and Jian Cao (42))

2.1 Summary

The biological functions of MMPs extend beyond extracellular matrix degradation. Non-proteolytic activities of MMPs are just beginning to be understood. Herein, the role of proMMPs was evaluated in cell migration. Employing a Transwell chamber migration assay, we demonstrated that transfection of COS-1 cells with various proMMP cDNAs resulted in enhancement of cell migration. Latent MMP-2 and MMP-9 enhanced cell migration to a greater extent than latent MMP-1, -3, -11 and -28. To examine if proteolytic activity is required for MMP-enhanced cell migration, three experimental approaches, including a fluorogenic substrate degradation assay, transfection of cells with catalytically inactive mutant MMP cDNAs, and addition of hydroxamic acid-derived MMP inhibitors, were employed. It was demonstrated that the proteolytic activities of MMPs are not required for MMP-induced cell migration. To explore the mechanism underlying MMP-enhanced cell migration, structure-function relationship of MMP-9 on cell migration was evaluated. By using a domain swapping approach, it was demonstrated that the hemopexin domain of proMMP-9 plays an important role in cell migration when examined by a Transwell chamber assay and by a phagokinetic migration assay. TIMP-1, which interacts with the hemopexin domain of proMMP-9, inhibited cell migration, whereas TIMP-2 had no effect. Employing small molecular inhibitors, MAPK and PI3K pathways were found to be involved in MMP-9 mediated cell migration. In conclusion, it was demonstrated that MMPs utilize a non-proteolytic mechanism to enhance epithelial cell migration and the homodimer formation of the hemopexin of MMP-9 is prerequisite required for MMP-9-mediated cell migration.

2.2 Introduction

Based on the failure to date of broad spectrum MMP inhibitors in treating human diseases, the scientific community is in the process of reevaluating the biological function of MMPs in order to design more selective MMP inhibitors (102, 103). All MMPs contain a signal peptide, a propeptide, and a Zn^{2+}-containing catalytic domain of 160-170 amino acids in length. With the exception of MMP-7, -23 and -26, all MMPs contain a proline-rich hinge region and a C-terminal hemopexin-like domain (PEX). The PEX domain of MMPs forms a propeller with four blades linked by a disulfide bonds between blade I and IV (10). Each individual blade is composed of one α-helix and four anti-parallel β-strands. The PEX domain of MMPs regulates substrate binding (4). In contrast to other MMPs, the PEX domain of proMMP-2 and proMMP-9 bind TIMP-2 and TIMP-1, respectively. MMP-9 is the only secreted MMP that forms a homodimer through its PEX domain. It also has the longest hinge region consisting of 50 amino acids (compared to ~10 amino acids in other MMPs) and is the only MMP containing a cysteine residue in this domain (104). Of interest, the PEX domain of proMMP-9 has been shown to have higher affinity for binding gelatin, collagen type I, collagen type IV, elastin and fibrinogen than the PEX domain of active MMP-9 (105).

Correlations have been made between the capacity of MMP-9 to degrade ECM collagens and laminin and its ability to regulate cell migration, increase angiogenesis and affect tumor growth (4, 14, 90, 105-107). Importantly, several reports do not clearly distinguish between migration (motility) and invasion. It was hypothesized that MMPs are able to induce cell migration (locomotion) independently of their proteolytic activity. We have therefore examined the cell locomotion of proMMPs in the absence of ECM. Based on our interest in the function of MMP-9 exosite (PEX domain), we have explored and identified novel functions of this domain in cell migration.

2.2 Results

Enhanced cell migration by over-expression of full-length MMPs in COS-1 cells

Substrate degradation and cell migration are key factors contributing to cancer invasion (14). MMPs function in these pathological processes by digesting basement membrane/extracellular matrix (ECM) and enhancing cell migration (4). Given the evidence that enhanced cell migration is often accompanied by secretion of activated MMPs, it has been proposed that the enzymatic activity of MMPs is required for the enhanced cell migration (4). However, direct evidence for this hypothesis is limited.

Wild-type human MMP cDNAs encoding full-length secretory MMP-1, -2, -3, -9, -11 and -28 were overexpressed in COS-1 cells, a monkey kidney epithelial cell line which produces negligible quantities of MMPs (108). Following transient transfections, cell migration was assessed in a Transwell chamber migration assay employing 8 μm pore size non-coated polycarbonate membranes. In comparison to non-transfected or Green Fluorescent Protein (GFP)-cDNA transfected cells, COS-1 cells transfected with each individual human MMP cDNA displayed significantly enhanced cell migration (Fig. 2.1A, B). Migration by MMP-2 and MMP-9 transfected cells was enhanced as compared to MMP-1, -3, 11, and -28. The enhancement of cell migration was not due to the expression level of MMPs in COS-1 cells as assessed by Western blotting (ratios between specific MMPs and a house-keeping gene product, tubulin; Fig. 2.1C, D). Of note, the molecular weight of individual MMP bands revealed no cleavage products consistent with activated enzyme. Similar results were obtained using minimally invasive human MCF-7 cells transfected with MMP cDNAs (Fig. 2.1E). These results indicate that overexpression of full-length MMPs leads to enhanced cell migration.

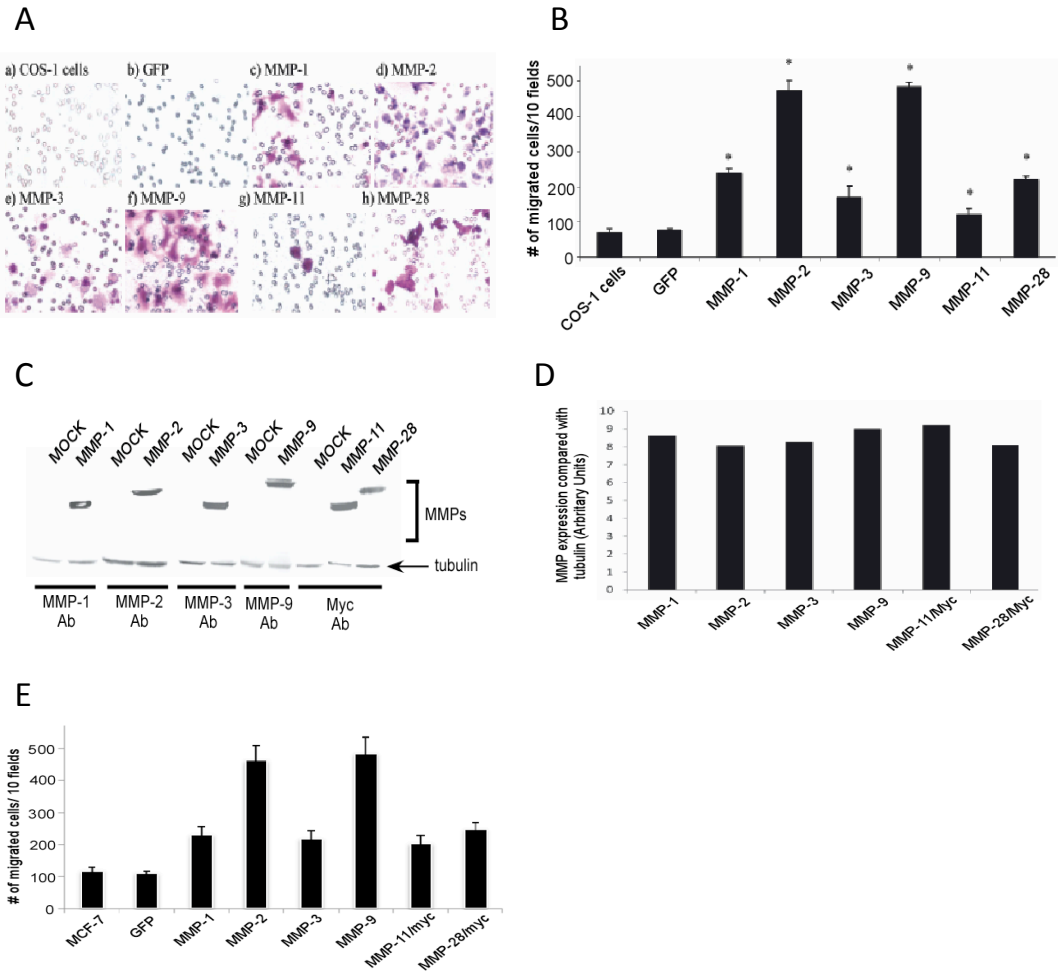

Figure 2.1. Effect of MMPs expressed in COS-1 cells and MCF-7 on random cell migration. (A, B): Expression of human MMPs in COS-1 cells enhances cell migration. COS-1 cells transfected with corresponding human cDNA as indicated were examined by a Transwell chamber migration assay. Migrated cells were microscopically examined (A) and counted (B). *Significant difference; *P<0.05*, as compared to COS-1 cells. (C, D): Comparable expression of MMPs in transfected COS-1 cells examined by Western blotting. COS-1 cells transfected with a vector encoding various cDNAs were lysed and immunoblot analysis was performed using the corresponding antibodies as indicated (C). Densitometric analyses of expression levels of MMPs and tubulin, respectively, in COS-1 cells were performed. Relative expression levels of MMPs in COS-1 cells were determined based on ratios between levels of specific MMPs and the corresponding respective levels of tubulin (D). (E) Expression of human MMPs in MCF-7 cells enhances cell migration. MCF-7 cells transfected with corresponding expression vector encoding human cDNAs as indicated were examined by a Transwell chamber migration assay and migrated cells were stained and microscopically counted.

MMP proteolytic activity is not required for enhanced cell migration

To specifically address the issue of a requirement of MMP activation for cell migration, we first examined if activated MMPs are present in the conditioned medium of transfected COS-1 cells. A highly sensitive fluorogenic peptide degradation assay was employed (109). MMP-2 and MMP-9 were selected as examples of MMPs that are effective in enhancing cell migration. Conditioned medium of COS-1 cells transfected with MMP-2 and -9 was collected and proteolytic activity was compared to APMA-treated cell conditioned medium containing activated MMP-2 and MMP-9; conditioned medium from vector transfected cells was utilized as a negative control. In contrast to APMA-treated conditioned media from cells transfected with MMP-2 and MMP-9 cDNA, non-APMA-treated conditioned media displayed negligible activity (Fig. 2.2A). This data confirms the absence of measureable quantities of activated MMPs in cell conditioned media.

To further explore the role of proteolytic activity of MMPs in cell migration, MMP inhibitors (TIMP-1 and -2) at effective concentrations were employed (7). MMP-2, -11 and -28 were transiently co-expressed in COS-1 cells along with either TIMP-1 or TIMP-2; cell migration was subsequently assessed. TIMP-1 and TIMP-2 displayed no effect on MMP-2, -11, and -28-mediated cell migration (Fig. 2.2B). When broad spectrum hydroxamic acid-derived inhibitors of MMPs CT1746 (Fig. 2.2C) and BB3103 (Fig. 2.2D) were incubated with COS-1 cells in the Transwell chambers, no effect of these MMP inhibitors was observed on MMP-9-induced cell migration. In addition, enzymatically inactive mutants of MMP-9 and MMP-28 were generated by converting glutamic acid in the active center of each MMP to alanine using a site-direct mutagenesis approach (MMP-9 E^{230} and MMP-28 E^{241}). The enhanced COS-1 cell migration observed in the enzymatically inactive mutants of MMP-9 and -28 was comparable to wild types (Fig. 2.2E). These results indicate that cell synthesis of MMPs leads to enhanced cell migration without a requirement of enzyme activity.

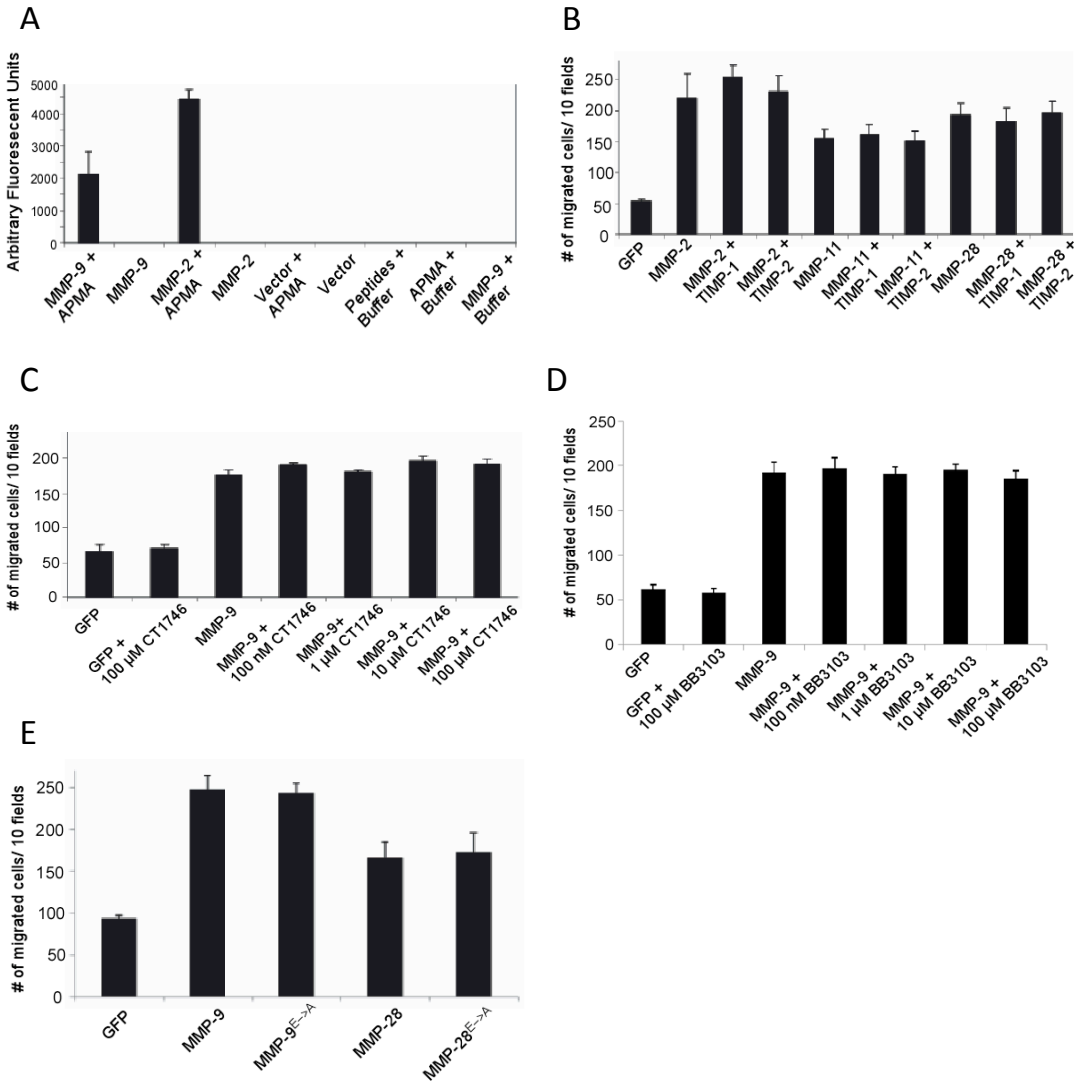

Figure 2.2. ProMMPs enhance cell migration of COS-1 cells. (A): No enzymatic activity is detected in the conditioned medium of COS-1 cells transfected with MMP-2 and MMP-9 cDNAs. Fluorogenic substrate peptide was incubated with APMA- or non-APMA-treated conditioned medium, as indicated, followed by measurement of the degradation products using a fluoresecent plate reader. (B): No effect of TIMP-1 and TIMP-2 on MMP-2, MMP-11 and MMP-28-enhanced cell migration. COS-1 cells transfected with a combination of MMPs and TIMP, as indicated, were examined by a Transwell chamber migration assay. Migrated cells were stained and microscopically counted. (C, D): Addition of synthetic MMP inhibitor in MMP-transfected COS-1 cells does not interfere with MMP-9-enhanced cell migration. Synthetic MMP inhibitor CT1746 (C) or BB3103 (D) at different does was incubated with cells transfected with MMP-9 cDNA, and Transwell migration assay was subsequently performed. Migrated cells were stained and microscopically counted. (E): Constitutively inactive MMP-9 and MMP-28 enhance cell migration as well as wild type enzymes. COS-1 cells

transfected with wild-type, mutant MMP-9, or MMP-28 were examined by the Transwell migration assay. Migrated cells were stained and microscopically counted.

Requirement of the hemopexin domain of MMP-9 in cell migration

Based on the prominent implication of MMP-9 in various disease processes and its profound effect on cell migration (14), this MMP was selected for more detailed analysis. There has been considerable recent interest in the unique function of the hemopexin and hinge regions (OG domain) of MMP-9 and homodimer formation (104). Hemopexin and hinge domains of MMP-9 were individually deleted using a two-step PCR approach (Fig. 2.3A) (110). The engineered expression vector encoding MMP-9 deletion mutants were transiently transfected into COS-1 cells and immunoblotting of cell lysates and conditioned media was performed (Fig. 2.3B). Both wild type MMP-9 and MMP-$9_{\Delta PEX}$ (deletion of PEX domain) were detected as high molecular weight glycosylated forms in the conditioned medium and low molecular weight non-glycosylated forms in the cell lysates (Fig. 2.3B) (111). As described by Van den Steen et al. (104), no molecular weight shift of MMP-$9_{\Delta OG}$ (deletion of hinge domain) was noted between conditioned medium and cell lysates, confirming the highly O-glycosylated region of hinge domain (Fig. 2.3B).

To determine the role of the hinge and hemopexin domains of MMP-9 in cell migration, COS-1 cells transfected with deletion mutants were compared to wild type MMP-9 cDNA in the Transwell chamber migration assay. Cells transfected with MMP-$9_{\Delta OG}$ cDNA exhibited enhanced cell migration as compared to MMP-$9_{\Delta PEX}$; deletion of either the hinge region or hemopexin domain resulted in significantly reduced cell migration enhanced by expression vector encoding the cDNA of MMP-9 ($p<0.01$) (Fig. 2.3C). However, deletion of the hemopexin domain of MMP-9 resulted in decreased protein secretion into the conditioned media (Fig. 2.3B), but no apparent effect on mutant MMP-9 protein expression (i.e., cell lysates) was noted, suggesting that deletion of this relative

large domain interferes with protein trafficking. To circumvent this problem, a substituted mutation was generated. Because the PEX domain of MMP-1 does not form homodimers (112), a chimera between MMP-9 and MMP-1 was engineered by replacing the hemopexin domain of MMP-9 with that of MMP-1 to generate MMP-9/MMP-1_{PEX} chimera and its biological properties were investigated. Both glycosylated (i.e., in conditioned medium) and non-glycosylated (i.e., in cell lysate) MMP-9/MMP-1_{PEX} were readily detected in cDNA-transfected COS-1 cells (Fig. 2.3B). Substitution of the PEX domain of MMP-9 with that of MMP-1 (i.e., MMP-9/MMP-1_{PEX}) resulted in decreased cell migration as compared to wild type MMP-9, but comparable to cells transfected with MMP-1 cDNA (Fig. 2.3C).

To further confirm the role of the hemopexin domain of MMP-9 in cell migration, wild-type and mutant MMP-9-transfected cells were subjected to phagokinetic migration analysis which permits quantification by clearance of colloidal gold particles within the cell migratory path (Fig. 2.3D and 2.3E). In agreement with the data from the Transwell chamber migration assay (Fig. 2.3C), cells transfected with vector encoding the cDNA of wild-type MMP-9 cDNA displayed enhanced migration (i.e., 4.7% particle phagocytosed) as compared to GFP-transfected cells (i.e., 1.2% phagocytosed). The stimulatory effect of MMP-9 on cell migration was decreased in cells transfected with MMP-9 mutations (MMP-$9_{\Delta PEX}$: 2.1%; MMP-$9/1_{PEX}$: 3.3%; MMP-9ΔOG: 3.6%, Fig. 2.3D,a-e).

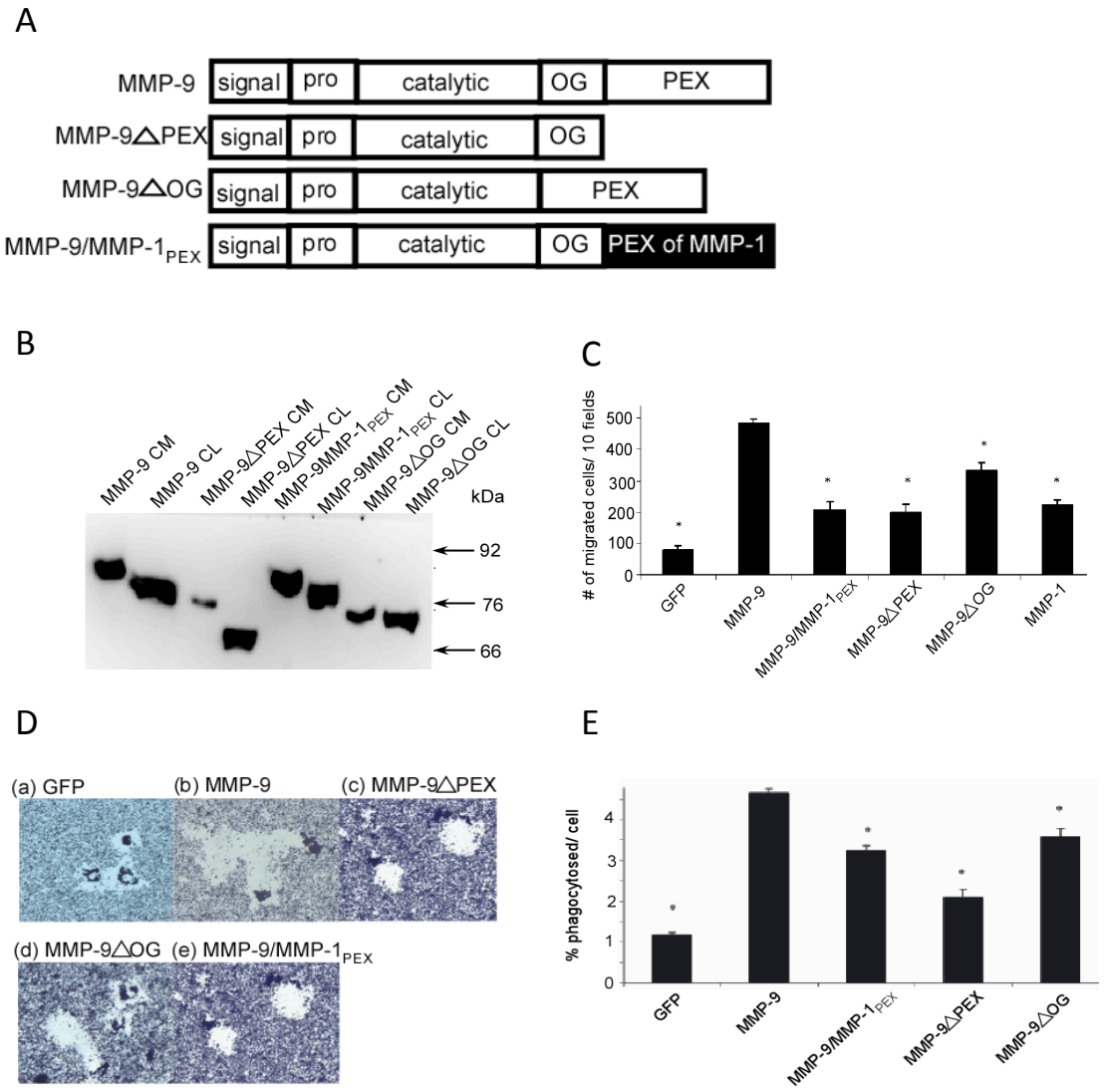

Figure 2.3. The hemopexin domain of MMP-9 is required for MMP-9-enhanced cell migration. (A): Schematic diagram of wild-type and mutant MMP-9. (B): Expression of wild-type and mutant with vector encoding the cDNA of MMP-9 in COS-1 cells. The conditioned medium (CM) and cell lysates (CL) of COS-1 cells transfected with wild-type or mutant MMP-9 cDNAs were examined by Western blotting under denaturing conditions using anti-MMP-9 monoclonal antibodies. (C-E): Decreased cell migration in COS-1 cells transfected with expression vector encoding the cDNA of MMP-9 PEX domain mutation. Migratory ability of COS-1 cells transfected with cDNAs as indicated was examined by a Transwell chamber migration assay (C, *P-values* reflect comparison with MMP-9 transfected cells: **P<0.01*) or phagokinetic assay (D). Cleared migratory tracks as depicted by the absence of gold particles in phagokinetic assay were measured by ImageJ NIH imaging software (E). *P-values* were calculated in comparison with MMP-9 transfected cells: **P<0.01*.

Differential effect of MMP inhibitors on MMP-9-enhanced cell migration

X-ray crystallographic analysis of MMP-9 suggests that the hemopexin domain is involved in homodimer formation (10). Using non-denaturing conditions in Western blotting, we confirmed that MMP-9 forms a homodimer in the conditioned medium of transfected COS-1 cells. Replacement of the hemopexin domain of MMP-9 with that of MMP-1 (MMP-9/MMP-1_{PEX}) failed to result in homodimer formation (Fig. 2.4A).

It has been demonstrated that the C-terminus of TIMP-1, but not TIMP-2, binds to the hemopexin domain of MMP-9 (113), whereas the N-terminus of both TIMP-1 and -2 binds to the catalytic center of active MMP-9. To explore if binding of TIMP-1 to proMMP-9 interferes with enhanced cell migration, COS-1 cells co-transfected with MMP-9 along with TIMP-1 and TIMP-2 cDNAs were examined in the Transwell migration assay (Fig. 2.4B). A significant decrease of MMP-9-enhanced cell migration was observed in cells expressing both MMP-9 and TIMP-1, but not MMP-9 and TIMP-2. These data suggests that TIMP-1 interference with MMP-9 homodimer formation results in diminished cell migration. As expected, TIMP-1 had no effect on MMP-9/MMP-1_{PEX}-induced cell migration, which is consistent with the lack of binding between the hemopexin domain of MMP-1 and TIMP-1 (111, 113). Addition of exogenous TIMP-1 inhibited cell migration but TIMP-2 did not (Fig. 2.4C).

To further determine if extracellular MMP-9 enhances cell migration, conditioned media from COS-1 cells transfected with wild-type MMP-9 cDNA (i.e., unprocessed (CM) and gelatin Sepharose purified proMMP-9) was added to MMP-$9_{\Delta PEX}$ transfected and to native COS-1 cells followed by the Transwell migration assay. We found that exogenous MMP-9 was ineffective at enhancing the migration of native or MMP-$9_{\Delta PEX}$ transfected cells (Fig 2.4D).

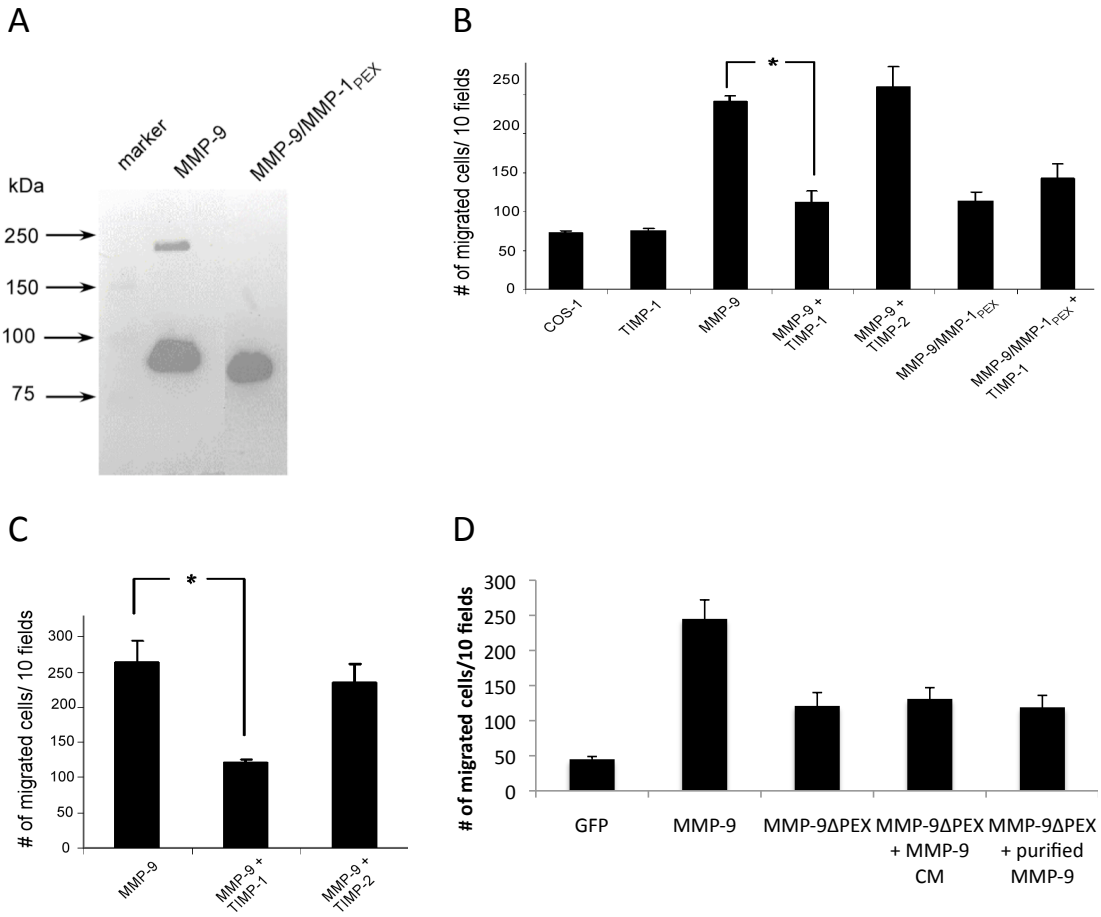

Figure 2.4. Interference of MMP-9-induced cell migration by TIMP-1, but not TIMP-2. (A): Detection of MMP-9 dimer in the conditioned medium of transfected COS-1 cells. The conditioned media from COS-1 cells transfected with MMP-9 or MMP-9/MMP-1_{PEX} cDNAs were examined by Western blotting under non-denaturing conditions using anti-MMP-9 antibodies. The homodimer was identified in COS-1 cells expressing wild-type MMP-9, but not in the MMP-9/MMP-1_{PEX}. (B): Expression of TIMP-1, but not TIMP-2 in cells interferes with MMP-9-mediated cell migration. COS-1 cells were co-transfected with MMP-9 or MMP-9/MMP-1_{PEX} along with TIMP-1 or TIMP-2 cDNAa and cell migration was assessed by a Transwell chamber migration assay. **P<0.01*. (C): Exogenous TIMP-1, but not TIMP-2 inhibits MMP-9-induced cell migration. COS-1 cells transfected with MMP-9 cDNAs were incubated with exogenous TIMP-1 (50 nM) or TIMP-2 (50 nM) followed by the Transwell chamber migration assay. **P<0.01*. (D) COS-1 cells were transfected with a vector encoding the cDNA of MMP-9 or MMP-9ΔPEX and cell migration was assessed by a Transwell migration assay. Addition of MMP-9 CM or gelatin-sepharose purified MMP-9 did not enhance the migration ability of COS-1 cells expressing MMP-9ΔPEX.

Lack of effect of MMP-9 on cell attachment

To determine whether the decreased cell migration in COS-1 cells transfected with MMP-9 mutants, as compared to wild-type MMP-9, was due to an effect on cell adhesion, a cell attachment assay was utilized. Cell attachment to culture plates after incubation for one and three hours was unaffected by wild-type and MMP-9 mutants (Fig. 2.5).

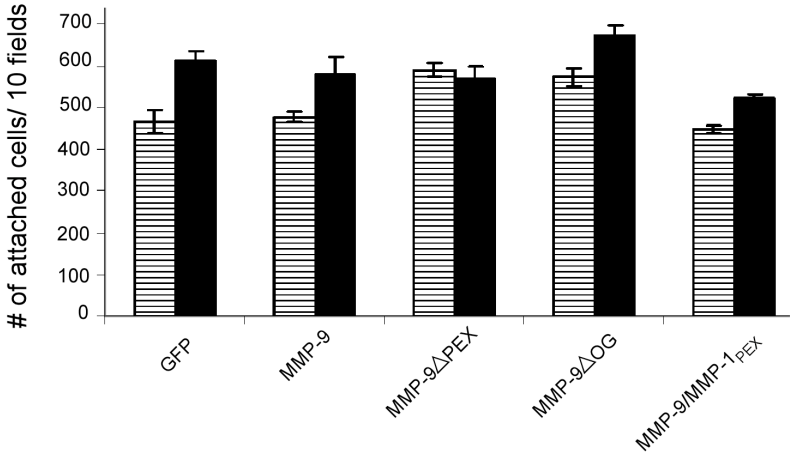

Figure 2.5. MMP-9 expression in transfected COS-1 cells has no effect on cell attachment. COS-1 cells transfected with GFP, MMP-9 and MMP-9 mutants cDNAs were incubated in polycarbonate wells and cell attachment was measured after 1 h (white) ad 3 h (black). Attached were stained with crystal violet and ten separate fields were counted. No significant differences in cell attachment were noted at either time point.

Effect of inhibitors of signal transduction pathways on MMP-9 induced cell migration

Inhibitors of signal transduction pathways were tested to investigate intracellular pathways involved in MMP-induced cell migration. We found that MAPK inhibitor (PD98059) (114) and PI3K inhibitors (LY294002 and wortmannin) (115) inhibited MMP-9-induced cell migration (Fig. 2.6). SP600125 inhibited baseline (GFP cDNA transfected) cell migration by 38%; MMP-9 induced cell migration was inhibited to a lesser extent (22%). These latter results link the JNK

pathway primarily to the basal level of cell migration (116). Y27632 and H89 exhibited no effect on either GFP or MMP-9 transfected cells, thus suggesting that protein kinase A and ROCK pathways are not involved in MMP-9 enhancement of COS-1 cell migration (117, 118).

Over-expression of MMP-7 in COS-1 cells

To further explore the importance of the hemopexin domain of MMPs, COS-1 cells were transfected with a vector encoding the cDNA of MMP-7 (MMP lacking a hemopexin domain) or MMP-9ΔPEX and evaluated in a Transwell migration assay. MMP-7 and MMP-9ΔPEX transfected cells display a similar enhancement on COS-1 cell migration but a lesser effect on cell migration as compared to MMP-9 wild type (Fig. 2.7).

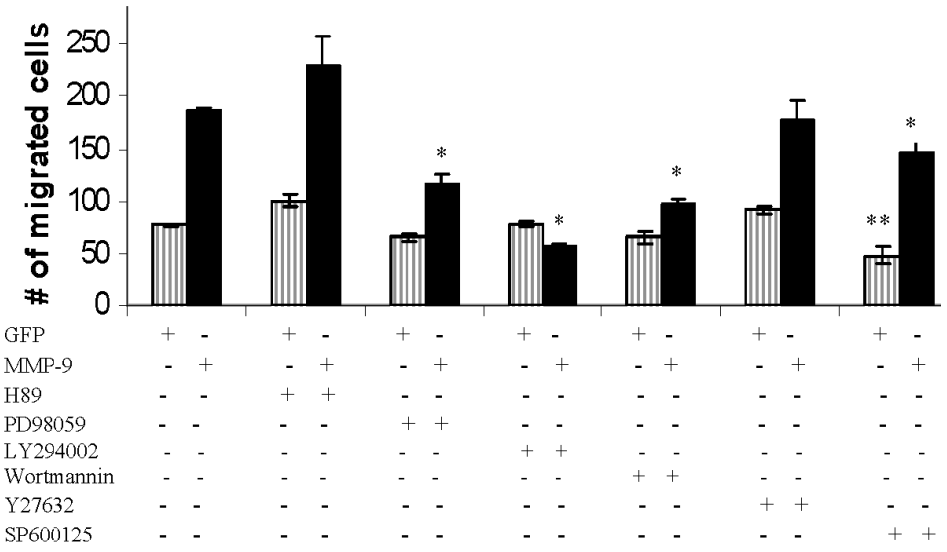

Figure 2.6. Differential effect of small molecular inhibitors on MMP-9-mediated cell migration. COS-1 cells transfected with a vector encoding GFP and MMP-9 cDNAs were incubated with PD98059 (10 μM), LY294002 (10 μM), Y27632 (1 μM), H89 (10 μM), wortmannin (10 μM) or SP600125 (10 μM) for 6 h in the Transwell chamber cell migration assay. **P<0.05* compared to MMP-9 and ***P<0.05* compared to GFP.

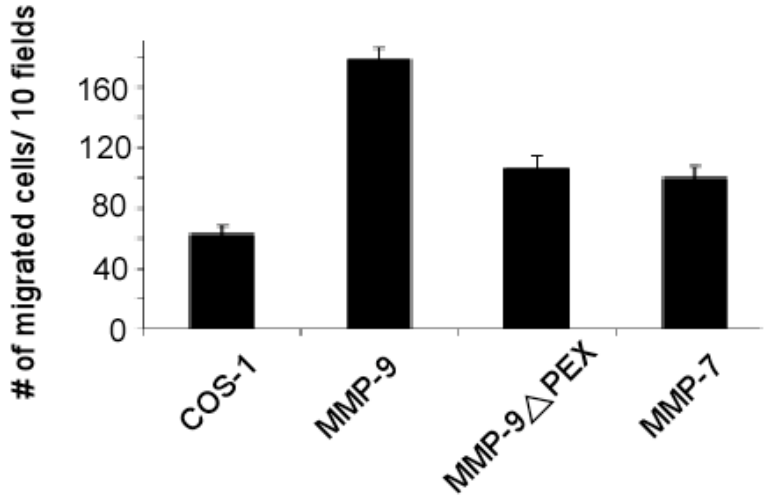

Figure 2.7. Enhancement of cell migration by overexpression of MMP-7 in COS-1 cells. COS-1 cells transfected with a vector encoding the corresponding cDNAs as indicated were examined by a Transwell chamber migration assay. Migrated cells were microscopically examined and counted. Migrated cells expressing MMP-7 were approximately equivalent to MMP-9 without PEX domain transfected cells.

2.3 Discussion

Cell migration and invasion are complex processes that have a key role in numerous biological and pathological conditions including embryonic development, wound healing, immune response, atherosclerosis, and cancer (119). Among the multiple proteases orchestrating cell migration, MMPs have been the most widely studied.

MMPs and other proteases have been shown to induce cell invasion by degrading the ECM, thereby facilitating migration through tissues. It is generally assumed that activation of proMMPs is required for this cell locomotion effect. Our experimental results run contrary to this expectation. Following transfection of a vector expressing human MMP cDNA into monkey kidney (COS-1) and human breast cancer (MCF-7) cells, it was demonstrated that several proMMPs enhanced cell migration (Fig 2.1A & 2.1E). By employing MMP inhibitors (Fig. 2.2C & 2.2D) or expressing constitutively inactive MMPs in COS-1 cells (Fig. 2.2E), it was demonstrated for the first time that enzymatic activity of MMPs is not a prerequisite for MMP-mediated cell migration.

Since proMMP-9 exerts a potent effect on cell migration, displays unique structural properties (e.g. long hinge domain, PEX homodimer formation), and is implicated in numerous pathological processes such as inflammation and cancer, we chose to mutate the domains of MMP-9 cDNA to better understand their role in cell migration. Using MMP-9 as a model, it was demonstrated that the PEX domain of MMP-9 is required for MMP-9-mediated cell migration, suggesting a novel role for the PEX domain of MMPs in enhancement of migration. Substitution of the PEX domain of MMP-9 with that of MMP-1 decreased MMP-9-enhanced cell migration, but the level of cell migration was still above the basal control level of GFP-transfected cells (Fig. 2.3C). However, it was also demonstrated that the hinge region (O-glycosylation domain) of MMP-9 contributes to MMP-9-mediated cell migration (Fig. 2.3C). It has been proposed

that the hinge region of MMP-9 correctly orients the PEX domain in order to facilitate binding to various molecules (104, 120). In terms of examination of other MMPs without a PEX domain, we have evaluated MMP-7 transfected cells and noted that migration was approximately equivalent to MMP-9 without PEX domain transfected cells (Fig. 2.7). It needs to be noted, however, MMP-7 contains an abbreviated hinge region, which complicates analysis of the function of the PEX versus hinge domain.

Although the hemopexin domain of different MMPs displays distinct features, for example, binding to different TIMPs, forming homo- and heterodimer, etc. (121), the PEX domain of MMPs exhibit similar three-dimensional structures composed of a disc-like shape, with the chain folded into a β-propeller structure that has a pseudo four-fold symmetry (10). Each propeller contains a sheet of four antiparallel strands with peptide loops linking one sheet to the next. Only strands 1-3 within each blade are topologically conserved and can be superimposed. The outer strand 4 of each blade is considerably different between MMP PEX domains (10). This suggests that the inner three strands constitute the shared common structural framework making up the β-propeller architecture, while the outer strand of each blade mediates contacts with other specific protein components and provide unique functions to the PEX domain, that is, capacity for cell migration (further explored in chapter 3). It was hypothesized that there are structural amino acids in the PEX domain of MMPs required for enhanced cell migration. Our observation that different MMPs displayed distinct capability for enhanced cell migration (Fig. 2.1B & 2.1 E) supports the structural difference of the PEX domain of MMPs.

Although MMP-9, like MMP-2, is a secreted protein and has been studied for its capacities to degrade the ECM, others have suggested that it may have additional roles either intracellularly (122) and/or the cell membrane (123). The PEX domain of MMP-9 is known to bind to several cell surface molecules including LRP-1, LRP-2, CD44, RECK, Ku and type IV collagen (4, 104, 124), but

the precise roles of these interactions remains speculative. To examine the role of secreted MMP-9 on cell migration, the effect of adding MMP-9 (isolated from transfected cell condition medium) to cells was examined. Exogenous MMP-9 did not enhance migration of non-transfected COS-1 cells. This negative data suggests that enhancement of cell migration by proMMP-9 may reflect an unidentified intracellular event.

In addition to binding to the catalytic domain of MMP-9, TIMP-1 forms a complex with the PEX domain of proMMP-9 (125). In my migration assay using either exogenous TIMP or TIMP cDNA transfected cells, TIMP-1 inhibited migration of proMMP-9 expressing cells in a PEX domain dependent manner, whereas TIMP-2 did not. Since both TIMP-1 and TIMP-2 inhibits activated MMP-9, these data suggest an inhibitory effect related to TIMP-1 binding to the PEX domain of proMMP-9. Whereas comprehensive studies by Olson et al. concluded that TIMP-1 binds to either monomeric or dimeric forms of proMMP-9 (111), an earlier publication reported that the proMMP-9:TIMP-1 complex interfered with MMP-9 homodimer formation (113).

Inhibitors of cell signaling were employed in order to illuminate pathways involved in MMP-9 induced cell migration. It was demonstrated that the MAPK and PI3K pathways, but not the protein kinase A and ROCK pathways are linked to MMP-9 induced cell migration. Inhibition of the JNK pathway affected basal cell migration to a greater extent than MMP-9 induced cell migration. In accordance with my results, Tian et al. (126) reported that interference with the ERK1/2 pathway affected epithelial cell migration. However, they also reported that activated MMP-9 participated in epidermal growth factor/transforming growth factor-β1 induced cell migration (126). It was found that the dose of MMP-2/-9 inhibitor required to interfere with cell migration by Tian et al. (126) also decreased cell secretion of MMP-9, thereby implying cell toxicity.

Of relevance to my observations, Hu and Ivashkiv (123) recently reported that MMP-9 is a key player in migration of dendritic cells through uncoated filters in a Transwell chamber assay. In contrast to the epithelial cells (COS-1 and MCF-7) employed in my experiments, dendritic cells secrete active MMP-9 that becomes membrane-bound to $\alpha_M\beta_2$ integrin and CD44, leading to modulation of CCL5 and activation of JNK signaling. Both the JNK inhibitor (SP600125) and a synthetic inhibitor of MMPs, abrogated dendritic cell migration. These data suggest that dendritic cell migration is dependent on activated MMP-9 and JNK signaling, whereas epithelial cell migration is independent of activated MMP-9, but dependent on the MAPK and PI3K signaling pathways (Fig. 2.6).

In summary, it was demonstrated that MMPs enhance epithelial cell migration, independent of proteolytic activity. The PEX domain of proMMP-9 is a prerequisite for enhancement of cell migration, possibly due to homodimer formation. Additional studies are needed to better understand the detailed dynamics of MMP-induced cell migration with the recognition that the underlying mechanism may differ depending on cell type. We propose that the development of selective inhibitors of the PEX domain of MMP-9 may provide an attractive option for treatment of diseases in which MMP-9 plays a pathologic role.

Chapter 3 - Roles of Matrix Metalloproteinase-9 dimers in Cell migration: Design of Inhibitory Peptides

(The work in this chapter has been published in the *Journal of Biological Chemistry* (2010) **[E-publication ahead of print]**, and the co-authors are Stanley Zucker, Nicole S. Sampson, Cem kuscu and Jian Cao (127))

3.1 Summary

Non-proteolytic activities of matrix metalloproteinases (MMPs) have recently been shown to impact cell migration, but the precise mechanism remains to be understood. It was previously demonstrated that the hemopexin (PEX) domain of MMP-9 is a prerequisite for enhanced cell migration. Using a biochemical approach, it is shown that dimerization of MMP-9 through the PEX domain appears necessary for MMP-9-enhanced cell migration. Following a series of substitution mutations within the MMP-9 PEX domain, blade IV was shown to be critical for homodimerization, whereas blade I was required for heterodimerization with CD44. Blade I and IV mutants showed diminished enhancement of cell migration compared to wild type MMP-9 transfected cells. Peptides mimicking motifs in the outermost strands of the first and fourth blades of MMP-9 PEX domain were designed. These peptides efficiently blocked MMP-9 dimer formation and inhibited motility of COS-1 cells overexpressing MMP-9, HT-1080 and MDA-MB-435 cells. Using a shRNA approach, CD44 was found to be a critical molecule in MMP-9-mediated cell migration. Furthermore, an axis involving a MMP-9-CD44-EGFR signaling pathway in cell migration was identified using specific receptor tyrosine kinase inhibitors. In conclusion, the mechanism of proMMP-9-enhanced cell migration was dissected and structure-based inhibitory peptides targeting MMP-9-mediated cell migration were developed.

3.2 Introduction

In the 1990's, several broad-spectrum MMP inhibitors were evaluated in clinical trials involving cancer, arthritis and later, heart failure. Based on the absence of clinical efficacy of these drug trials and the conviction that MMPs are critical players in disease processes, a more thorough investigation of the biological roles of individual MMPs has subsequently been undertaken (14, 102).

Crystal structures of various domains have been solved for several MMPs including MMP-1, -2, -3, -9, -13 and -14. Bridging biochemical information with *in vitro* and *in vivo* experiments has been helpful in better understanding the specific roles of individual MMPs. Since the catalytic site of most MMPs are highly homologous, leading to difficulty producing specific inhibitors, intense scrutiny of other MMP domains has followed. Based on the substrate binding function of the hemopexin (PEX) domain, this domain is recognized to play an important role in MMP function (4). With the exception of MMP-7, -23 and -26, which lack the PEX domain, all other MMPs form a propeller structure composed of four blades and each blade consists of one α-helix and four anti-parallel β-strands.

Among secreted MMPs, only MMP-9 is capable of forming a homodimer; the precise role of this homodimerization has yet to be elucidated. Solving the crystal structure of MMP-9 demonstrated that the homodimer is formed through blade IV of the PEX domain (10). In contrast to all other secreted MMPs, proMMP-9 and proMMP-2 bind TIMP-1 and TIMP-2, respectively, through their PEX domain. Other MMPs require activation in order for TIMP to bind to the catalytic domain of MMPs.

MMP-9 has been shown to bind to several cell surface receptors including CD44, LRP-1, LRP-2, Ku, and β1-integrin (89, 104, 124, 128). CD44, a cell-surface glycoprotein involved in cell-cell and cell-matrix interactions, has been associated with the ability to regulate cell migration and cell shape by association

with actin microfilaments (129, 130). CD44 has an extracellular domain that binds hyaluronic acid and this interaction has been shown to promote intracellular signaling involving ERK and Rho (131, 132).

Since MMPs are involved in multiple diseases, it has been proposed that better understanding of MMP domains might reveal crucial information for specific and novel inhibitory drug design (14, 102, 133). Based on lower similarity between PEX domains as compared to catalytic domains of different MMPs (homology sequence alignment: www.ebi.ac.uk /Tools/clustalw2), targeting the PEX domain is proposed as an option to inhibit a specific MMP.

In contrast to general concepts regarding the requirement for activation of proMMPs to generate biological activity, it was demonstrated that proMMP-9 enhances COS-1 cell migration independent of its proteolytic activity (42). To shed light on this novel observation, we investigated biochemical and biological properties of MMP-9 dimerization and dissected the signaling pathways involved in MMP-9-mediated cell migration. Based on structure-functional analysis, inhibitory peptides targeting MMP-9-induced cell migration were designed and assessed. This novel structure-based peptide approach serves as a proof of principle for design of the next generation of MMP inhibitors.

3.3 Results

Dimerization of MMP-9 in transfected COS-1 cells

It was previously demonstrated that the hemopexin (PEX) domain of proMMP-9 is required for the enhanced cell migration; this effect is independent of MMP-9 proteolytic activity (Chapter 2, (42)). In order to dissect the mechanism underlying MMP-9-induced cell migration, the PEX domain of MMP-9 was examined using biochemical and molecular approaches.

Among all secreted MMPs, only MMP-9 has been found to form a homodimer. Employing proteins purified from an E. coli expression system (Fig. 3.1A, ribbon diagram based on PDB file: 1ITV), Cha et al. (10) showed that MMP-9 homodimer formation requires an interaction of the fourth blade of adjacent PEX domains. Since proteins purified from a bacterial system lack posttranslational modifications, e.g. glycosylation and phosphorylation, which can impact the function of most mammalian proteins (134), it is essential to test if the dimerization of MMP-9 also occurs in a mammalian cell expression system. To this end, we fused HA and Myc tags into the MMP-9 cDNA, to generate MMP-9/HA and MMP-9/Myc chimeras, respectively (Fig. 3.1B), followed by transfection of the cDNAs into COS-1 monkey kidney epithelial cells. Insertion of either HA tag between the propeptide domain and catalytic domain or Myc tag at the end of the PEX domain of MMP-9 does not interfere with the overall properties of wild type MMP-9 as evidenced by gelatin zymography and western blotting (Fig. 3.1C & 3.1D). Immunoprecipitation with either HA or Myc antibodies resulted in identifying MMP-9 in both the cell lysates and conditioned media of transfected COS-1 cells (Fig. 3.1E).

COS-1 cells co-transfected with HA- and Myc-tagged MMP-9 cDNAs were then employed to examine homodimer formation using a co-immunoprecipitation approach. The HA-tagged MMP-9 proteins in the conditioned medium of

transfected COS-1 cells were immunoprecipitated with anti-HA antibodies followed by a Western blot probed with anti-Myc antibodies. This approach revealed the identification of Myc-tagged MMP-9 in the complex immunoprecipitated by anti-HA antibody, suggesting that MMP-9 forms homodimers in cell condition medium (Fig. 3.1F). To further confirm this observation, the reciprocal co-immunoprecipitation was performed. Anti-Myc antibodies were employed to precipitate Myc-tagged MMP-9 complexes in the conditioned medium of co-transfected COS-1 cells followed by Western blotting using anti-HA antibodies. This reciprocal approach confirms that MMP-9 does form a homodimer in the condition medium of transfected COS-1 cells. To further explore if homodimer formation of MMP-9 occurs within the cell or following secretion from the cell, the cell lysate of transfected COS-1 cells was also examined by the co-immunoprecipitation method (Fig. 3.1F). MMP-9 homodimer formation was demonstrated in the cell lysate, suggesting that MMP-9 dimerization occurs during MMP-9 secretion.

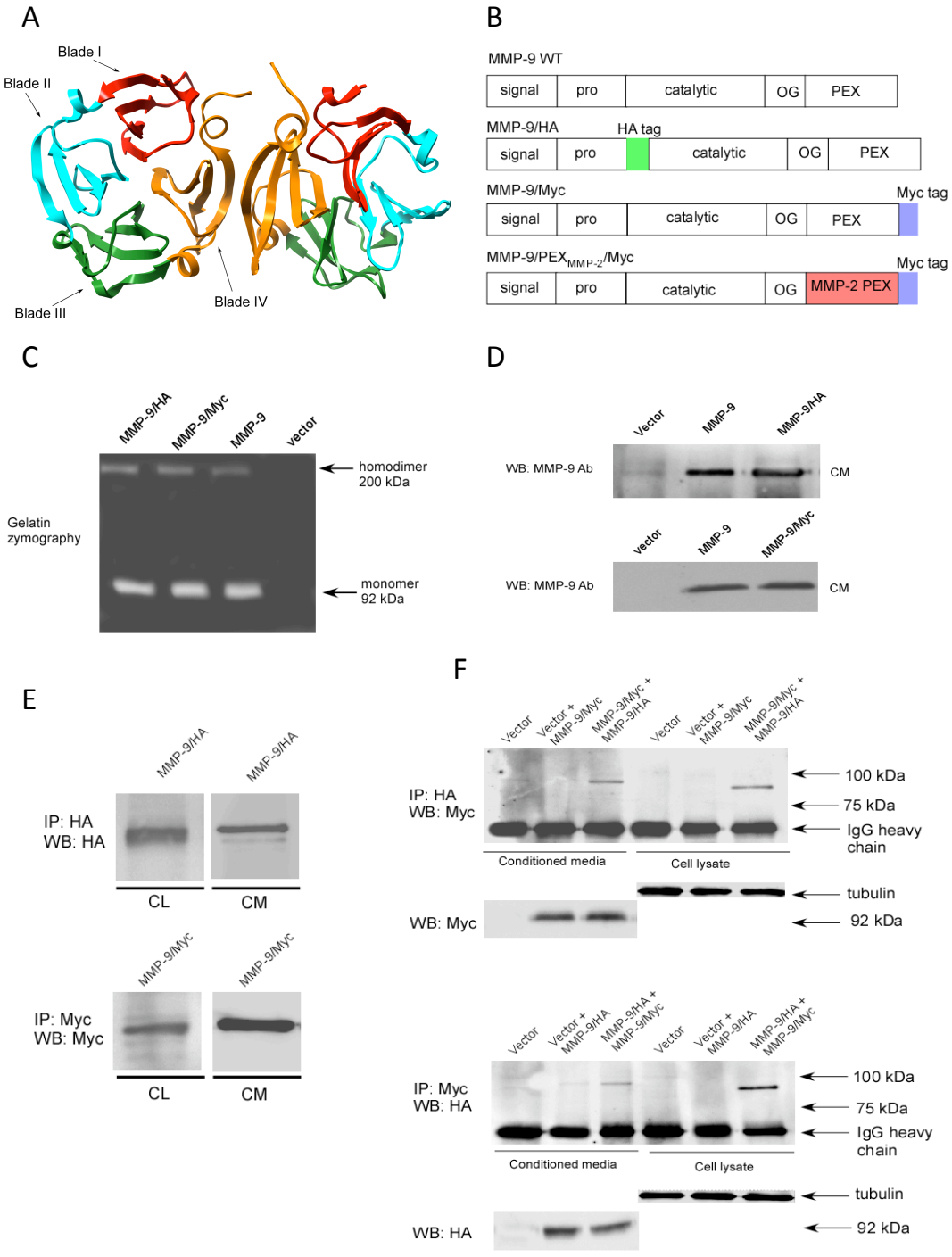

Figure 3.1. MMP-9 homodimerizes through its PEX domain. (A) Ribbon diagram of MMP-9 PEX domain (PDB: 1ITV). Homodimerization of MMP-9 is through the fourth blade of the MMP-9 PEX domain. (B) Schematic diagram of wild type MMP-9, MMP-9/HA, MMP-9/Myc and MMP9/PEX$_{MMP2}$/Myc. Five typical domains of MMP-9 from the N-terminus to C-terminus are the signal peptide

(signal), propeptide (pro), catalytic domain (catalytic), hinge region (OG), and hemopexin-like domain (PEX). HA and Myc tags were inserted as shown. The PEX domain of MMP-9 was replaced by that of MMP-2 to generate MMP-9/PEX_{MMP-2}/Myc. (C) Expression of wild type, HA- and Myc-tagged MMP-9 in COS-1 cells transfected with the cDNAs. The conditioned medium from COS-1 cells transfected with cDNAs was examined by gelatin zymography. (D) Expression of MMP-9 and HA- or Myc- tagged MMP-9 in COS-1 cells examined by Western blotting. The conditioned medium from transfected COS-1 cells was precipitated followed by Western blotting. (E) Insertion of HA or Myc tag in MMP-9 cDNA does not affect antibodies to precipitate MMP-9 chimera. The conditioned medium and cell lysate from COS-1 cells transfected with cDNAs as indicated were immunoprecipitated with anti-HA antibody (upper panel) and anti-Myc antibody (lower panel) followed by Western blotting using the same antibodies. (F) MMP-9 forms a homodimer in the COS-1 cells transfected with vector encoding human MMP-9 cDNAs. COS-1 cells were transfected with a combination of cDNAs as indicated. The conditioned medium and cell lysates were examined by a co-immuneprecipitation assay (upper panel) and a reciprocal co-immuneprecipitation assay (lower panel). 20 µg of total cell lysates or 20 µl of the conditioned medium were used as loading controls by anti-α/β tubulin antibody for cell lysates and anti-Myc or anti-HA antibodies for the conditioned medium.

Prerequisite of MMP-9 dimerization in proMMP-9-induced cell migration

To test if dimerization of the MMP-9 PEX domain is a prerequisite for MMP-9-induced cell migration, MMP-9 PEX domain mutations were generated. Since MMP-2 does not form homodimers (41), the PEX domain of MMP-9 was replaced by that of MMP-2 to generate MMP9/PEX_{MMP-2} chimeric cDNA using a two-step PCR approach (135). The resultant PCR product containing MMP9/PEX_{MMP-2} was then inserted into a pcDNA3.1/Myc vector to generate a final construct of MMP9/PEX_{MMP-2}/Myc chimeric cDNA (Fig. 3.1B). Substitution of the PEX domain of MMP-9 with that of MMP-2 failed to couple with the wild type MMP-9 in co-transfected COS-1 cells in the conditioned medium (Fig. 3.2A). The failure of the dimerization of the PEX domain mutation was not due to the loss of protein synthesis, trafficking, or proteolytic activity as evidenced by Western blotting and gelatin zymography (Fig. 3.2B).

In order to determine if the loss of homodimerization of this MMP-9 PEX domain mutation affects MMP-9-induced cell migration, a Transwell chamber migration assay was employed (42). COS-1 cells transfected with a vector encoding the cDNA of the PEX mutant MMP-9 (MMP-9/PEX_{MMP-2}/Myc) failed to enhance cell migration to the extent of wild type MMP-9, suggesting a role of MMP-9 homodimer in cell migration (Fig. 3.2C). To further confirm the biological role of MMP-9 homodimers in cell migration, wild-type and mutant MMP-9-transfected cells were subjected to phagokinetic migration analysis which permits quantification by clearance of colloidal gold particles within the cell migratory path (Fig. 3.2D). Similarly to the data from the Transwell migration assay (Fig. 3.2C), cells transfected with MMP-9/Myc cDNA displayed enhanced migration as compared to vector-transfected cells determined by the NIH ImageJ software (Fig. 3.2E). Enhanced cell migration did not occur in cells transfected with a vector encoding the cDNA of MMP-9/PEX_{MMP-2}/Myc. Taken together, these data indicate that homodimerization through the MMP-9 PEX domain plays an important role in MMP-9-induced cell migration.

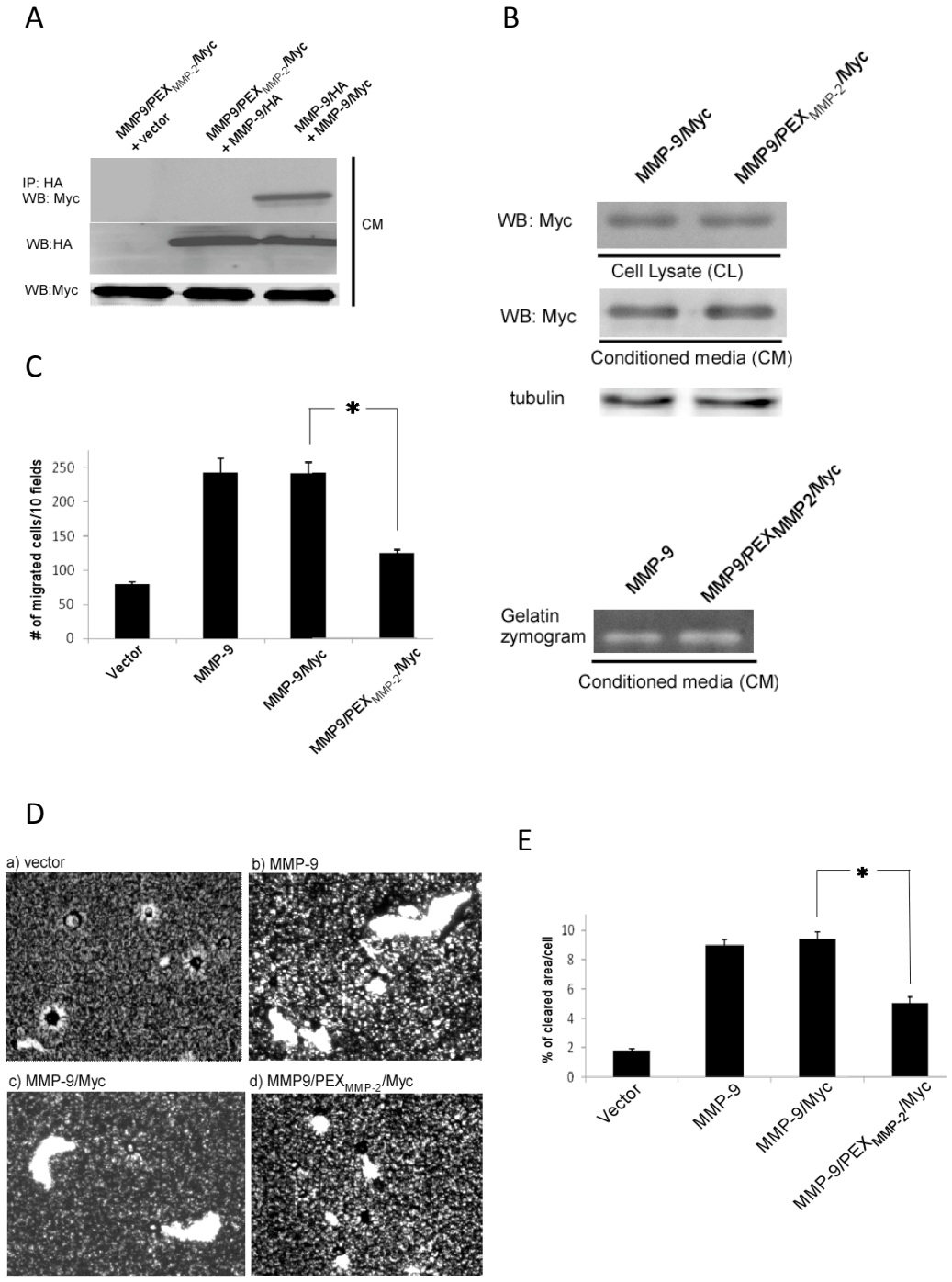

Figure 3.2. MMP-9 homodimer is required for MMP-9-enhanced cell migration. (A) Replacement of the MMP-9 PEX domain with the corresponding region of MMP-2 prohibited dimerization with wild type MMP-9 as examined through a co-immunoprecipitation assay. The conditioned medium of COS-1 cells transfected with a combination of cDNAs as indicated was examined by a co-immuneprecipitation assay. 20 µl of the conditioned medium were examined by Western blotting using anti-Myc antibody for monitoring expression of MMP-

9/Myc and MMP9/PEX_{MMP2}/Myc. (B) Mutant MMP-9 by swapping the PEX domain with that of MMP-2 (MMP-9/MMP-2_{PEX}) expresses comparable level of proteins with wild-type MMP-9 examined by Western blotting (upper panel) and by gelatin zymography (lower panel). (C) COS-1 cells transfected with wild-type and mutant MMP-9 cDNAs were examined by a Transwell chamber migration assay (C) and phagokinetic assay (D). Migratory ability of cells using the phagokinetic assay was quantitatively determined using Image J software (E). ($^{*}p < 0.05$).

Inhibition of MMP-9 dimerization by TIMP-1 resulting in diminished cell migration

The role of TIMP-1 in interfering with MMP-9 homodimer formation remains controversial (111, 113). This discrepancy led to a reevaluation of the specific interference of TIMP-1 on proMMP-9 homodimer formation using the biochemical approach described above. Since MMP-9 homodimer formation is a prerequisite for enhancing cell migration (Fig. 3.2C-E) and TIMP-1 blocks MMP-9-induced cell migration (42), it was hypothesized that binding of TIMP-1 to the PEX domain might prevent proMMP-9 homodimerization, thus, interfering with MMP-9-induced cell migration. To test this hypothesis, COS-1 cells transfected with both proMMP-9/Myc and proMMP-9/HA cDNAs along with TIMP-1 or TIMP-2 cDNAs were examined by the co-immunoprecipitation assay, as described above. As shown in figure 3.3A, co-expression of TIMP-1 with proMMP-9 cDNAs resulted in blocking MMP-9 homodimer formation both in the conditioned media and cell lysate of transfected cells. As demonstrated by co-immunoprecipitation studies, abrogation of proMMP-9 homodimer formation by TIMP-1 coincided with heterodimer formation between proMMP-9 and TIMP-1 (Fig. 3.3B & 3.3C). In contrast, TIMP-2 has no effect on proMMP-9 homodimer formation (Fig. 3.3A), which is in agreement with previous observation that TIMP-2 only bound to the PEX domain of MMP-2, but not MMP-9 (Fig. 3.3D) (41).

Since TIMP-1 was shown to interfere with MMP-9 homodimerization, it was then tested if the loss of homodimer formation of MMP-9 by TIMP-1 fails to enhance cell migration. By employing a Transwell migration assay, it was

observed that co-expression of TIMP-1, but not TIMP-2, with proMMP-9 in COS-1 cells inhibited proMMP-9-enhanced cell migration, but had no apparent effect on proMMP9/PEX$_{MMP-2}$/Myc transfected cells (Fig. 3.3E). In addition, both TIMP-1 and TIMP-2 did not significantly inhibit MMP9/PEX$_{MMP-2}$/Myc enhancement of COS-1 cell migration (Fig. 3.3E). These results suggest a unique role for TIMP-1 interference of both MMP-9 homodimerization and enhancement of cell migration.

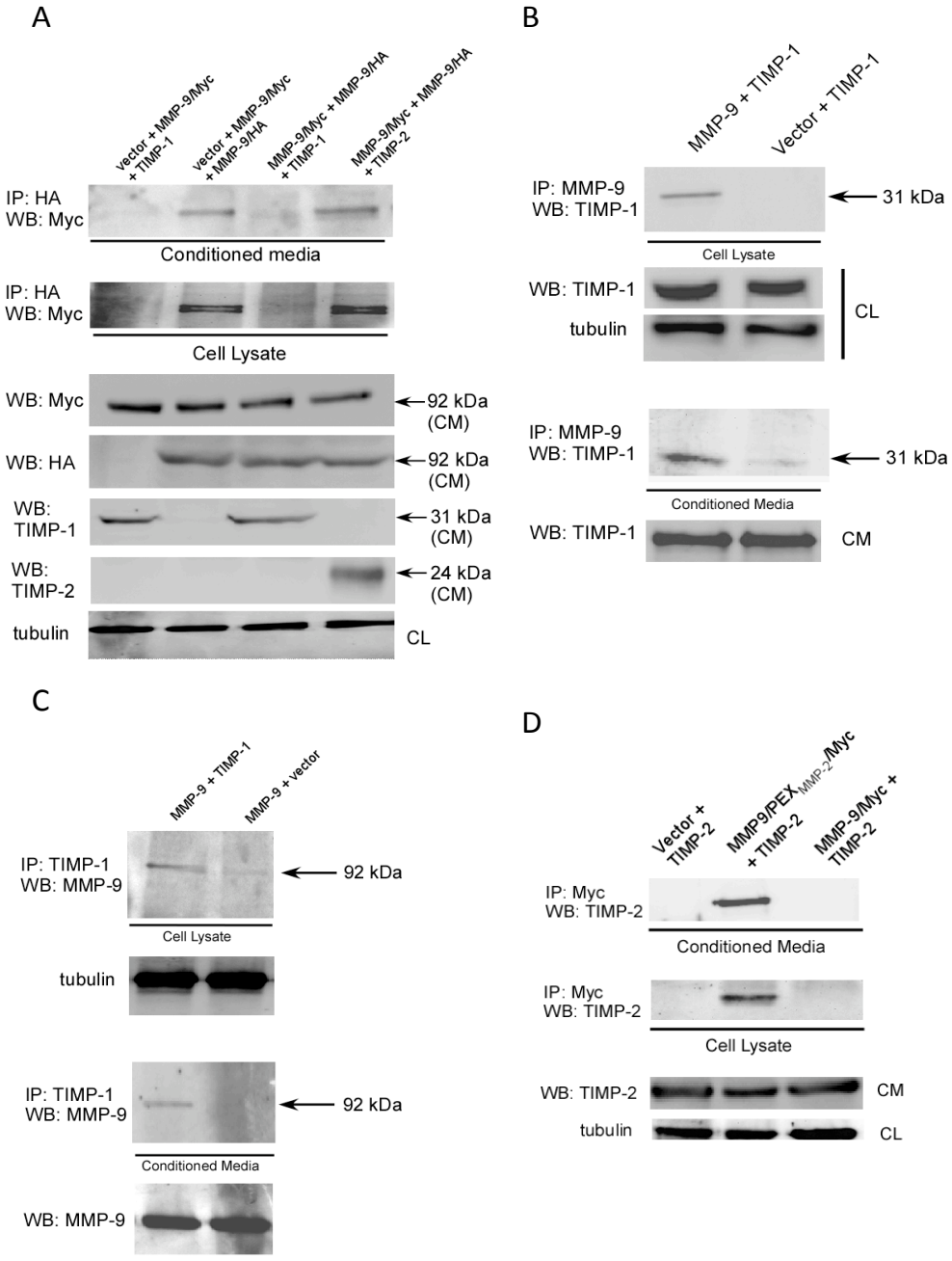

E

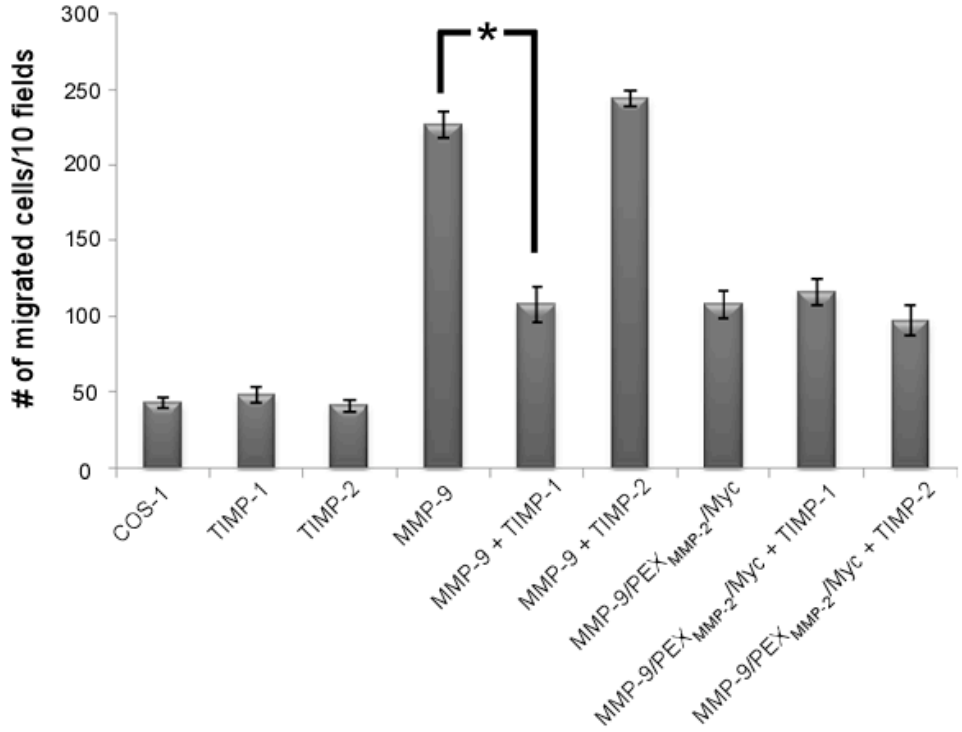

Figure 3.3. TIMP-1 interferes with MMP-9 homodimerization. (A) TIMP-1, but not TIMP-2 interferes with MMP-9 dimerization in transfected COS-1 cells examined by a co-immunoprecipitation assay for conditioned medium and cell lysates (upper and middle panels). Western blotting using aliquot of the conditioned medium and cell lysates was performed using anti-Myc, HA, TIMP-1, TIMP-2 and α/β tubulin antibodies (lower panel, loading control). (B) TIMP-1 co-precipitated with MMP-9 in both the cell lysate and the conditioned medium of transfected COS-1 cells examined by a co-immunoprecipitation assay. The reciprocal co-immunoprecipitation experiment is shown in (C). The conditioned medium and cell lysate were examined by Western blotting using anti-TIMP-1 and α/β tubulin antibodies for control of protein expression. (D) MMP-9/PEX_{MMP-2}/Myc, but not wild type MMP-9, co-precipitates with TIMP-2. COS-1 cells were co-transfected with a combination of cDNAs as indicated. The conditioned medium and cell lysate were examined by a co-immunoprecipitation assay. Aliquot of conditioned medium and cell lysate were examined by Western blotting using anti-TIMP-2 and MMP-9 antibody, respectively, for control of protein expression. (E) TIMP-1, but not TIMP-2, interferes with MMP-9-induced cell migration. COS-1 cells transfected with corresponding cDNAs as indicated were subjected to a Transwell migration assay. *Three triplicate repeats* were performed for each transfection and the experiment was repeated three times. *$p < 0.05$.

Minimal motif required for MMP-9 homodimer formation

The PEX domain of MMPs exhibit similar structures composed of a disc-like shape, with the chain folded into a β-propeller structure that has a pseudo four-fold symmetry. Each blade contains four anti-parallel β-strands with peptide loops linking one strand to the next as illustrated in figure 3.1A. Based on the crystal structure analysis of purified MMP-9 PEX domain from E. coli (10), the homodimerization of MMP-9 occurs through an interaction of the outermost strand of the fourth blade of the PEX domains. However, the crystal structure of MMP-9 PEX domain using the recombinant protein from E. coli has not been completely validated in a mammalian cell system. To test if the interaction interface of MMP-9 homodimer formation occurs through the outermost strand of the fourth blade of the PEX domains in mammalian cells, a genetic approach was employed to generate substituted mutations for the outermost β-strands of each blade within the MMP-9 PEX domain. The outermost β-strand of the fourth blade of the MMP-9/HA PEX domain (N_{688}QVDQVGY$_{695}$) was substituted by the corresponding region from MMP-2 PEX domain (K_{586}SVKFGS$_{592}$) to generate MMP-9/IVS4 chimera (Fig. 3.1A & 3.4A). As controls, three additional mutations for the outermost strands of blades I, II and III were engineered by replacing with the corresponding sequence of MMP-2 (MMP-9/IS4, MMP-9/IIS4 and MMP-9/IIIS4) (Fig. 3.4A). Employing a co-immunoprecipitation assay for COS-1 cells co-transfected with different combination of cDNAs, we observed that mutations of blades I, II and III of MMP-9 PEX domain had no effect on MMP-9 homodimer formation; whereas mutation of blade IV (MMP-9/IVS4) failed to dimerize (Fig. 3.4B). This defect was not due to the loss of secretory ability of the mutant as evidenced by Western blot and gelatin zymography of the conditioned medium from transfected COS-1 cells (Fig. 3.4B). The four mutants and wild type MMP-9 were then evaluated for their ability to enhance cell migration using a Transwell migration assay (Fig. 3.4C). Mutation of the fourth β-strand of the PEX domain of MMP-9 (MMP-9/IVS4) failed to enhance COS-1 cells migration, as compared to

wild type MMP-9, whereas mutations of blade II and III induced cell migration as well as wild type MMP-9 (Fig. 3.4C). Unexpectedly, mutation of the first blade of the PEX domain of MMP-9 (MMP-9/IS4) also failed to induce cell migration. These data suggest that both blades I and IV of the MMP-9 PEX domain are required for the enhanced cell migration. Since the outermost β-strand of blade I is not involved in homodimer formation, another explanation for failure of migration of the MMP-9/IS4 mutant needs to be sought.

Blocking MMP-9-induced cell migration by targeting the homodimerization of MMP-9

Increased cell migration is involved in many pathological conditions including atherosclerosis and cancer; upregulated MMP-9 has been implicated in these processes (4). One approach to blunt MMP-9 induced cell migration might be to target homodimer formation, which is a prerequisite for MMP-9-induced cell migration. Given the observation that the outermost β-strand of the fourth blade of the MMP-9 PEX domain is required for MMP-9 homodimerization formation, an 8-amino acids peptide (NQVDQVGY) was synthesized to mimic the outer β-strand of blade IV of MMP-9 PEX domain (IVS4 peptide). As a control, a scrambled peptide with the same amino acids but rearranged in different order (VQYDNGQV) was designed and synthesized. To test if **IVS4** peptide blocked MMP-9 homodimer formation, COS-1 cells transfected with a vector encoding the MMP-9 cDNA were treated with 100 μM peptide for 24 hours prior to a co-immunoprecipitation assay. As shown in figure 3.4D, the **IVS4** peptide, but not the scrambled peptide, efficiently blocked MMP-9 homodimer formation both in the conditioned medium and the cell lysate. To examine the potential therapeutic effect of this peptide, a Transwell migration assay was performed. Interference of homodimerization by the peptide inhibited MMP-9-induced cell migration in a dose-dependent manner, whereas, the scrambled peptide had no apparent effect (Fig. 3.4E). This **IVS4** peptide had no effect on cell migration induced by MT1-MMP (Fig. 3.4F), an integral membrane matrix metalloproteinase capable of

stimulating cell migration (11). These data suggest that the **IVS4** peptide specifically inhibits MMP-9-induced cell migration through interference with MMP-9 homodimer formation.

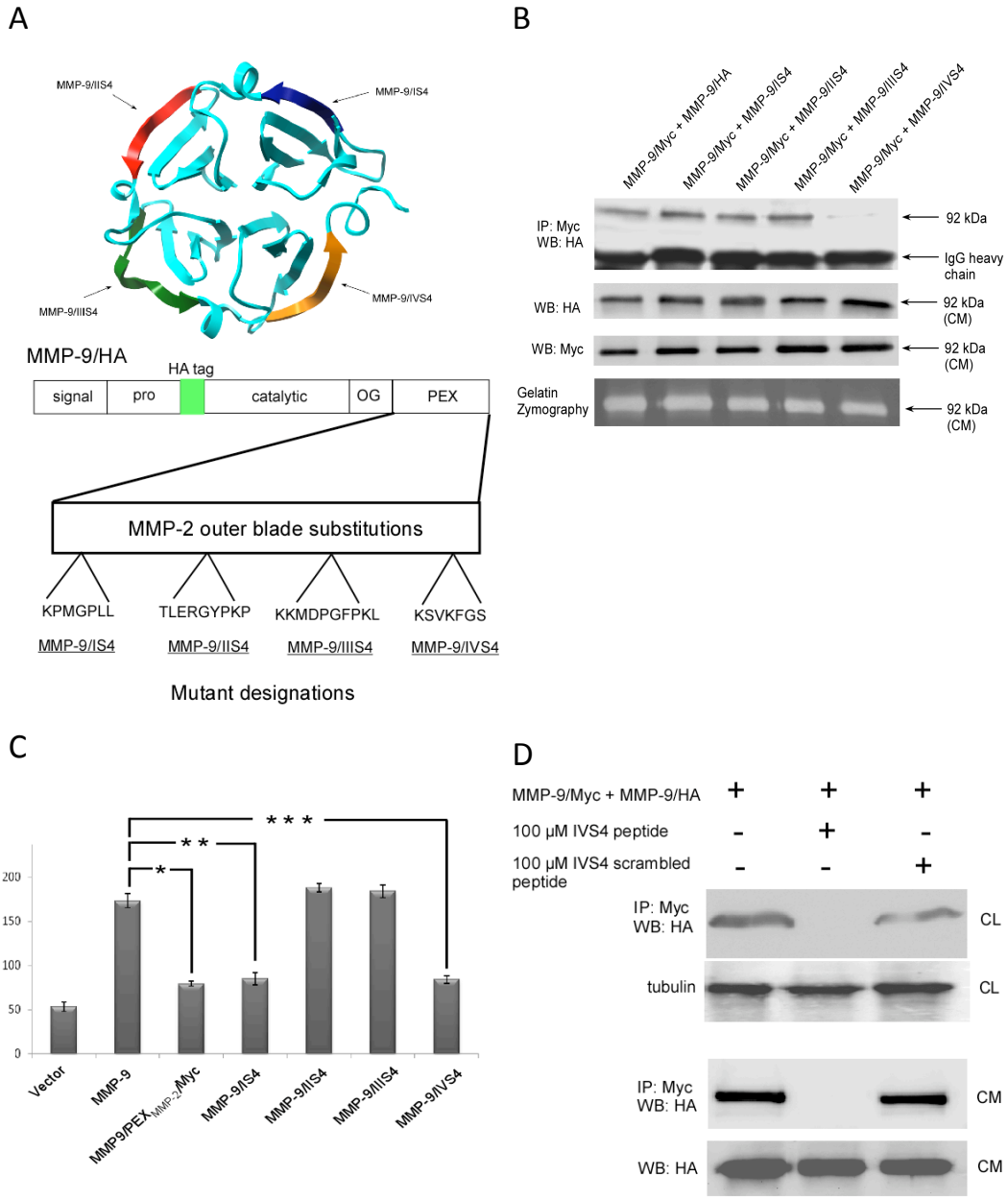

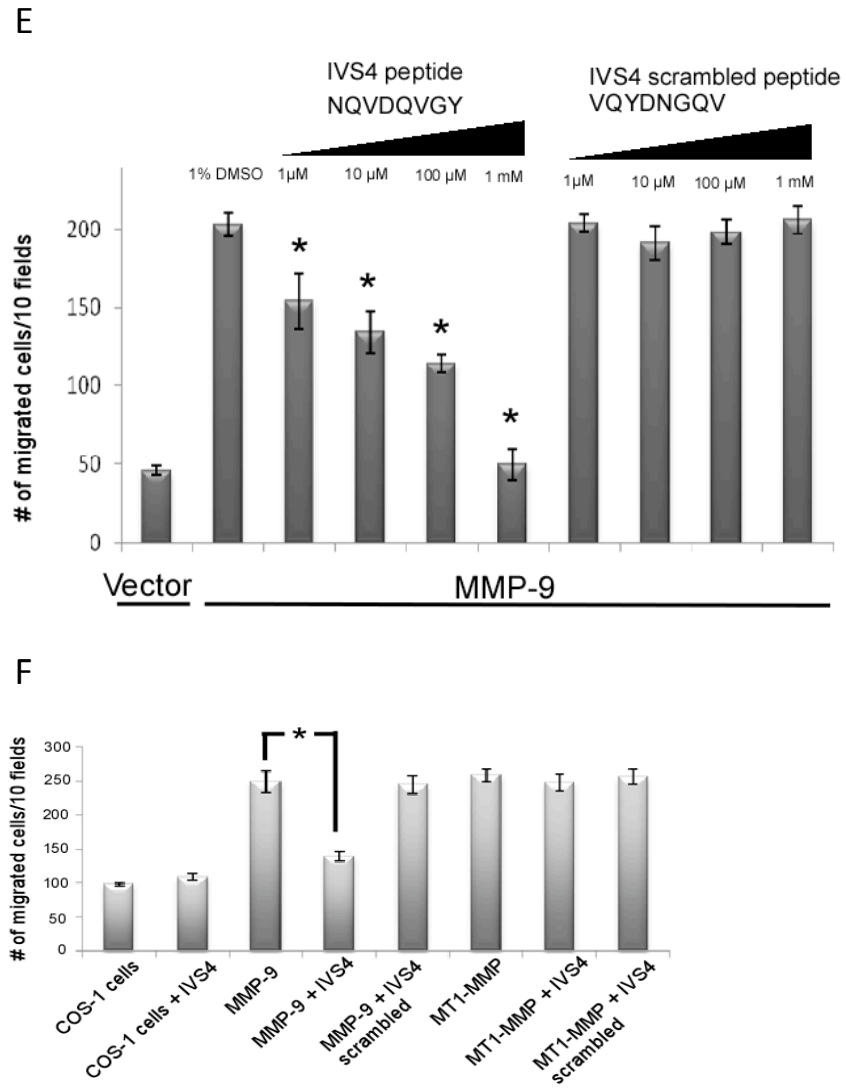

Figure 3.4. Blade IV of the PEX domain of MMP-9 is required for homodimerization and cell migration. (A) Ribbon diagram of MMP-9 PEX domain (PDB: 1ITV). Each outermost β-strand from the four blades was swapped with the corresponding MMP-2 PEX domain sequences (upper panel). Lower panel: Schematic diagram of substitution mutations at the outermost β-strands of four blades of MMP-9 by corresponding MMP-2 sequences. (B) Requirement of the blade IV for MMP-9 homodimerization: COS-1 cells transfected with MMP-9 chimeric cDNAs were examined by co-immunoprecipitation assay. Mutation at blade IV of the PEX domain of MMP-9 fails to co-precipitate with wild type MMP-9 (upper panel). The aliquot of condition medium was examined by Western blotting using anti-HA and anti-Myc antibody (middle panel) and by gelatin zymography (lower panel) for control of protein expression. (C) Mutations of the PEX domain or the outermost IS4 and IVS4 motifs of MMP-9 fail to enhance cell migration. COS-1 cells transfected with wild-type and mutant MMP-9 cDNAs were examined by a Transwell cell migration assay. *Three triplicate repeats* were

performed for each transfection and the experiment was repeated three times. $^{*}p < 0.05$. (D) Design of an inhibitory peptide interfering with MMP-9 homodimer formation. A peptide mimicking MMP-9/IVS4 was chemically synthesized and incubated (100 μM) with COS-1 cells transfected cDNAs as indicated. Scrambled peptide was used as a control. Both the cell lysates and conditioned medium were examined by a co-immunoprecipitation assay (upper and middle panel). An aliquot of the conditioned medium and cell lysate were examined by Western blotting using anti-HA and anti-α/β tubulin as a control. (E) Dose dependent inhibition (from 1 μM to 1 mM) of MMP-9-mediated cell migration by **IVS4** peptides. COS-1 cells transfected with an empty vector or MMP-9 cDNAs were pre-incubated with 1% DMSO, the **IVS4** peptide (NQVDQVGY) and **IVS4** scrambled peptide (VQYDNGQV) for 30 min. followed by a Transwell chamber migration assay in the presence of different concentrations of peptides for 6 hours. Each data point was performed in triplicate and the experiments were repeated three times ($^{*}P < 0.05$). (F) Specificity of **IVS4** peptide on inhibition of MMP-9-induced cell migration. COS-1 cells transfected with MMP-9 or MT1-MMP cDNAs were pre-treated with **IVS4** peptide and **IVS4** scrambled peptide for 30 min followed by Transwell migration assay. Each data point was performed in triplicate and the experiment was repeated three times ($^{*}P < 0.05$).

Cross-talk between MMP-9 and CD44 regulates cell migration

Although the outermost β-strand of blade I of MMP-9 is not required for MMP-9 homodimer formation (Fig. 3.4A), this motif is essential for MMP-9-induced cell migration (Fig. 3.4B). Given the evidence that MMP-9 interacts with CD44, a cell surface glycoprotein involved in cell-cell interactions, cell adhesion and migration (54, 89, 128), we reasoned that MMP-9 may also form a heterodimer with CD44 which signals for cell migration. As examined by real time RT-PCR and immunofluorescent staining (Fig. 3.5B & 3.5C), COS-1 cells express endogenous CD44. Co-immunoprecipitation between CD44 and MMP-9 was assessed to determine the interaction between MMP-9 and CD44 in MMP-9 transfected COS-1 cells. Indeed, MMP-9 and CD44 co-precipitated in the transfected COS-1 cells (Fig. 3.5A), which confirms heterodimer formation of the two molecules. In contrast, swapping the PEX domain of MMP-9 with that of MMP-2 (MMP9/PEX_{MMP-2}/Myc) resulted in failure to complex with CD44, suggesting that heterodimer formation between CD44 and MMP-9 is through the PEX domain of MMP-9. To further determine which motif is required for the

heterodimer formation, CD44 was co-expressed with MMP-9 mutants (MMP-9/IS4, MMP-9/IIS4, MMP-9/IIIS4 and MMP-9/IVS4) in transfected COS-1 cells, followed by co-immunoprecipitation. MMP-9/IS4 failed to form a complex with CD44, indicating that the outer β-strand of blade I interacts with CD44 at the cell surface (Fig. 3.5A). Mutations of outer β-strand of blades II, III and IV of the MMP-9 PEX domain did not interfere with CD44/MMP-9 heterodimerization (Fig. 3.5A).

To explore the role of CD44 in MMP-9-induced cell migration, endogenous CD44 expression in COS-1 cells was silenced using a short hairpin RNA (shRNA) approach. As determined by a real time RT-PCR, mRNA of CD44 was suppressed more than 20 fold in CD44 shRNA expressing COS-1 cells (Fig. 3.5B). No detectable CD44 protein was found in COS-1 cells expressing CD44 shRNA examined by immunofluorescent staining and flow cytometry analysis (Fig. 3.5C & 3.5D). By functional assay, the enhanced cell migration of MMP-9 transfected COS-1 cells was reduced significantly when CD44 was silenced, indicating that CD44 is a critical molecule in the MMP-9 cell migration signaling pathway (Fig. 3.5E). Interestingly, CD44 silenced COS-1 cells migrated to relatively higher levels as compared to shRNA luciferase control and wild type COS-1 cells. This observation might be due to decreased cell-cell and cell-matrix interactions by silence of CD44 expression in COS-1 cells (136).

To further examine the importance of cross-talk between CD44 and MMP-9 in cell migration, an 8-amino acid peptide (SRPQGPFL) was synthesized to mimic the outermost β-strand of the first blade of the MMP-9 PEX domain. As a control, a scrambled peptide with the same amino acids but rearranged in different order (GLSQPRFP) was synthesized. COS-1 cells transfected with CD44 and MMP-9 cDNAs were treated with **IS4** and **IS4** scrambled peptides for 24 hours followed by monitoring complex formations between CD44 and MMP-9 using a co-immunoprecipitation assay. **IS4** peptide interfered with CD44/MMP-9 heterodimer, whereas the **IS4** scrambled peptide had minimal effect (Fig. 3.5F).

In addition, the **IS4** peptide displayed dose-dependent inhibition of MMP-9-induced cell migration, but not the scrambled peptide (Fig. 3.5G). The **IVS4** peptide also inhibited cell migration. Although the potency of **IS4** and **IVS4** peptides (IC_{50}: 12 μM and 50 μM, respectively) are suboptimal from a therapeutic standpoint, generation of the mimicking inhibitory peptides provide a proof of concept for specific targeting an important molecule in human disease. To further validate the efficiency of the **IS4** and **IVS4** peptides, human cancer cell lines HT-1080 and MDA-MB-435, that naturally produce MMP-9 (137, 138), were tested. Using the Transwell migration assay, both **IS4** and **IVS4** peptides significantly inhibited migration of these two cell lines (Fig. 3.5H and 3.5I).

A

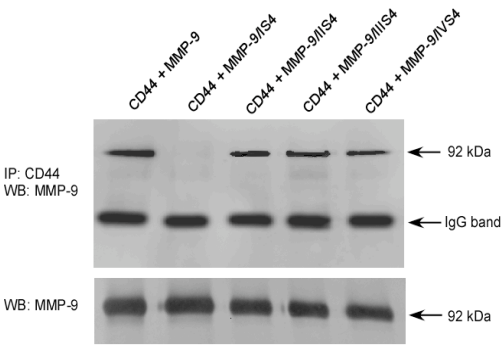
CD44 + MMP-9
CD44 + MMP-9/IS4
CD44 + MMP-9/IIS4
CD44 + MMP-9/IIIS4
CD44 + MMP-9/IVS4
IP: CD44
WB: MMP-9
92 kDa
IgG band
WB: MMP-9
92 kDa

B

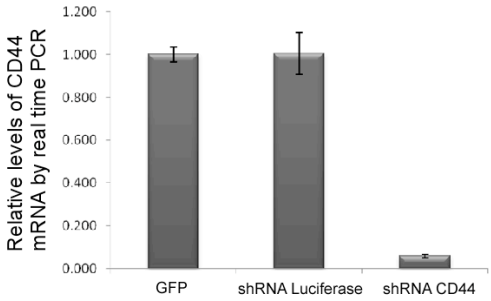
Relative levels of CD44 mRNA by real time PCR
1.200
1.000
0.800
0.600
0.400
0.200
0.000
GFP
shRNA Luciferase
shRNA CD44

C

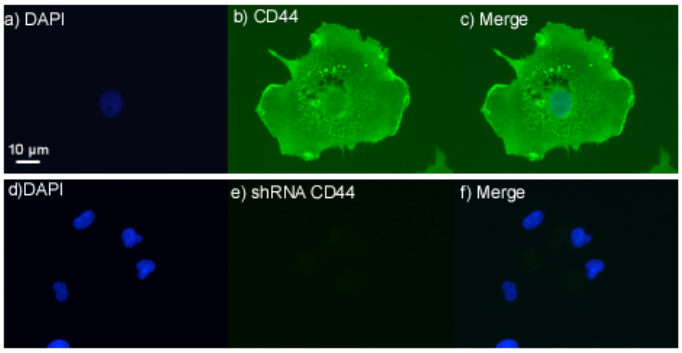
a) DAPI
b) CD44
c) Merge
10 µm
d)DAPI
e) shRNA CD44
f) Merge

D

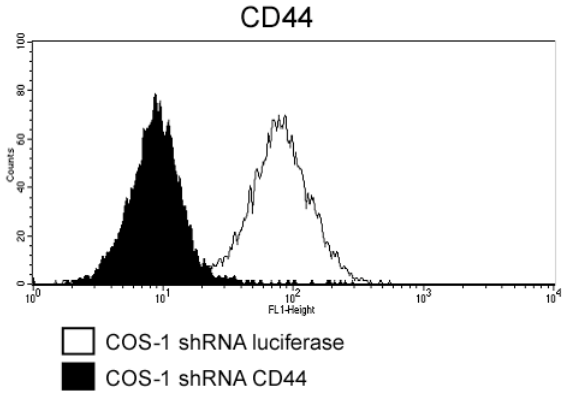
CD44
Counts
FL1-Height
COS-1 shRNA luciferase
COS-1 shRNA CD44

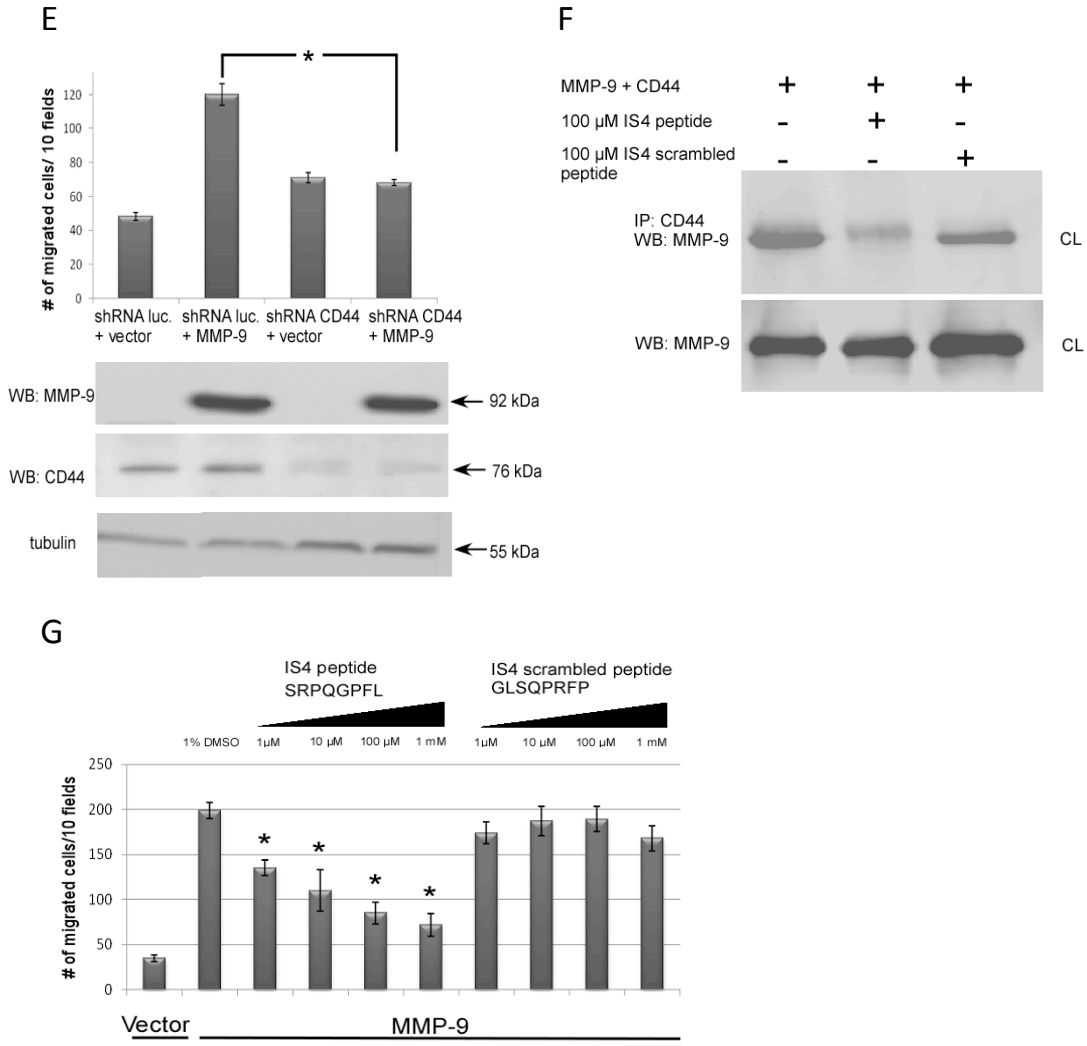
E
F
G
# of migrated cells/ 10 fields
shRNA luc. + vector
shRNA luc. + MMP-9
shRNA CD44 + vector
shRNA CD44 + MMP-9
WB: MMP-9
92 kDa
WB: CD44
76 kDa
tubulin
55 kDa
MMP-9 + CD44
100 µM IS4 peptide
100 µM IS4 scrambled peptide
IP: CD44
WB: MMP-9
CL
WB: MMP-9
CL
IS4 peptide
SRPQGPFL
IS4 scrambled peptide
GLSQPRFP
1% DMSO
1µM
10 µM
100 µM
1 mM
# of migrated cells/10 fields
Vector
MMP-9

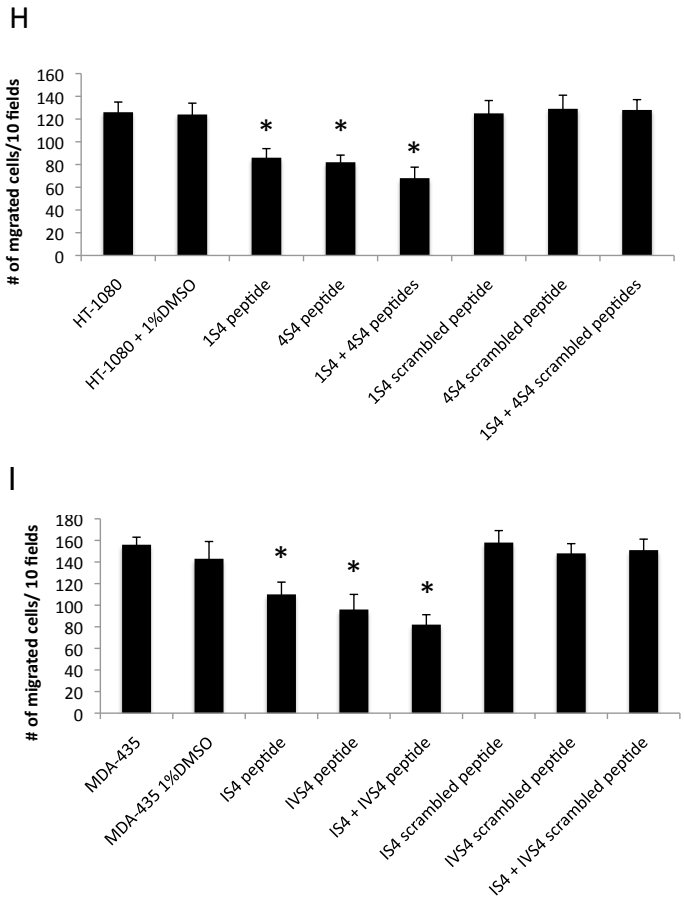

Figure 3.5. CD44 serves as a docking molecule for MMP-9 on the cell surface and facilitates MMP-9-mediated cell migration. (A) The outermost of blade I of the MMP-9 PEX domain interacts with CD44. COS-1 cells co-transfected with cDNAs as indicated were immunoprecipitated with anti-CD44 antibody followed by Western blotting using MMP-9 antibody. An aliquot of the conditioned medium was examined by Western blotting for MMP-9 to monitor expression level of MMP-9 in each transfection. (B) Silencing of CD44 in COS-1 cells using a shRNA approach. COS-1 cells were infected with retrovirus containing shRNA against CD44 and luciferase control. Total RNAs were extracted followed by a real time RT PCR analysis. The relative quantitative value of CD44 expression was normalized against housekeeping genes, HPRT1 and GAPDH. Each bar represents the mean ± S.E. (C) Silencing of CD44 in COS-1 cells by a shRNA approach. Expression of CD44 in COS-1 cells stably infected with retrovirus containing shRNA luciferase (a-c) or CD44 shRNA (d-f) was analyzed by immunofluorescence staining using anti-CD44 antibodies. Nuclei were counterstained with DAPI (blue). (D) Expression of CD44 in silenced COS-1 cells examined by flow cytometry. COS-1 cells expressing shRNAs for luciferase or CD44 were examined by flow cytometry using anti-CD44 antibody. (E) MMP-9 enhancement of cell migration is dependent on CD44. CD44 silenced

COS-1 cells were transfected with MMP-9 or vector control followed by a Transwell migration assay (upper panel). Each data point was performed in triplicate and the experiment was repeated three times (P^* < 0.05; P^{**} < 0.01). Western blotting for MMP-9, CD44 and α/β tubulin (lower panel) was performed to monitor protein expression in the transfected COS-1 cells. (F) Peptides mimicking the outermost β-strand of the blade I interfere with MMP-9 heterodimer formation (upper panel). 20 μg of total cell lysates were examined by Western blotting using anti-MMP-9 antibody to determine equal expression of MMP-9 (lower panel). **IS4** and **IS4** scrambled peptides (100 μM) were incubated with the cell lysate for 24 hours prior to a co-immunoprecipitation assay. (G) Dose-dependent inhibition (from 1 μM to 1 mM) of MMP-9-mediated cell migration by **IS4** peptides. COS-1 cells transfected with MMP-9 cDNAs or vector control were pre-incubated with 1% DMSO, **IS4** peptide (SRPQGPFL) or **IS4** scrambled peptide (GLSQPRFP) at different dose for 30 min followed by a Transwell chamber migration assay. Each data point was performed in triplicate and the experiment was repeated three times ($^*P$ < 0.05). (H) and (I) Inhibition of cell migration by MMP-9 specific peptides in human cancer cells expressing endogenous MMP-9. Human fibrosarcoma HT-1080 (H) and MDA-MB-435 (I) cells were pre-incubated with control and specific peptides (100 μM) for 30 min followed by Transwell chamber migration assay. Each data point was performed in triplicate and the experiment was repeated three times ($^*P$ < 0.05).

MMP-9-CD44-EGFR axis in cell migration

It has been reported that CD44 activates receptor tyrosine kinases (RTKs) initiating signaling for cell migration (129). To further investigate which RTKs are involved in the MMP-9-CD44 signaling pathway for cell migration, eight small molecule inhibitors (AG 1024, PD173074, PHA665752, Genistein, PP2, AG 490, AG 1296 and AG 1478) targeting different RTK pathways were employed and tested in a Transwell migration assay. Among the eight tested inhibitors, three inhibitors (AG1478, AG1024 and PD173074) significantly reduced cell migration in MMP-9 transfected COS-1 cells as compared to the DMSO control (Fig. 3.6A). The most efficient inhibitor was EGFR inhibitor (AG1478), which demonstrated a dose-dependent inhibition of cell migration (Fig. 3.6B). These data suggest that EGFR may be activated in MMP-9 transfected COS-1 cells.

To test if MMP-9-CD44 interactions result in the activation of EGFR, COS-1 and CD44-silenced COS-1 cells transfected with MMP-9 cDNA as well as vector

control were examined by Western blotting using a specific anti-phosphorylated EGFR antibody. As shown in Figure 3.6C, expression of MMP-9 in wild type COS-1 cells resulted in increased phosphorylation of EGFR as compared to vector control. This activation of EGFR did not occur in CD44-silenced COS-1 cells transfected with MMP-9 cDNA. These data are consistent with a pathway by which a complex formation between MMP-9 and CD44 leads to activation of EGFR. To further dissect the MMP-9-CD44-EGFR pathway, we examined downstream effectors of activated EGFR, including pERK, pAKT, and pFAK, which have been implicated in EGFR-induced cell migration (129). An increase of pERK1/2, pAKT, pFAK (less visibly evident) and pEGFR was observed in MMP-9 transfected COS-1 cells, but not MMP-9 transfected CD44-silenced COS-1 cells or vector control, confirming MMP-9-CD44-EGFR signaling axis in MMP-9-induced cell migration (Fig. 3.6C & 3.6D).

Taken together, this study demonstrates that MMP-9-enhanced protease-independent cell migration involves the coordination of PEX domain homodimerization and CD44 heterodimerization leading to EGFR activation.

A

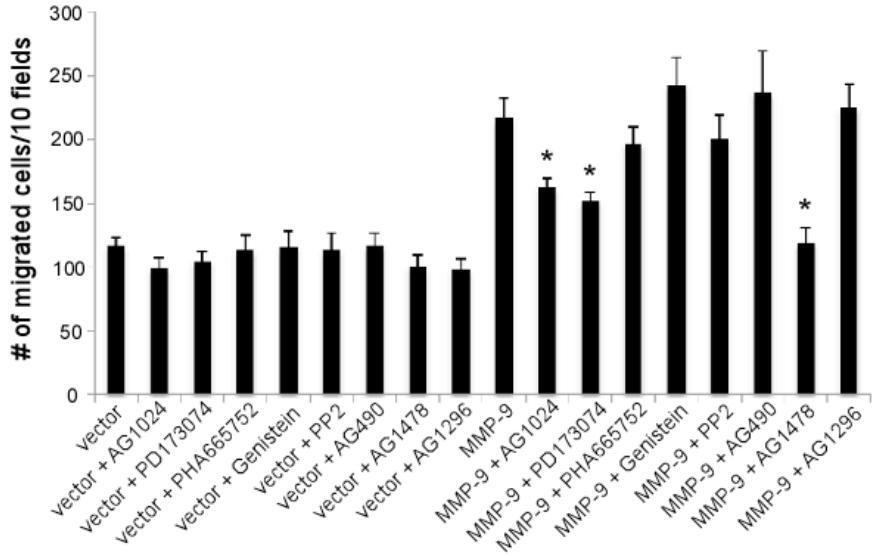
# of migrated cells/10 fields
300
250
200
150
100
50
0
vector
vector + AG1024
vector + PD173074
vector + PHA665752
vector + Genistein
vector + PP2
vector + AG490
vector + AG1478
vector + AG1296
MMP-9
MMP-9 + AG1024
MMP-9 + PD173074
MMP-9 + PHA665752
MMP-9 + Genistein
MMP-9 + PP2
MMP-9 + AG490
MMP-9 + AG1478
MMP-9 + AG1296
*
*
*

B

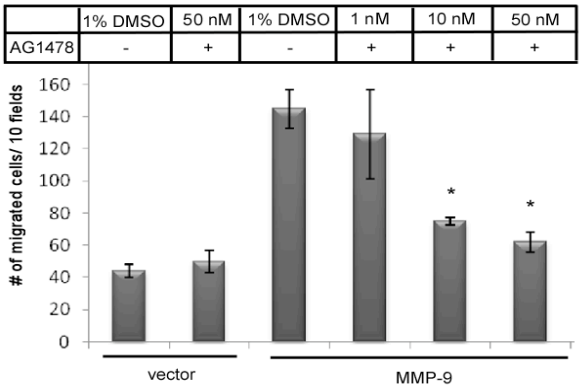
1% DMSO
50 nM
1% DMSO
1 nM
10 nM
50 nM
AG1478
-
+
-
+
+
+
# of migrated cells/ 10 fields
160
140
120
100
80
60
40
20
0
*
*
vector
MMP-9

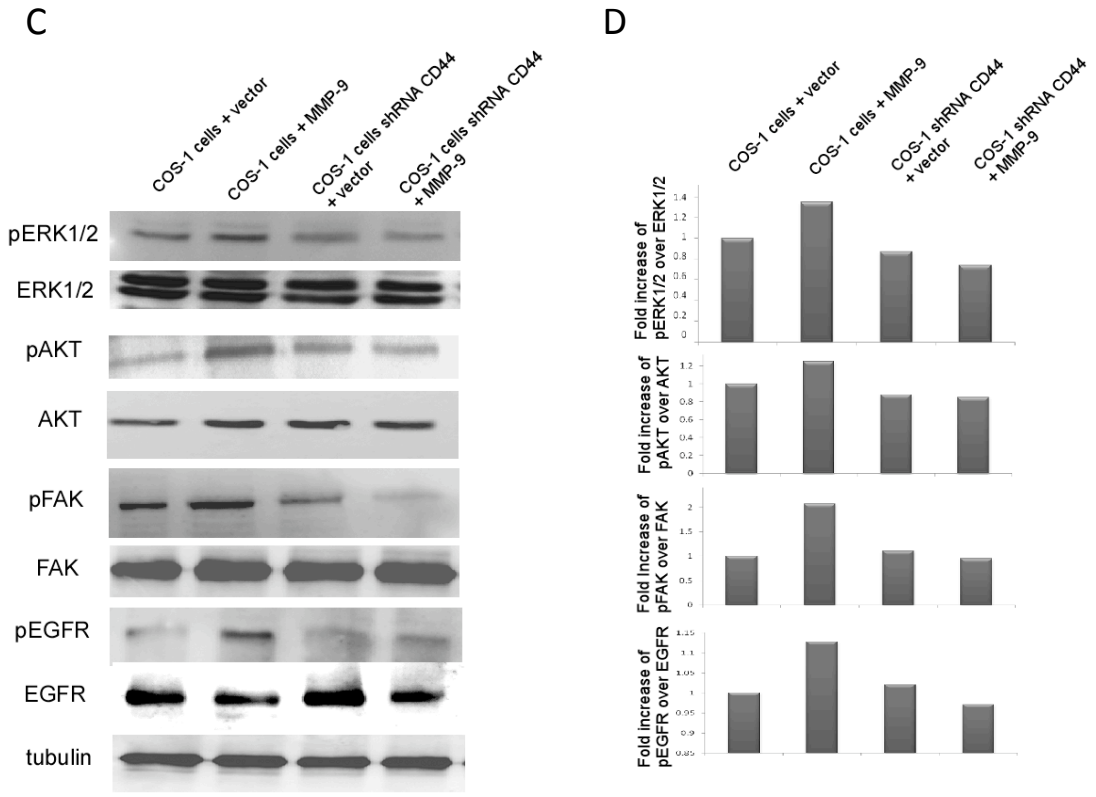

Figure 3.6. CD44 activates EGFR to regulate MMP-9 enhanced cell migration. (A) COS-1 cells transfected with vector or MMP-9 cDNAs were pre-treated with 8 different inhibitors targeting distinct receptor tyrosine kinase pathways (AG1024 (50 nM), PD173074 (50 nM), PHA665752 (50 nM), Genistein (50 μM), PP2 (10 nM), AG490 (50 nM), AG1478 (50 nM) or AG1296 (500 nM)) for 30 min followed by a Transwell migration assay. Each data point was performed in triplicate and the experiment was repeated three times (*P < 0.05). (B) Dose dependent inhibition of MMP-9-mediated cell migration using an EGFR inhibitor (AG1478). COS-1 cells transfected with vector or MMP-9 cDNAs were treated with different concentration of AG1478 for 30 min before being subjected to a Transwell migration assay. (P-values reflect comparison with MMP-9 transfected cells: $^{*}P$ < 0.05). (C) Activation of EGFR downstream effectors in COS-1 cells transfected with MMP-9 cDNAs, but not in CD44-silenced COS-1 cells. Cell lysates of transfected COS-1 cells were prepared and subjected to Western blot analysis using antibodies against pERK1/2, ERK1/2, pAKT, AKT, pFAK, FAK, pEGFR, EGFR and α/β-tubulin antibodies. (D) Densitometric analysis of the ratio of phosphorylation of pERK, pAKT, pFAK and pEGFR to corresponding pan antibodies.

3.4 Discussion

The proteolytic activity of MMP-9 has been implicated in various physiologic and pathologic conditions. Inhibition of the catalytic domain has been a long-term focus of MMP research. More recently, the PEX domain of MMPs has been demonstrated to be critical for mediating protein-protein interactions and enhancing cell migration (42, 128, 139). By swapping the MMP-9 PEX with that of MMP-2, we demonstrated the unique homo- and hetero- dimerization properties of the MMP-9 PEX domain in cell migration. Based on the mutagenesis analysis, specific peptides preventing MMP-9 dimerization have been developed and demonstrated to interfere with MMP-9-induced cell migration.

The proteolytic activity of secreted MMPs is inhibited by TIMP binding in a 1:1 ratio to the catalytic core domain. It has also been shown that the MMP-9 PEX domain binds specifically to TIMP-1, whereas the PEX domain of MMP-2 binds to TIMP-2 (41, 113). Based on a crystallography analysis, TIMP-2 forms a complex with proMMP-2 through interaction with the blade IV of the PEX domain of MMP-2 (41). A precise interaction between the proMMP-9 PEX domain and TIMP-1, however, has not been solved by crystallography. Using a biochemical approach, we herein confirm that TIMP-1 interacts with proMMP-9. This observation raises the question: can TIMP-1 competitively interfere with proMMP-9 homodimerization and hence, inhibit MMP-9 biological properties? Using a biochemical assay, it was shown that TIMP-1 interfered with MMP-9 homodimerization either competitively, caused by overlapping contact areas, or allosterically, caused by conformational changes to PEX-9 that render it incompetent for homodimerization. This interaction reduced MMP-9-mediated cell migration.

TIMP-1 has been demonstrated to form a complex in a 1:1 ratio with MMP-9 (140). Roderfeld et al. (141) reported that TIMP-1:MMP-9 forms in the Golgi

apparatus prior to secretion using a fluorescence resonance energy transfer (FRET) approach. A similar result was reported using pulse-chase analysis (111). However, given the evidence that most MMP-9 bound to the cell surface is TIMP free (142, 143) and specific peptides blocking MMP-9 dimerization inhibit MMP-9-enhanced cell migration (Fig. 3.5G, 3.5H and 3.5I), it was hypothesized that proMMP-9-TIMP-1 complexes dissociate before interacting with cell surface molecule(s), e.g. CD44. Docking of TIMP-1 free-MMP-9 monomer at the cell surface by CD44 leads to MMP-9 dimerization and cell migration. In support of this hypothesis, it has been demonstrated that cell surface-bound MMP-9 is less accessible for binding to TIMPs than soluble MMP-9, which is possibly due to the dimerization of MMP-9. A 21-fold higher IC_{50} in terms of inhibition of membrane bound MMP-9 by TIMPs as compared to soluble MMP-9 has been reported (143). Due to the limitation of current technology, direct evidence for the effect of TIMP-1 on MMP-9 dimerization and migration remains to be fully understood.

Homodimer formation of MMP-9 features functions that are not present in monomeric PEX of MMP-9, such as electrostatic potential at the physical-chemical level (10). Moreover, an extended hydrophobic surface patch, accessible to solvent in the monomeric MMP-9 PEX domain, becomes buried upon dimerization. Finally, the dimeric complex brings all domains, including the catalytic domains of the two MMP-9 monomers, within a defined distance from each other. This distance restraint is likely to influence a multitude of functions, including accessibility for proteolytic activation (111), localization to the extracellular matrix (144) and substrate recognition and processing (145).

It has been demonstrated that MMP-9 plays an important role in cell migration (14, 42, 105, 138). However, given technical limitations, the individual role of MMP-9 dimers versus monomers in cell migration has not been previously determined. By using mutagenesis and biochemical approaches, it was demonstrated that MMP-9 dimers, but not monomers, are required for full enhancement of MMP-9-mediated cell migration. Based on diminished migration

of cells transfected with MMP-9 mutants, which are unable to form dimers, it was concluded that this minor population of MMP-9 is responsible for functional activity. Furthermore, peptides interfering with MMP-9 dimerization abrogated MMP-9-enhanced cell migration in COS-1 cells transfected with MMP-9 cDNA and in cells expressing endogenous MMP-9 (HT-1080 and MDA-435), (Fig. 3.5H and 3.5I). These data further support the conclusion that dimerization of MMP-9 is required for MMP-9-enhanced cell migration.

Expression of MMP-9 in cells has been found to result in activation of MAPK and PI3K pathways; activation of these signaling molecules has been linked to the phosphorylation status of receptor tyrosine kinases (146, 147). However, it remains to be explained how MMP-9 initiates signaling transduction leading to enhanced cell migration. To pinpoint this signaling mechanism, the effect of inhibitors against different receptor tyrosine kinase pathways on MMP-9-mediated cell migration was screened. It was identified that phosphorylation of EGFR is involved in the MMP-9 signaling cascade. This observation was supported by three lines of evidence: 1) inhibition of EGFR activation by specific inhibitors abrogates MMP-9-mediated cell migration; 2) enhanced phosphorylation of EGFR in MMP-9-transfected cells was confirmed by Western blotting; and 3) downstream effectors of active EGFR, including pERK1/2, pAKT and pFAK in MMP-9 expressing cells were upregulated or phosphorylated, as examined by antibody array and immunoblotting assays.

It has been reported that CD44 and EGFR interactions promote cell migration involving activation of Akt, FAK and MMP-2 (129). In a separate report, Yu et al. (89) demonstrated that CD44 serves as a cell surface docking molecule for MMP-9. We now present data showing that MMP-9 transduces signals to activate EGFR through crosstalk with CD44 to initiate a cell migration signaling cascade. This conclusion is based on the fact that silencing of CD44 in MMP-9 expressing cells abrogated activation of EGFR. In addition, mutations of blade II, III and IV did not interfere with the binding of CD44, whereas blade I of the MMP-

9 PEX domain mediates MMP-9 and CD44 interactions, increases phosphorylation of EGFR which, in turn, activates FAK, AKT and ERK leading to cell migration. Collectively, these data suggest that homodimerization of MMP-9 is not a prerequisite for binding CD44 as evidenced by the co-immunoprecipitation between MMP-9/Blade IV (only observed as a monomeric form) and CD44 (Fig. 3.5A).

Docking of proMMP-9 at the cell surface by CD44 was reported to lead to activation of proMMP-9 in osteoclasts and results in enhanced cell migration (148). In contrast, we demonstrate that proteolytic activity of MMP-9 is not a prerequisite for MMP-9-mediated cell migration. Four lines of evidence support our previous conclusion that MMP-9-mediated COS-1 cell migration is independent of enzymatic activity (42): 1) constitutively inactive MMP-9 (MMP-9^{E-A} mutation) induced cell migration in COS-1 cells as well as wild type MMP-9; 2) synthetic MMP inhibitors did not interfere with MMP-9-mediated COS-1 cell migration; 3) TIMP-1, but not TIMP-2 abrogates MMP-9-mediated cell migration; and 4) no activated MMP-9 is detected by fluorogenic peptide assay, gelatin zymography and Western blotting in COS-1 transfected cells.

Targeting the PEX domain of MMP-9 has been our goal in recent years since most MMP inhibitors blocking enzymatic activities failed to prove useful in several clinical trials (96, 149). Three approaches have been used to target the PEX domain of MMP-9: 1) anti-functional antibody: an anti-functional antibody targeting the MMP-9 PEX domain blocked Schwann cell migration (150); 2) recombinant protein of the PEX domain of MMP-9: Ezhilarasan et al. (151) reported that excess recombinant MMP-9 PEX protein retarded endothelial cell migration; and 3) inhibitory peptides: Bjorklund et al., (152) reported that random peptides isolated from a phage display peptide library inhibit cell migration and tumor formation by targeting either the MMP-9 catalytic domain or PEX domain. These studies emphasized the importance of the PEX domain of MMP-9 in cell migration and targeting this domain is a viable approach to abrogate pathologic

cell migration. Our strategy for the development of synthetic compounds targeting the functional MMP-9 PEX domain is to identify targeting motifs within the PEX domain based on a mutagenesis approach followed by chemical synthesis. The peptides mimicking the outermost β-strand of blades I and IV of the MMP-9 PEX domain inhibited MMP-9-mediated cell migration in a dose-dependent manner. The core structure of these peptides is being evaluated by NMR spectroscopy.

In summary, we demonstrated a novel axis of MMP-9-CD44-EGFR in which MMP-9 initiates crosstalk between CD44 and EGFR, which in turn activates downstream effectors for cell migration. We further pinpoint two critical motifs in the PEX domain of MMP-9 required for cell migration. The synthetic inhibitory peptides mimicking these motifs demonstrate proof of principle that developing pharmaceutical compounds targeting these regions is a useful approach to impair cell migration during pathological processes.

Chapter 4 - Discovery of Novel Inhibitors Binding the Hemopexin domain of Matrix Metalloproteinase-9 using *In Silico* Modeling

4.1 Summary

After the failure of MMP inhibitors for the treatment of cancer in phase III clinical trials, a reevaluation of MMPs' biological roles has been undertaken. Since MMPs can display either pro-tumorigenic or anti-tumorigenic effects, and in some cases both, more specific inhibitors targeting a single MMP could potentially lead to an effective drug for clinical use. The PEX domain of MMP-9 was previously demonstrated to be critical for enhancement of cell migration. Using an *in silico* approach, a quick and simple method is presented for finding specific inhibitors of MMP exosites that can inhibit their biological roles. Utilizing DOCK6.0, a library of commercially available compounds was screened against MMP-9 hemopexin domain monomer. The hits were scored according to several parameters including cluster size, grid score (energy), van der Waals energies and electrostatic energies. Compounds with the top 5 scores were purchased and tested in a Transwell migration assay. Two of the five compounds (#3735 and #1403) inhibited MMP-9-mediated cell migration in COS-1 transfected cells and cancer cell lines expressing endogenous MMP-9: HT-1080 and MDA-MB-435. Both compounds also inhibited the invasion of the HT-1080 cells in a 3D type I collagen invasion assay. In conclusion, a quick and simple method that combined molecular docking and *in vitro* migration assays was employed to discover novel small molecules that bind to a specific domain of a protein and serve as inhibitors of cell migration.

4.2 Introduction

Several classes of compounds have been designed in order to bind and inhibit the activity of MMPs' catalytic site including peptidomimetic, tetracycline, and biphosphonate inhibitors (101, 153). These classes of inhibitors are of low specificity and target multiple MMPs due to the highly conserved active site. After the failure of broad-spectrum MMP inhibitors in clinical trials, efforts have been made to understand the biological role of each MMP. Since the catalytic site of most MMPs is highly homologous, leading to difficulty designing specific inhibitors, the PEX domain has been shown to be an alternative site to inhibit MMPs' biological roles (6, 127). Novel therapeutics targeting MMPs' exosites are currently being investigated (96, 102, 103).

Latent and active MMP-9 has been linked to many biological processes including cancer invasion, metastasis and angiogenesis, cardiovascular disease and inflammatory diseases. Active MMP-9 can remodel the ECM, impact angiogenesis and increase cell invasion. However, high levels of proMMP-9 can increase cell motility and have also been found in tissue samples of inflammatory arthritis patients (4, 14, 42, 154). The distinction between the biochemical roles of proMMP-9 and MMP-9 remains unclear. For instance, proMMP-9 has a higher affinity for type I collagen than MMP-9, whereas for type IV collagen, MMP-9 has a higher affinity (155). The ability of MMP-9 to degrade many types of collagens and laminin correlates to its ability to regulate cell migration, increase angiogenesis and affect tumor growth (14, 90, 106, 107). Importantly, several groups have also demonstrated that proMMP-9 can induce cell migration (42, 90). This enhancement of epithelial cell migration, independent of its proteolytic activity, has been linked to the PEX domain of MMP-9, which is capable of forming homodimers and heterodimers with cell surface molecules (42, 127).

In the past decade, molecular modeling has emerged as a powerful tool for drug design. Docking has emerged to be an effective *in silico* tool for drug design

in several cases (156, 157). Although there are also some obstacles with using this approach as a screening method e.g. the conformational states of compounds are poorly defined and many solvent-related terms are ignored thereby creating false positives (156-158). Nevertheless, molecular docking offers advantages such as the ability to screen out compounds that do not fit in a binding site or that have the wrong electrostatic properties (156). Thus, it allows for more selective experimental assays on a small number of compounds from a database. Docking can also be used to screen molecules for which there is no physical sample at hand and can thereby be helpful to select a particular subset of compounds. These advantages present molecular docking as a unique technique to generate novel inhibitors at a high enough frequency to compete with other screening methods. By combining a crude *in silico* screening method with a simple biological assay (i.e. migration, invasion or angiogenic *in vitro* assays), time and money can be saved to discover novel lead compounds to bind a desired domain of an enzyme. Requirements include a solved crystal structure of the target protein and a simple *in vitro* biological assay to test the efficacy of the generated hits. This chapter presents a “proof of principle” for identifying a novel binding site in the MMP-9 PEX domain for inhibition of cell migration and invasion.

4.3 Results

Screening of ZINC database using molecular docking

ZINC is a free database of commercially-available compounds for virtual screening (http://zinc.docking.org). The advantage of its use is that the compounds may be purchased for rapid testing in biological assays (159). Before screening the ZINC database, the reliability of our docking studies was assessed using two known MMP-9/inhibitor and MMP-3/inhibitor crystallographic complexes (PDB codes: 1GKC and 1HY7) (Fig. 4.1). The structures of these complexes were taken from the Brookhaven Protein Data Bank. Complexes that had been determined at a resolution of 2.3 Å or better were selected to ensure the best performance of the docking algorithms. The results obtained using our computational tools to dock the ligand back into the MMP-3 or MMP-9 active site are shown in Table 4.1. Solutions were evaluated on the basis of the RMSD from the experimental orientation (160).

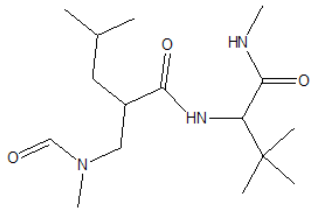

1GKC

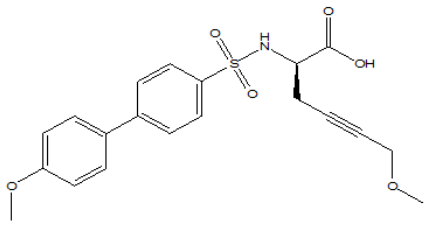

1HY7

Figure 4.1: Chemical structures of two MMP inhibitors for which the crystallographic structure of the complex formed with MMP-3 or MMP-9 have been reported.

The X-ray structure for the PEX domain of MMP-9 (PDB: 1ITV) demonstrates that MMP-9 homodimerizes through interactions of the fourth blades of its PEX domain (10). For the *in silico* analysis using DOCK6.0 (157, 161), a single monomer was utilized. Preparation of the parameters for MMP-9 PEX domain was identical to those used for the two control experiments (Fig. 4.1, Table 4.1 and 4.2). Electrostatic calculations of the PEX surfaces were performed using PYMOL (162, 163). Spheres generated from the DOCK program were superimposed onto the PEX domain (Fig. 4.2). As a "proof of principle" approach, 100 compounds from the ZINC database were randomly selected and docked against the MMP-9 PEX monomer. The following parameters were used for ranking the hits: cluster size, grid score (energy), van der Waals energies and electrostatic energies. The top five hits are displayed in Table 4.3 and their chemical structures are shown in Figure 4.3. Compound ZINC03296592 (#3735) displayed the highest number of binding possibilities to MMP-9 PEX domain (cluster size), the lowest grid score (-69.89 kcal/mole) and van der Waals (-60.94 kcal/mole) energies, as shown in Table 4.3. These top five hits were purchased for *in vitro* testing to further characterize if these compounds could be utilized as inhibitors of MMP-9-mediated cell migration.

Table 4.1: Four selected X-Ray Structures for docking experiments

PDB Code	Protein/Ligand	Rotable bonds of ligands	Resolution (Å)
1ITV	Hemopexin of MMP-9	No ligand	1.95
1GKC	MMP-9/BUM+STN	10	2.30
1HY7	MMP-3/MBS	7	1.50

Table 4.2: RMSD between computational predictions and experimentally observed binding modes for MMP-3 and MMP-9 crystallographic complexes.

PDB code	Resolution (Å)	RMSD (Å) best solution[1]	RMSD (Å) top ranked solution[2]
1GKC	2.30	1.43	1.91
1HY7	1.50	1.61	1.69

[1] Best solution as determined by X-Ray crystallography PDB files.
[2] Top solution as determined by DOCKing simulations using DOCK6.0.

Table 4.3: Ranking of the top five selected compounds from the ZINC library

Name	Cluster size	Grid score energy (-kcal/mole)	van der Waals energy (-kcal/mol)	Electrostatic energy (-kcal/mol)
ZINC03296592 (#3735)	30	69.89	60.94	8.95
ZINC03292299 (#1403)	15	60.49	51.56	8.94
ZINC03293170 (#1846)	14	55.03	48.67	6.37
ZINC03303676 (#6440)	4	55.08	51.02	4.07
ZINC03293506 (#2024)	2	47.78	44.11	3.65

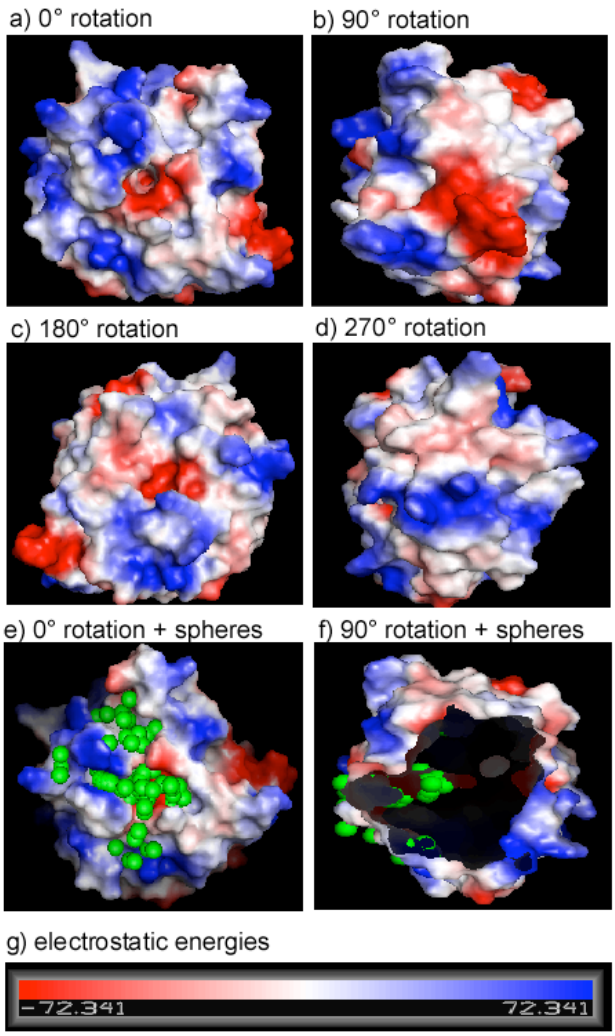

Figure 4.2: Electrostatic energy surfaces of the monomeric unit of MMP-9 generated in PYMOL (162, 163)**.** Rotations were made around the y-axis. a) 0° rotation, b) 90° rotation, c) 180° rotation, d) 270° rotation, e) 0° rotation and selected spheres using DOCK program, f) 90° rotation transparent picture and selected spheres using DOCK program. g) Legend of electrostatic energies. Red is negative electrostatic energy, white is neutral and blue is positive electrostatic energy.

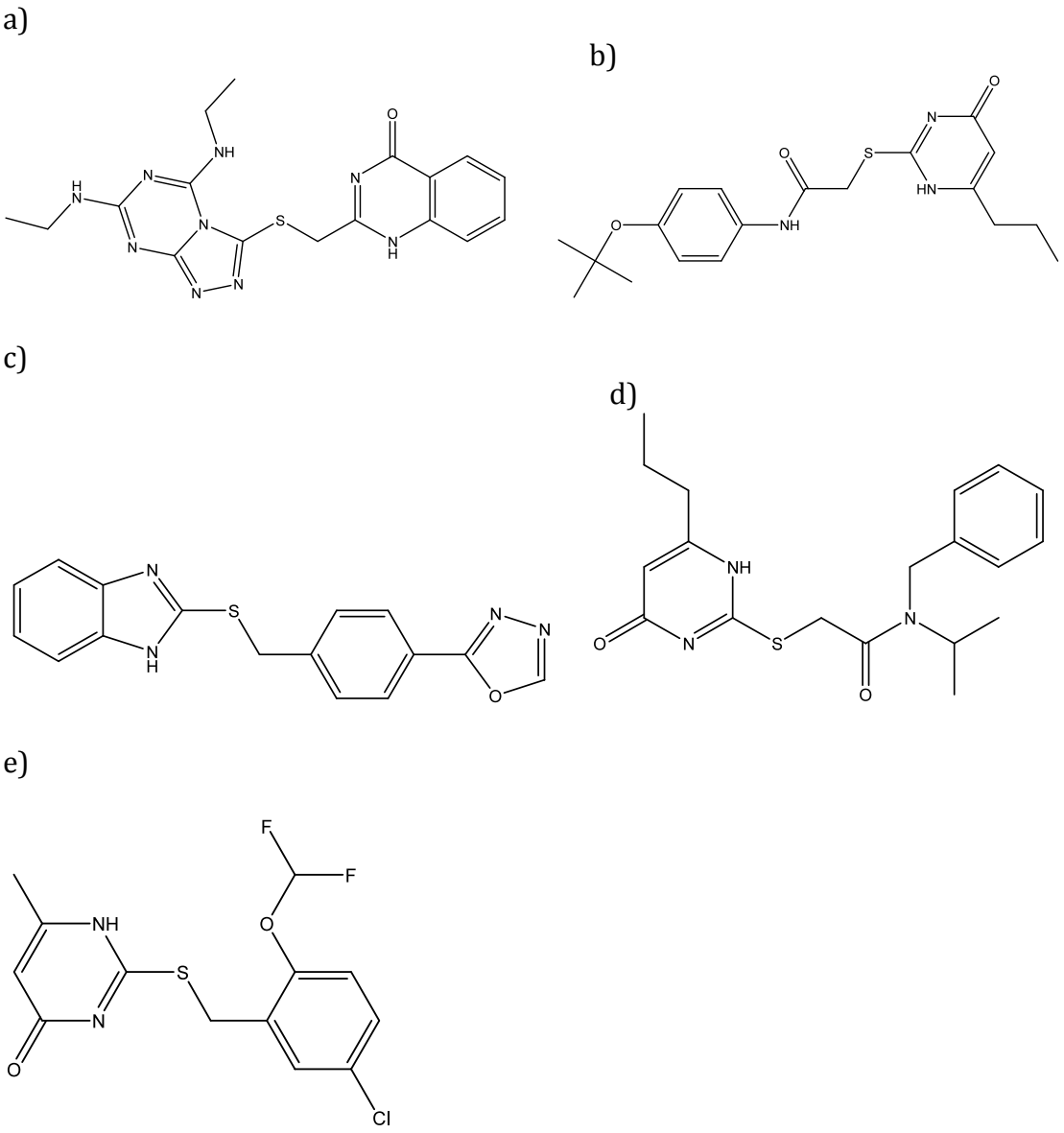

Figure 4.3: Structures of the top 5 DOCK hits. a) #3735 (ZINC03296592 = 2-[[3,5bis(ethylamino)-2,4,6,8,9-pentazabicyclo[4.3.0]nona-2,4,7,9-tetraen-7yl] sulfanyl-methyl]-1H-quinazolin4-one.) b) #1403 (ZINC03292299 N-[4-(difluoromethoxy)phenyl]-2-[(4-oxo-6-propyl-1Hpyrimidin-2-yl)sulfanyl]-acetamide c) #1846 (ZINC03293170 = 2-[[4-(1,3,4-oxadiazol-2-yl)phenyl] methylsulfanyl]-1H-benzoimidazole). d) #6440 (ZINC03303676 = N-benzyl-N-isopropyl-2-[(4-oxo-6-propyl-1H-pyrimidin-2-yl)sulfanyl]acetamide). e) #2024 (ZINC03293506 = 2-[[5-chloro-2-(difluoromethoxy)phenyl]methylsulfanyl]-6-methyl-1H-pyrimidin-4-one).

Inhibition of cell migration of MMP-9-transfected COS-1 cells by three of the five compounds

COS-1 cells were incubated with each compound (ranging from 100 nM to 100 μM) independently for 30 minutes, followed by a Transwell migration assay. Compounds #3735, #1403, #1846 and #2024 (ranked #1, #2, #3, and #5 respectively) inhibited the migration of MMP-9 transfected COS-1 cells, whereas compound #6440 did not have any inhibitory effects (Fig. 2A-E). Compound #2024 inhibited cell migration only at the highest treated dose (100 μM). Importantly, compounds #1846 and #2024 also inhibited the control cells (GFP-transfected) suggesting potential cell toxicity and/or nonspecific inhibition (Fig. 4.4 A-E).

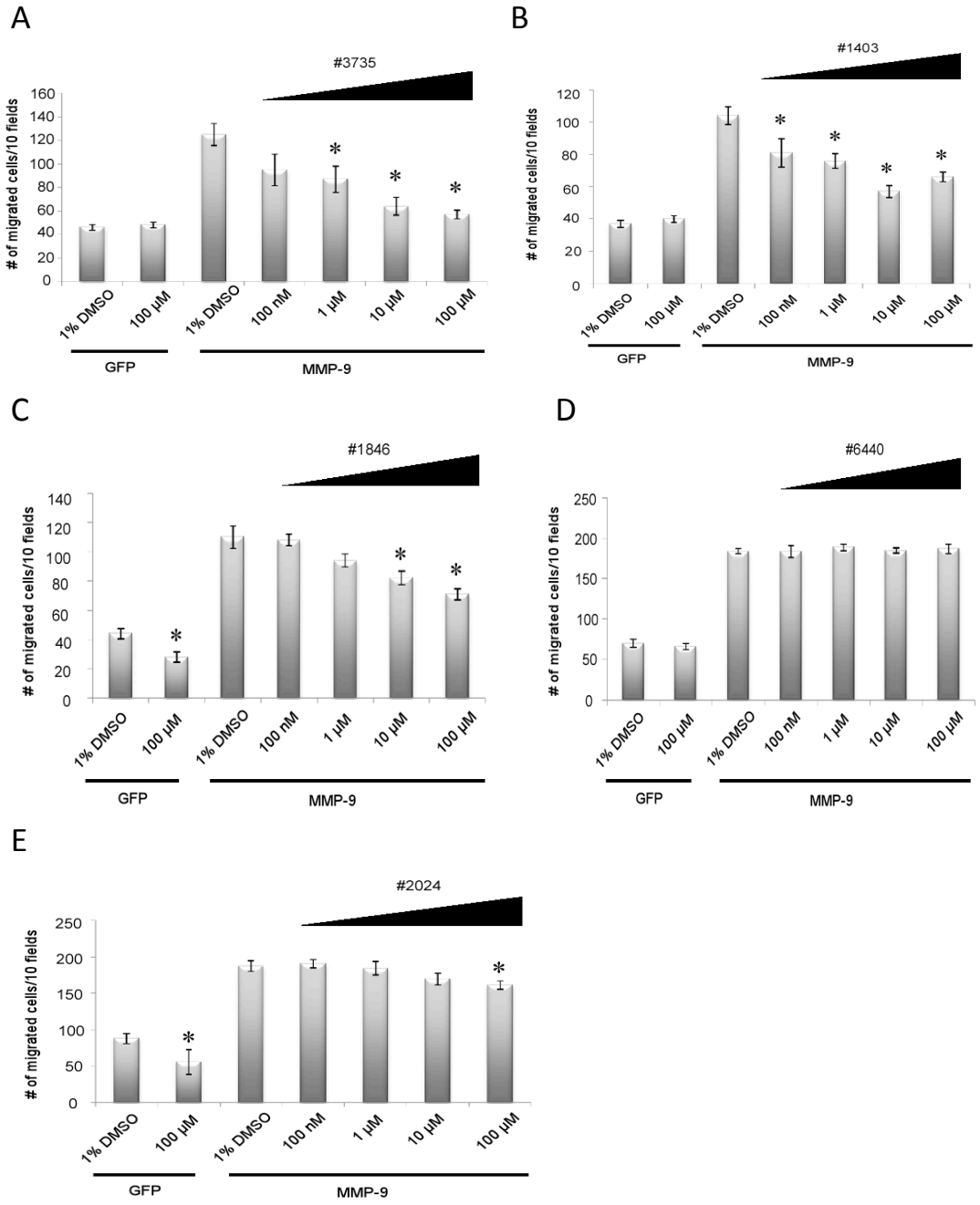

Figure 4.4: Compounds #3735 and #1403 inhibit MMP-9-mediated cell migration. COS-1 cells were transfected with a vector encoding the cDNA of GFP or MMP-9 and incubated with five compounds (#3735 (A), #1403 (B), #1846 (C), #6440 (D), # 2024 (E)) for 30 min. before being subjected to a Transwell chamber migration assay for 8 h. Each data point was performed in triplicate and the experiments were repeated three times ($^{*}P < 0.05$).

Two of the five selected compounds display cell toxicity

Since compounds #1846 and #2024 also inhibited the migration of GFP-transfected COS-1 cells, a cell viability assay was performed to verify toxicity to the cells. COS-1 cells were treated for 24 hours with a 100 μM dose of each compound and thapsigargin, an ER stress inducer that inhibits intracellular Ca^{2+} ATPases (164), was used as a positive control to trigger cell death. Compounds #3735, #1403 and #6440 did not display toxicity at 100 μM, whereas compounds #1846 and #2024 induced cell death (Fig. 4.5A). Compounds #1846 and #2024 were then discarded since they were toxic to COS-1 cells. Compound #6440 was also abandoned since it did not inhibit MMP-9-mediated cell migration (Fig. 4.4). Furthermore, a dose-dependent (ranging from 100 pm to 10 mM) cell viability assay was performed using compounds #3735 and #1403 to determine the lethal dose of these two compounds to cells (Fig. 4.5B & C). Toxicity EC_{50} was then calculated: the EC_{50} for #3735 was found to be ~300 μM (Fig. 4.5B) and ~4 mM for #1403 (Fig. 4.5C).

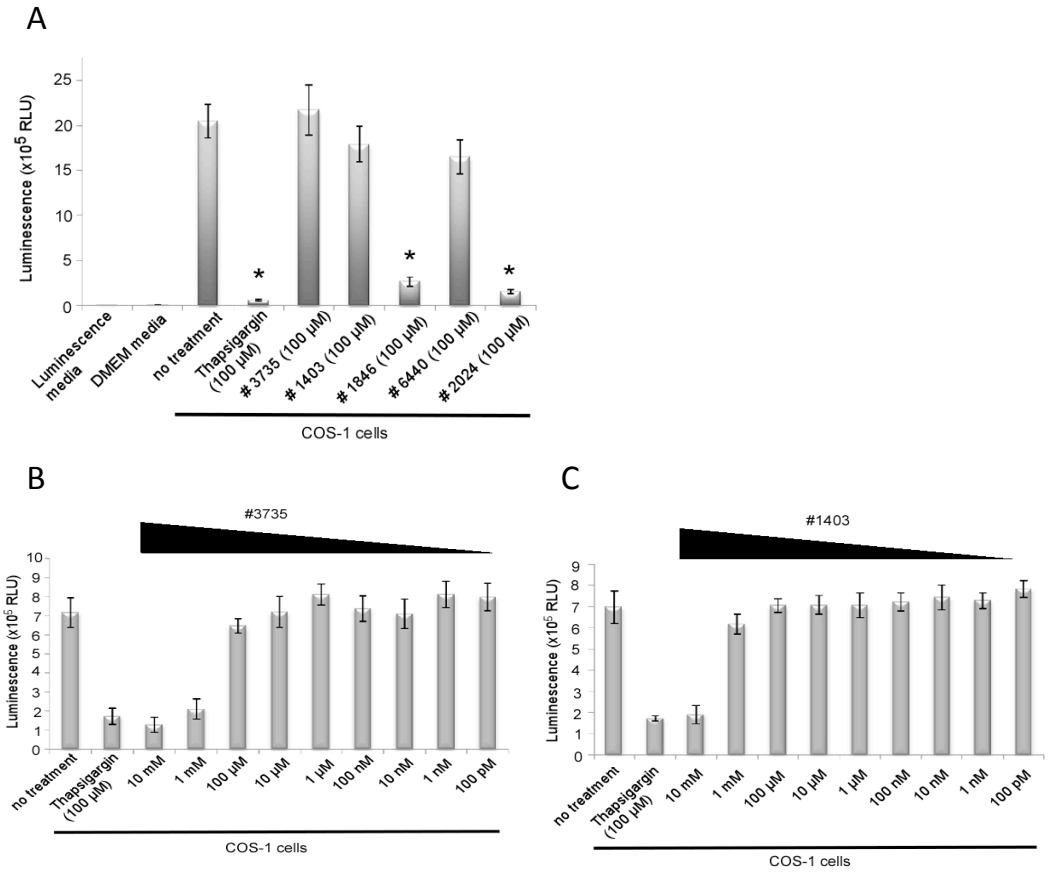

Figure 4.5: Cell toxicity of the five compounds. *A)* COS-1 cells were incubated for 24 hours with 100 µM of thapsigargin (positive control), #3735, #1403, #1846, #6440 and #2024 before being subjected to a cell toxicity assay. *B)* COS-1 cells were incubated with a dose-dependent treatment of #3735 for 24 hours before being subjected to a cell toxicity assay. *C)* COS-1 cells were incubated with a dose-dependent treatment of #1403 for 24 hours before being subjected to a cell toxicity assay.

Compounds #3735 and #1403 inhibited cell migration and invasion of HT-1080 and MDA-MB-435 cancer cell lines

Because transient transfection with a vector encoding the cDNA of MMP-9 in COS-1 cells might not represent physiological conditions, we wanted to test the efficiency of compound #3735 and #1403 in a cell line expressing endogenous levels of MMP-9. Two cancer cell lines were used: human fibrosarcoma HT-1080 and breast cancer MDA-MB-435 (137, 138). Both cell

lines were incubated with compounds #3735 and #1403 in a dose-dependent manner (ranging from 1 μM to 100 μM) for 30 minutes before a Transwell migration was assayed. Both compounds inhibited the migration of HT-1080 and MDA-MB-435 cells (Fig. 4.6A & 4.6B). To further characterize the efficiency of the two compounds, HT-1080 cells were assayed in a 3D type 1 collagen invasion model. Invasion was inhibited by both #3735 and #1403 at a dose of 100 μM (Fig. 4.6C). These data further demonstrate the biological efficacy of both compounds at inhibiting MMP-9 mediated cell migration and invasion.

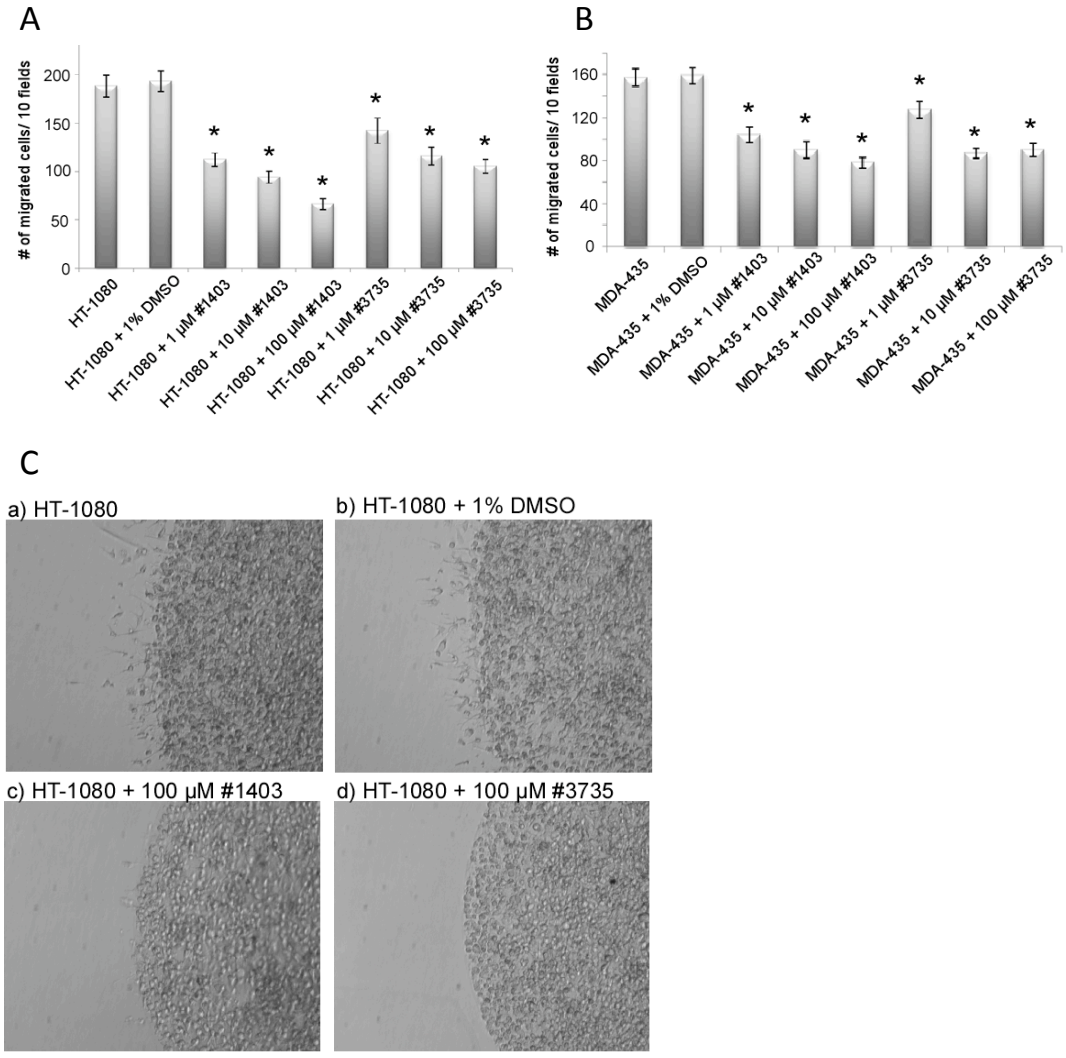

Figure 4.6: #3735 and #1403 inhibited cell migration and invasion of two human cancer cell lines. *A)* Human fibrosarcoma HT-1080 cells were incubated with 1% DMSO, #3735 or #1403 for 30 minutes followed by assay of Transwell migration. Each data point was acquired in triplicate and the experiment was repeated three times. (*$p < 0.05$) *B)* MDA-MB-435 cancer cells were incubated with 1% DMSO, #3735 or #1403 for 30 minutes followed by assay of Transwell migration. Each data point was acquired in triplicate and the experiment was repeated three times. (*$p < 0.05$) *C)* HT-1080 cells (1×10^4) were incubated with 1% DMSO, 100 µM of #3735 or 100 µM of #1403 and were dotted in a 96-well plate followed by covering with type 1 collagen (1.5 mg/ml). Invading cells at the cell-collagen interface were enumerated by microscopy after 18 hours of incubation and the images are shown.

Specificity to MMP-9, and not MMP-2 or MT1-MMP, of inhibition of cell migration

To verify that both #3735 and #1403 are specific inhibitors of MMP-9 PEX domain function, as designed by previous DOCKing studies (Fig. 4.2 and Table 4.3), inhibition of induced cell migration by other MMPs was investigated. COS-1 cells were transfected with the cDNAs of MMP-9 and two other MMPs that have been shown to impact cancer progression and metastasis by increasing cell migration: MMP-2 and MT1-MMP (11, 14). COS-1 transfected cells were incubated with #3735 or #1403 for 30 minutes before assay by Transwell migration. Both compounds inhibited the migration of MMP-9 transfected cells but not MMP-2 or MT1-MMP transfected cells (Fig. 4.7).

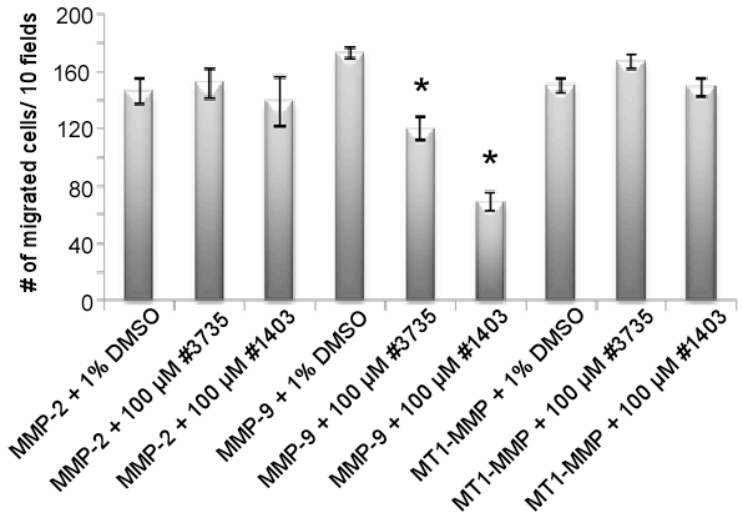

Figure 4.7: Compounds #3735 and #1403 specifically inhibit MMP-9 and not MMP-2 or MT1-MMP. COS-1 cells were transfected with MMP-2, MMP-9 or MT1-MMP and incubated with #1403 (100 µM) or #3735 (100 µM) for 30 minutes followed by assay by Transwell chamber migration. Each data point was performed in triplicate and the experiments were repeated three times ($^{*}P < 0.05$).

Biochemical Interactions of Compounds #1403 and #3735 with MMP-9

To support the DOCKing analysis, further biochemical characterization of the interactions of the two small molecules (#1403 and #3735) with the PEX domain of MMP-9 were investigated. Due to differences in their fluorescence properties, two separate approaches have been undertaken to demonstrate binding of the two compounds to MMP-9 PEX domain. 1) The change in protein fluorescence (ex 280 nm, em 290 to 450 nm) due to the 14 tryptophans of MMP-9 was monitored as a function of #1403 concentration (165, 166). The λ_{max} of tryptophan fluorescence was plotted as a function of #1403 concentration (Fig. 4.8A). Addition of buffer had no effect on the protein fluorescence but the addition of #1403 caused a 7 nm blue shift in the emission spectrum of MMP-9; no shift was detected when #1403 was added to MMP-9/PEX-2 (Fig. 4.8A). The k_D of MMP-9 binding to #1403 was calculated to be 2.1 μM ± 0.2 (Fig. 4.8B). 2) The change in fluorescence anisotropy (ex 290 nm, em 300 to 400 nm) of compound #3735 upon addition of MMP-9 was monitored in a fluorescence polarization assay (in progress) (167). Importantly, addition of compound #3735 or #1403 did not affect the ability of activated MMP-9 (with APMA) to cleave the MCA peptide (Fig. 4.8 C) (109). These date further support that both compounds did not interfere with the catalytic activity of MMP-9.

A

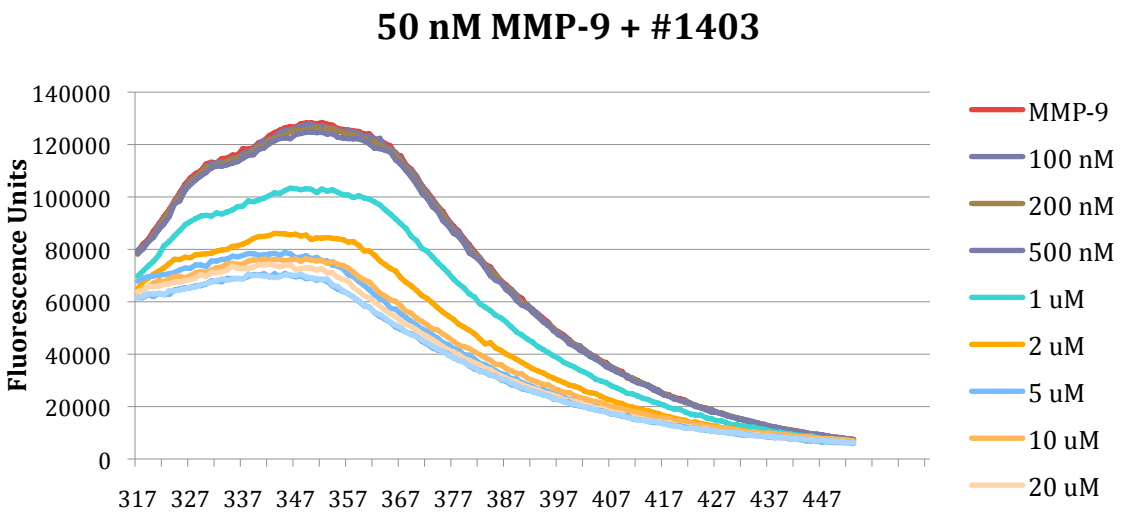
50 nM MMP-9 + #1403
Fluorescence Units
140000
120000
100000
80000
60000
40000
20000
0
317 327 337 347 357 367 377 387 397 407 417 427 437 447
MMP-9
100 nM
200 nM
500 nM
1 uM
2 uM
5 uM
10 uM
20 uM

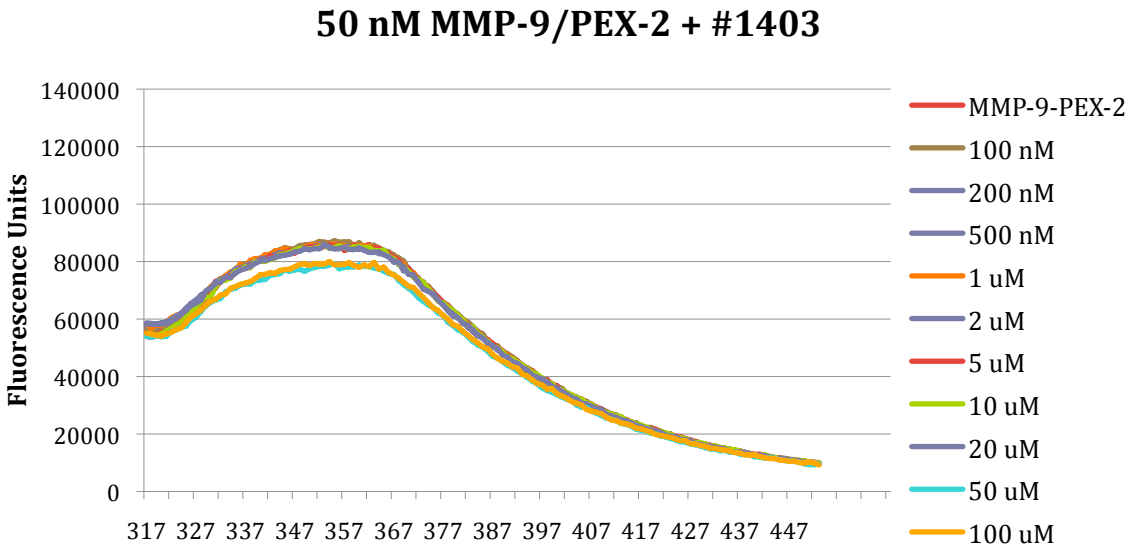
50 nM MMP-9/PEX-2 + #1403
Fluorescence Units
140000
120000
100000
80000
60000
40000
20000
0
317 327 337 347 357 367 377 387 397 407 417 427 437 447
MMP-9-PEX-2
100 nM
200 nM
500 nM
1 uM
2 uM
5 uM
10 uM
20 uM
50 uM
100 uM

B

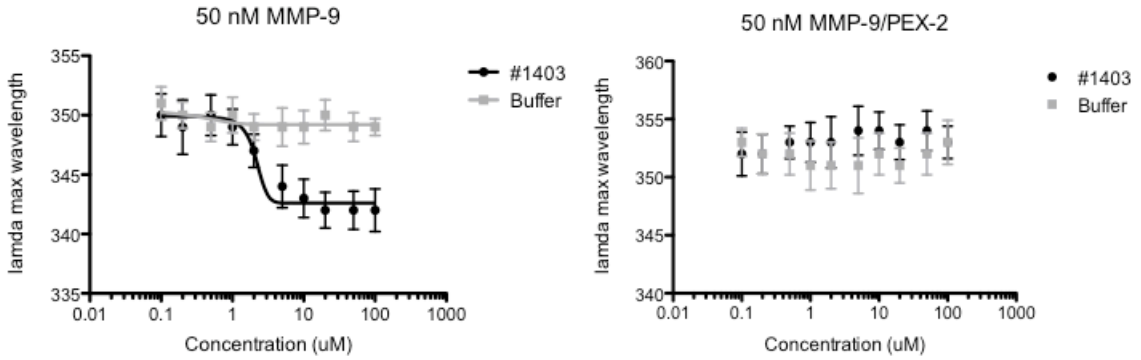

C

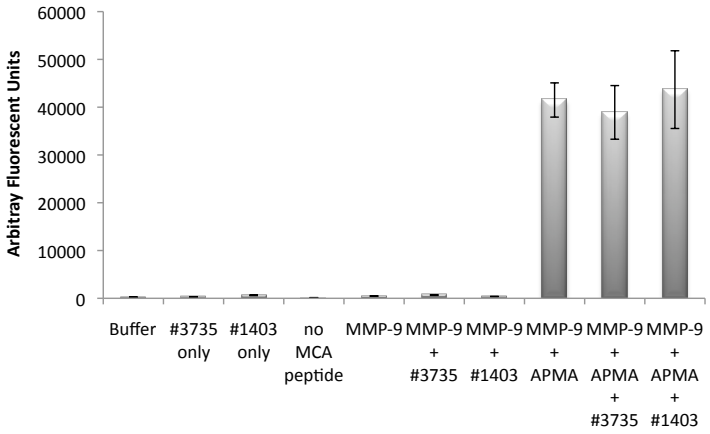

Figure 4.8 Binding of small molecule inhibitors to the PEX domain of MMP-9 *A)* The λ_{max} for tryptophan fluorescence emission of recombinant MMP-9 (50 nM, excitation 280 nm, emission 290 to 450 nm) titrated with compound #1403. The data shown are the average of 3 independent replicates and the errors are the standard error. *B)* Curve fit for the dissociation constant (K_d) between MMP-9 and compound #1403. *C)* Enzymatic activity of AMPA activated MMP9 is not affected by addition of #3735 or #1403. Fluorogenic substrate peptide was incubated with APMA- or non-APMA-treated conditioned medium and the addition of #3735 or #1403, followed by measurement of the degradation products using a fluorescent plate reader.

4.4 Discussion

After the failure of MMP inhibitors in phase III clinical trials, which was explained by lack of specificity for a single MMP, a reevaluation of MMP specificity determinants has been undertaken. Due to extensive homology between MMP catalytic domains, several drugs targeting the active site did not exclusively bind to the targeted MMP. The catalytic activity of MMPs is not required for enhancement of cell migration, suggesting an important role by other domains of this enzyme (42). Therefore, other domains were evaluated as potential inhibitor targets (48). The PEX domain, an MMP exosite, is important for mediating protein-protein interactions and therefore, affects cellular biological processes e.g. cell migration, angiogenesis and invasion (42, 128, 139, 168).

MMP-9 was selected as a drug target since it has been implicated in various pathologic conditions. The structures of its catalytic and hemopexin domains have been solved by x-ray crystallography, which allows for *in silico* drug screening (10, 163). Therefore, we investigated if the compounds that bound the MMP-9 PEX domain crystal structure in the DOCKing simulations can also impact the *in vitro* biological role of MMP-9. Validation of the MMP-9 PEX domain as a target has been explored using different approaches. 1) Anti-PEX antibody blocked Schwann cell migration (169). 2) Addition of excess recombinant PEX domain inhibited migration, an angiogenic feature of endothelial cells, as well as intracranial glioblastoma growth (170). 3) Bjorklund et al. (171) demonstrated that peptides isolated from a phage display peptide library can inhibit cell migration and tumor formation. Dufour et al. (127) designed peptides mimicking motifs in the outermost strands of the first and fourth blades of the PEX domain. These peptides inhibit the migration of MMP-9 transfected COS-1 cells, HT-1080 and MDA-MB-435 cancer cells. To date, no small molecule compounds have been developed for specifically targeting the PEX domain of MMP-9.

To find new molecules to target the MMP-9 PEX domain, an *in silico* method was utilized. DOCK was selected as a computational assay since it has been designed, by default, to handle protein-ligand interactions and suggest novel *in silico* bindings between the targeted protein and a small molecule. The efficiency of the calculated protein-ligand interactions can be distinguished and ranked by binding energies generated by DOCK. No small molecules have previously been demonstrated to interact with an MMP exosite; as a "proof of principle" approach, one hundred compounds from the ZINC database were randomly selected. The top five compounds, classified upon cluster size, grid score (energy), van der Waals energies and electrostatic energies, were purchased. Four of the five compounds inhibited *in vitro* cell migration of MMP-9 transfected COS-1 cells. Compound #6440 did not inhibit MMP-9-enhanced cell migration but the reason is not yet known. Compounds #1846 and #2024 had an inhibitory effect on cell motility. However, they also inhibited the migration of control cells (GFP-transfected), most likely due to cell toxicity as demonstrated in the cell viability experiments (Fig. 4.4C, 4.4E and 4.5A). These three compounds were then excluded. The toxicity EC_{50} of the remaining two compounds was calculated (~300 μM for #3735 (Fig. 4.5B) and ~4 mM for #1403 (Fig. 4.5C)); both EC_{50}'s were 3-fold higher and 40-fold higher, respectively, than the highest inhibitory dose utilized in the Transwell cell migration assay. Compounds #1403 and #3735 were selected for a more thorough analysis.

Since overexpression of MMP-9 in COS-1 cells might not represent the physiological state of tumor cells, two additional cell lines were studied, the HT-1080 human fibrosarcoma and MDA-MB-435 breast cancer cell lines which naturally express MMP-9. Both small molecules inhibited cell migration (Fig 4.6A and 4.6B) and cell invasion in a 3D type I collagen invasion assay (Fig 4.6C). HT-1080 cells also express several MMPs including MMP-2 and MT1-MMP, which have been demonstrated to enhance cell migration and invasion (11, 14). To test the specificity of our small molecules, COS-1 transfected cells with the cDNAs of MMP-2, MMP-9 and MT1-MMP were treated with #1403 and #3735. Importantly,

only MMP-9 transfected COS-1 cells were inhibited by the small molecules but not MMP-2 nor MT1-MMP (Fig. 4.7). Furthermore, compound #1403 was demonstrated to specifically bind to MMP-9 (K_D 2.1 μM ± 0.2).

MMP-9 has been demonstrated to enhance cell migration through an EGFR-CD44 signaling pathway with other downstream effectors including the phosphorylation of FAK, AKT and ERK (127). The exact mechanism of MMP-9-mediated cell migration inhibition by compounds #3735 and #1403 remains to be investigated; whether or not these two small molecules can decrease the phosphorylation of EGFR, FAK, AKT or ERK need to be determined. Compounds #3735 and #1403 were demonstrated to be active in other biological screens (Table 4.4); no correlations have been previously established between the activity of compounds #3735 or #1403 and cell migration.

Table 4.4: Active Hits in Tested Bioassays as indicated in pubchem.

Compound #3735	Assay	Protein target
	Cell signaling CRE-BLA (Fsk stim)	Not specified
	Confirmatory screen of Pyruvate Kinase	pyruvate kinase [Geobacillus stearothermophilus]
	Primary screen of primary cell-based high-throughput screening to identify agonists of the sphingosine 1-phosphate receptor 2 (S1P2)	endothelial differentiation, sphingolipid G-protein-coupled receptor, 5 [Homo sapiens]
	Primary screen of allosteric modulators of D1 receptors	Not specified
	Secondary screen of allosteric modulators of D1 receptors	Not specified
	Confirmation screen of allosteric modulators of D1 receptors	Not specified
	Primary screen of primary cell based high throughput screening assay for antagonists of the 5-Hydroxytryptamine Receptor Subtype 1E (5HT1E)	5- hydroxytryptamine receptor 1E (5-HT-1E) (Serotonin receptor 1E) (5-HT1E) (S31)

Compound #1403	Assay	Protein target
	Primary screen of high content assay for compounds that inhibit the assembly of the perinucleolar compartment	polypyrimidine tract-binding protein 1 isoform a [Homo sapiens]
	Profiling compound fluorescence on GSH beads with 488 nm excitation and 530 nm emission	Not specified

MMP-9 PEX domain is a disc-like shaped structure composed mostly of hydrophobic surfaces making this domain difficult to target with drugs (10, 48). One way to circumvent this issue was the design of inhibitory peptides mimicking the outer blades of the PEX domain (127). Our *in sillico* results indicate that the inside space within the MMP-9 PEX domain can be targeted by small molecules

(Fig. 4.9). When examining the structural components of the three highest-ranked compounds, all three displayed a six-membered ring docked within the space of the four blades of the PEX domain (Fig. 4.9). Hydrophobic groups preferentially bind to the inside space of the MMP-9 PEX domain's blades while hydrophilic groups (i.e. ethylamide group of compound #3735) bind to the outside of the middle pocket located in the blades' middle part (Fig. 4.9). It was observed that hydrophobic groups binding in the middle of the PEX domain blades and hydrophilic groups binding to the outside increased the binding affinity of the small molecules. To increase the IC_{50} of compounds #1403 and #3735, structure-activity relationship (SAR) studies will follow. The newly synthesized compounds will then be tested in a Transwell migration assay and a 3D type I collagen invasion assay to determine their *in vitro* efficiency.

In conclusion, these data demonstrate that the MMP-9 PEX domain is a targetable exosite. DOCKing was demonstrated to be a valid approach to discover novel drugs to inhibit cell migration and invasion caused by MMP-9.

A #3735

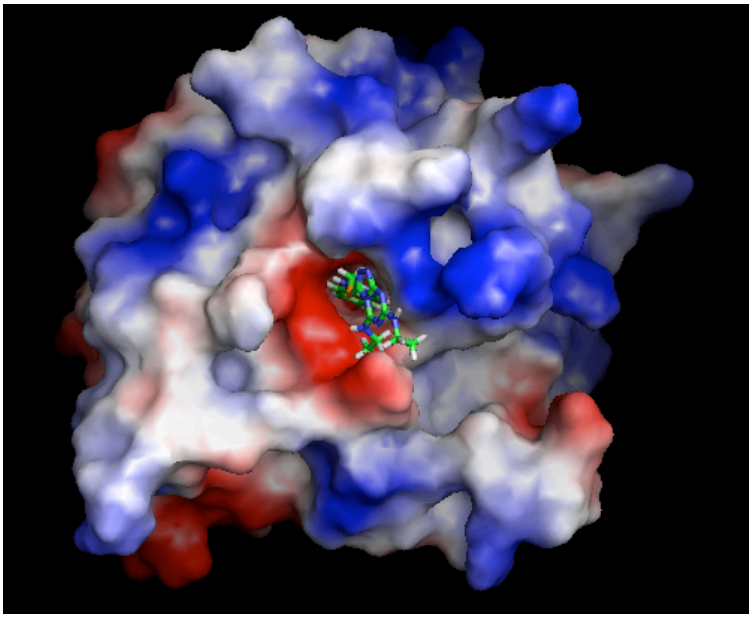

B #3735

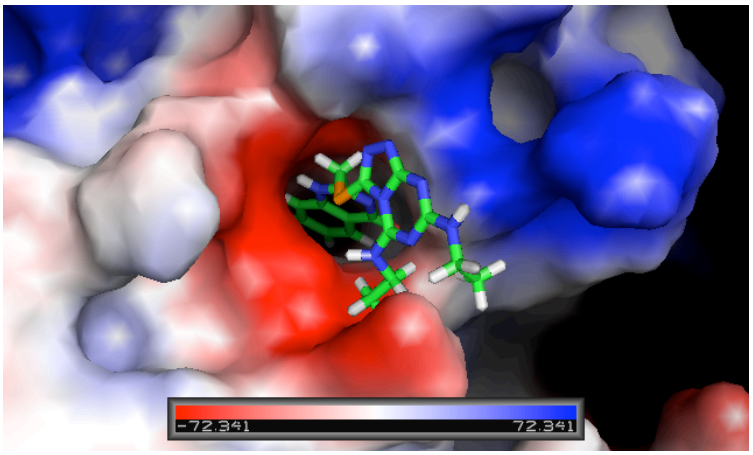

C #1403

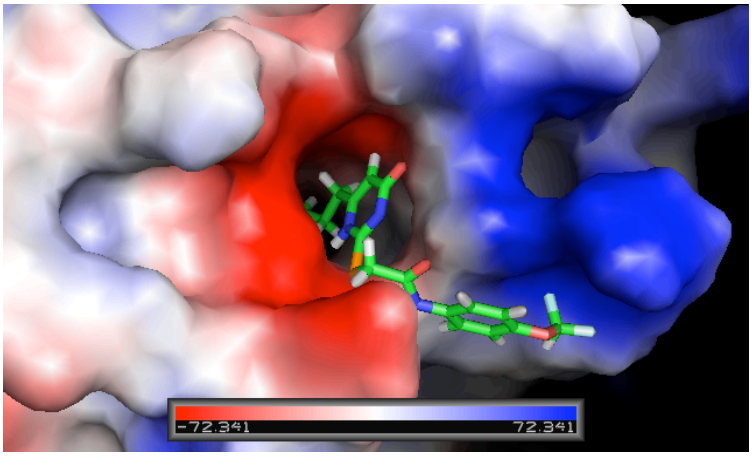

Figure 4.9: Electrostatic surfaces of MMP-9 PEX monomer generated by PYMOL. Atom colors: hydrogen (white), carbon (green), oxygen (red), nitrogen (blue), sulfur (orange). *A)* Compound #3735 docked to MMP-9 PEX domain monomer. *B)* Close up of compound #3735 docked to MMP-9 PEX domain monomer. *C)* Close up of compound #1403 docked to MMP-9 PEX domain monomer.

Chapter 5 – Future Perspectives

The MMP research in the past decade has mainly focused on unraveling the specific roles of each of the 24 known MMPs. After the failure of MMP inhibitors in clinical trials, several new approaches were undertaken to design effective drugs to treat diseases implicated by MMPs. The importance of the PEX domain in substrate binding specificity and biological processes highlights this domain as an important drug target. My work has focused on demonstrating that an MMP exosite, the PEX domain, is a reasonable target to alter the function of MMP-9 in cell migration and invasion. Three areas need to be further investigated before these peptides and compounds can reach clinical studies.

1- The two peptides and small molecules will be tested in *in vivo* models (e.g. nude mice, chick chorioallantoic membrane (CAM) assay) to further verify their stability and efficiency.

2- Structure activity relationship (SAR) studies will be undertaken for compounds #3735 and #1403 to lower their IC_{50}. Sequences of the two peptides (**IS4** and **IVS4**) bound to MMP-9 solved by X-Ray crystallography will be analyzed to determine what amino acids are critical for inhibition of cell migration and invasion.

3- A more complete understanding of the mechanism that causes proMMP-9 to enhance epithelial cell migration needs to be investigated to determine what are the mechanistic modes of action of the peptides and small molecules.

Potentially, the PEX domain of other MMPs could also be targeted with specific peptides and small molecules. This approach presents an alternative method to overcome the multiple specificity problems encountered in past clinical trials.

Chapter 6 - Experimental Methods

Reagents- Oligo primers were purchased from Operon (Huntsville, AL). The pcDNA3.1-myc and pSG5 expression vectors were described previously (135). Recombinant proMMP-1, -2, -3, -9, -11, -28 and TIMP-1 were produced by COS-1 cell transfected with corresponding proMMP and TIMP-1 cDNAs as previously described (135). Recombinant proMMP-1, 2, -3, -9, -11/myc, -28/myc and TIMP-1 were produced by COS-1 cell transfected with corresponding proMMP and TIMP-1 cDNA as previously described (135). Anti-human MMP-2 (hemopexin domain) monoclonal antibodies were purchased from Oncogene Research Products (Cambridge, MA). Anti-Myc, anti-HA antibodies were purchased from Roche (Indianapolis, IN). MMP-9 antibodies were described previously (135, 172). Anti-tubulin, anti-AKT, anti-pAKT, anti-ERK, anti-pERK, anti-EGFR, anti-pEGFR were purchased from Cell Signaling Technology (Davers, MA). Anti-FAK and anti-pFAK antibodies were purchased from BIoSource (Camarillo, CA). Anti-TIMP-1 and anti-TIMP-2 antibodies were purchased from Calbiochem (Cambridge, MA). Anti-CD44 antibodies were purchased from Novus Biologicals (Littleton, CO). PD89059 (ERK), LY294002 (PI3K), Y27632 (ROCK), H89 (protein kinase A), wortmannin (PI3K), SP600125 (JNK) were purchased from Sigma chemicals (St. Louis, MO). Genistein, PP2 (SRC), AG490 (JAK-2), AG1296 (PDGFR), AG1478 (EGFR) were purchased from Calbiochem (Cambridge, MA). AG1024 (IGFR), PD173074 (FGFR and VEGFR) and PHA665752 (c-MET) were purchased from EMD chemicals (Gibbstown, NJ). Peptides were synthesized from EZbiolab (Carmel, IN) and purity was verified by HPLC. MMP-9 was purified from transfected cell condition media by gelatin-Sepharose chromatography.

Cell Culture and Transfection- COS-1 monkey epithelial, human fibrosarcoma HT-1080, breast cancer MCF-7 and breast cancer MDA-MB-435 cell lines were

purchased from ATCC (Manassas, VA) and were maintained in Dulbecco's modified Eagle's medium (Invitrogen). Transfection of plasmid DNA (human) into cells was achieved using polyethylenimie (Polysciences) or Transfectin^{TM} reagent (Bio-Rad, CA) and the transfected cells were incubated for 48 h at 37 °C followed by biochemical and biological assays. Peptides and inhibitors were incubated with cells for 24 hours prior to coimmunoprecipitation and Transwell migration assays.

Construction of Plasmids- MMP-9ΔPEX lacking the C-terminal hemopexin domain of MMP-9 was generated by introducing a stop codon after Asp513 based on a PCR strategy using the primer sets: forward primer, #1315: 5'-3': CGGAATTCCGCCACCATGAGCCTCTGGCAGCCCCT and reverse primer, #1342 AAAAAGCTTTTAGTCCACCGGACTCAAAGGCAC. The primers were designed with an *EcoRI* site at the 5' and a *HindIII* site at the 3' end. The PCR products were digested with *EcoRI* and *HindIII* enzymes (Roche, IN). The PCR fragments were then ligated into pcDNA3.1(-)/Myc-His C vector (Invitrogen, CA). Correct sequences were verified by DNA sequencing.

MMP-9/MMP-1_{PEX} denotes a substitution mutation produced by replacing the PEX domain of MMP-9 with that of MMP-1. It was incorporated using a modified two-step PCR technique previously described (110). In brief, MMP-9 signal peptide/propeptide/ catalytic/hinge domains (fragment A) (primer sets: forward primer #1315 and #1316, 5'-3': TAGCTTACTGTCACACGCTTTGTCCACC GGACTCAAAGGCAC), MMP-1 PEX domain (fragment B) (primer sets: forward primer #1317, 5'-3': AAAGCAT GTGACAGTAAGCTA, and reverse primer #1318, 5'-3': CCCAAGCTTATTTTTCCTGCAGTTGAACCA) were first amplified by PCR separately using similar conditions as described above for MMP-9ΔPEX. Using resultant PCR products as templates (fragment A and B), the signal/propeptide/catalytic/hinge region of MMP-9 were then fused together with MMP-1 PEX domain by PCR using forward primer #1315 and reverse primer #1318. The PCR fragments were then ligated into pcDNA3.1(-)/Myc-His C vector

(Invitrogen, CA). Correct sequences were verified by DNA sequencing.

MMP-9ΔOG refers to MMP-9 without the O-glycosylated site. PCR was performed using synthetic oligonucleotide primers (Operon, AL) complementary to the MMP-9 gene without including its OG domain. The construct was done using site directed mutagenesis. A pair of primers was designed based on product instructions. The primer sequences were primer sets: forward primer #1357: 5'-3': ATCCGGCACCTCTATGGTGATGCCTGCAACGTGAAC and reverse primer #1358, 5'-3': ACCATAGAGGTGCCGGAT. The restriction enzymes used was *DpnI,* the PCR fragments were then ligated into pcDNA3.1(-)/Myc-His vector (Invitrogen, CA). Correct sequences were verified by DNA sequencing.

MMP-9E^{230}→A refers to a mutation of the glutamic acid at position 230 for an alanine in MMP-9 wild type. PCR was performed using synthetic oligonucleotide primers (Operon, AL) complementary to the MMP-9 gene. The construct was done using site directed mutagenesis. A pair of primers was designed based on product instructions. The primer sequences were primer sets: forward primer #2523: 5'-3':GACGATGACGCGTTGTGGTCC and reverse primer #2524, 5'-3':GGACCACAACGCGTCATCGTC. The restriction enzymes used was *DpnI,* the PCR fragments were then ligated into pcDNA3.1(-)/Myc-His vector (Invitrogen, CA). Correct sequences were verified by DNA sequencing.

MMP-9 with a carboxy-terminal Myc tag (MMP-9/Myc) was generated by using the pcDNA3.1 expression vector (Invitrogen). The MMP-9 cDNA containing the open reading frame of MMP-9 was amplified by a PCR approach using the primers sets: forward primer, #1315:5'-3': CGGAATTCCGCCAACATGAG CCTCTGGCAGCCCCT and reverse primer, #2507: 5'-3' GGAAGATCTC TAGTCCTCAGGGCACTGCAGGATGTC. The resultant PCR fragment was then cloned into the pcDNA3.1 vector to generate MMP-9/Myc chimeric cDNA.

To generate HA (human influenza hemagglutinin)-tagged MMP-9 chimeric cDNA, the HA tag was placed between the propeptide and catalytic domains of MMP-9 by a site-directed mutagenesis approach (Quick Change Site Directed Mutagenesis kit, Stratagene) using wild type MMP-9 as a template with mutagenesis primers containing HA sequence (forward primer, #2512: 5'-3': GGGGTCCCAGACCTGGGCAGATACCCCTACGACGTGCCCGACTCGCCTCC AAACCTTTGAGGGCGAC and reverse primer, #2513: 5'-3':GTCGCCCTCAAA GGTTTGGAAGGCGTAGTCGGGCACGTCGTAGGGGTATCTGCCCAGGTCTG GGACCCC) .

To determine the role of the PEX domain of MMP-9, a substitution mutation was engineered by replacing the PEX domain of MMP-9 with that of MMP-2. A modified two-step PCR was employed as previously described (110). In brief, MMP-9 signal peptide/ propeptide/ catalytic/ hinge domains (fragment A) (primer sets: forward primer #1315 and reverse primer #2534, 5'-3': TACAATGTC CTGTTTGCAGATCTCGTCCACCGGACTCAAAGGCAC), and MMP-2 PEX domain (fragment B) (primer sets: forward primer #2535, 5'-3': GAGA TCTGCAAACAGGACATTGTATTTGAT, and reverse primer #1356, 5'-3': CCCAAGCTTCTA GCAGCCTAGCCAGTCGGATTT) were first amplified by PCR respectively. Using the resultant PCR products as templates (fragment A and B), the signal/propeptide/catalytic/hinge region of MMP-9 were then fused together with MMP-2 PEX domain by PCR using forward primer #1315 and reverse primer #1356. The resultant PCR fragments were then inserted into the pcDNA3.1 vector (invitrogen) to generate MMP9/PEX_{MMP2}/Myc chimeric cDNAs.

Similarly, we generated substitution mutations of MMP-9/Blade I, II, III and IV by replacing the outermost β-strand of each blade with the corresponding sequence of MMP-2. Primers used to generate these chimeric cDNAs were designed as follow: 1) MMP-9/Blade I, fragment A: #1315, and #2557 (5'-3': GGGAGCCGGCCGGGGCCCCTGC TGATCGCCGAC); and fragment B: #2558 (5'-3': GTCGGCGATCAGCAGGGGCCCCGGCCGGCTCCC) and #2507; 2)

MMP-9/Blade II, Fragment A: #1315, and #2596 (5'-3': GTGTACACAGGCGC GACCTTGGAGCGAGGGTACCCCAAGCCACTGGACAAGCTGGGC); and fragment B: #2597 (5'-3':CACATGTGTCCGCGCTGGAACCTCGCTCCCATGG GGTTCGGTGACCTGTTCGACCCG), and #2507; 3) MMP-9/Blade III, fragment A: #1315, and #2540 (5'-3': GTTCGACGTGAAGGCGAAGAAAATGGATC CTGGCTTCCCCAAGCTCGTGGACCGGATGTTCC); and fragment B: #2541 (5'-3':GGAACATCCGGTCCACGAGCTTGGGGAAGCCAGGATCCATTTTCTTC GCCTTCACGTCGAAC), and #2507; and 4) MMP-9/Blade IV: fragment A: #1315, and #2538 (5'-3': GTTCCCGGAGTGAGTTGAAGAGCGTGAAGTTTGG AAGCGTGACCTATGACATCCTG); and fragment B: #2539 (5'-3': CAGGATGTCATAGGTCACGCTTCCAAACTTCACGCTCTTCAACTCACTCCGG GAAC), and #2507. All the constructs were confirmed by DNA sequencing.

Construction of Short Hairpin RNA Vectors and Retroviral Infection- Small interfering oligonucleotides specific for human and monkey CD44 and control luciferase to express short hairpin RNA were designed using a Worldwide Web-based online software system (Block-iT RNAi Designer, Invitrogen) for mammalian RNA interference. Two specific 21-nucleotide sequences spanning positions 173-193 (CD44shRNA-1) and 678-698 (CD44-shRNA-2) of the human CD44 gene (Gen-Bank accession number L05424) were synthesized. The sense and antisense template oligonucleotides encoding a hairpin structure were annealed and cloned into the RNAi-Ready pSIREN-Retro Q vector (Clontech). As a control, a luciferase protein from firefly Pyrocoelia pectoralis as a target gene was employed as previously reported (173). A retroviral supernatant was obtained by co-transfection of a vector encoding the envelope gene (pAmphotropic) and a retroviral expression vector containing the CD44 shRNA, or luciferase shRNA control into human embryonic kidney GP2–293 packaging cells (Clontech) according to the manufacturer's protocol. COS-1 cells were infected with the supernatant containing retrovirus, and the cells were then selected with 4 μg/ml puromycin for 1–2 weeks. The effects of shRNA on gene expression were evaluated by real time RT-PCR using RNA of pooled resistant

cells. The most effective stable CD44 knockdown cell lines were selected.

Immunofluorescence- Cultured cells were fixed with 4% paraformaldehyde (PFA)/phosphate-buffered saline (PBS) followed by blocking with 3% bovine serum albumin (BSA)/PBS. CD44 was detected with anti-CD44 antibody (Novus Biologicals, CO) followed by secondary antibodies conjugated with Alexa 568 (Invitrogen). Nuclei were counterstained with DAPI (Invitrogen).

Flow Cytometry- 1x 10^6 cells/ml cells suspended in Dulbecco's modified Eagle's medium containing 2% BSA were incubated with CD44 primary monoclonal antibody for 60 min at 4 ºC followed by incubation with anti-mouse FITC labeled (1:1000) secondary antibody for 60 min at 4 ºC. After extensively washing, the cells were stained with propidium iodide (PI) to determine viability of the cells. CD44 expression was measured using a FACS Calibur flow cytometer (Becton Dickinson, San Jose, CA).

Co-Immunoprecipitation- Twenty-four hours following transfection, the conditioned medium in the absence of serum was collected from the transfected COS-1 cells. The cells were then lysed in lysis buffer containing 150 mM NaCl, 25 mM HEPES (pH 7.4), 1% CHAPS, and protease inhibitors Cocktail (Sigma, St Louis, Missouri). Both the conditioned media and the cell lysates were incubated with specific antibodies for 24 hour at 4°C. Antigen-antibody complexes were precipitated with protein A agarose beads followed by brief centrifugation, washing, and then electrophoresis in a 10% SDS-polyacrylamide gel. Western blotting was then followed using a corresponding antibody.

Preparation of Plasma Membrane-enriched Cell Fractions- Cell membranes were prepared from MMP-9 transfected COS-1 cells following nitrogen cavitation as described previously (174). The post-nuclear supernatant (770 x g for 10 min.) was collected, and heavy organelles were removed by centrifugation at 6,000 x g

for 15 min. This supernatant was centrifuged at 100,000 x g for 1 h at 4 °C to recover the plasma membrane enriched lighter cell organelles in the pellet.

Phagokinetic Cell Migration Assay- The basic procedure was described earlier (175). In brief, coverslips treated with poly-L-lysine (50 µg/ml) were coated with 0.5% BSA followed by airdrying. The coverslips, placed in 12 well plates, were incubated with freshly made colloidal gold particles for 1 h followed by washing with PBS. Cells (1 x 10^4/well) were replated onto colloidal gold particle-coated coverslips and incubated at 37 °C for 6h followed by fixation with 4% paraformaldehyde in PBS. Migratory cells were observed and photographed under light microscopy (Nikon). Images were processed and measured using NIH image software (ImageJ). The percent of phagocytosis was analyzed by imageJ which calculated the area cleared of gold particles.

Transwell Cell Migration Assay- Polycarbonate membranes of 13 mm diameter with 8 µm pore size (Neuro Probe, MD) were inserted into the Blind-Well Chemotactic chambers (Neuro Probe, MD). Prior to seeding into the Transwell inserts, COS-1 cells were released from plates with trypsin-EDTA followed by the addition of DMEM with 10 % FCS media. The lower chemotactic chamber was filled with DMEM containing 10% FCS (200 µL). Cells were counted using a hemacytometer (Hausser Scientific, PA). The upper chamber was filled with 25,000 cells suspended in DMEM plus 10 % FCS to a final volume of 200 µL. Chambers were incubated for 6 h and 18 h at 37 °C and 5% CO_2 in a humidified tissue culture incubator. The cells on the upper surface were then removed from the filter with a cotton swab and washed three times with PBS. The cells remaining on the lower surface were fixed in 4% PFA/PBS solution overnight in a 4 °C refrigerator. Cells were stained with 0.1% crystal violet for 20 min and examined under a microscope. The number of cells in 10 areas of the filters was counted to obtain the number of migrating cells. For the inhibition experiments, cells were mixed with inhibitors 30 minutes prior to 6h and 18h migrations.

Gelatin Zymography- Zymography was performed in 10% polyacrylamide gels that had been cast in the presence of 0.1% gelatin as described previously (176). After electrophoresis, SDS was removed by Triton X-100 followed by incubation in a Tris-based buffer for 24 h. Gels were stained with Coomassie Brilliant Blue, and gelatinolytic activity was detected as a clear band in the background of uniform staining.

Immunoblotting- Immunoblotting was performed using monoclonal antibodies to MMP-1, -2, -3, -9, -14, TIMP-1, TIMP-2, CD44, HA and Myc. Transient transfected COS-1 cell-conditioned medium was precipitated with 10% trichloroacetic acid, and the precipitated proteins were dissolved in SDS sample buffer. Cells were lysed by 2 X SDS gel-loading buffer. The samples were resolved by 10% polyacrylamide gel electrophoresis, and proteins were transferred to nitrocellulose membranes and probed with antibodies. After extensive washing with TBS-T ((20 mM Tris-HCl, pH 7.6, 137 mM NaCl, 0.1% Tween), the membrane was probed with anti-rabbit or anti-mouse IgG for corresponding MMP, TIMP and Myc primary antibodies. Molecular weight was determined using prestained protein standards.

Cell Attachment Assay- Cells (5×10^4) suspended in DMEM containing 10% fetal calf serum were dispensed into 6-well culture plates and incubated in 5% CO_2 at 37 °C for 1h and 3h. After the incubation period, cells were gently washed 3 times with PBS. Cells attached to the membrane were stained with 0.1% crystal violet and counted under the microscope.

Fluorogenic Assay of Enzyme Activity- MCA Fluorogenic peptide substrate (50 µM) was added to MMP-2 and MMP-9 conditioned media and incubation buffer (109). As a positive control, MMP-2 and MMP-9 conditioned media were activated with 1 mM APMA (4-aminophenyl mercuric acetate). Samples were incubated in the dark for 1 h at 25 °C before detection. Fluorescence was measured with excitation at 328 nm and emission at 393 nm, in a fluorescent

plate reader (SpectraMAx M5, Molecular Devices, Union City, CA).

Fast Protein Liquid Chromatography (FPLC)- Conditioned media of COS-1 cells transfected with MMP-9 cDNA was isolated and clarified by centrifugation. Cell-free conditioned media was subjected to gelatin Sepharose 4B column chromatography as previously described (177). The DMSO eluted fractions were dialyzed against buffer (150 mM NaCl, 10 mM Tris, 0.03% sodium azide at pH 7.4), concentrated, and subjected to a Hiload 16/60 Superdex 200 prep grade column (GE Healthcare, Piscataway, NJ) mounted on an FPLC apparatus (GE Pharmacia Aktapurifier, GE Healthcare, Piscataway, NJ). One ml of sample was injected and the flow rate was 1 ml min^{-1}. One ml fractions were collected and 10 µl of each fraction was examined by gelatin zymogram.

Dataset of MMP/ligand complexes and PDB files- Three-dimensional coordinates of MMPs structures were obtained from the PDB files: 1ITV (Hemopexin domain of MMP-9), 1GKC (MMP-9 inhibitor complex) and 1HY7 (MMP-3 with different inhibitors) (10, 163, 178). The primary criterion of selection was the flexibility of the selected ligands, which varies from 2 to 10 rotable bonds (179). Another selection factor was the resolution and all selected X-ray structures were ranging from 1.50 to 2.30 Å (supplementary figure 1). The ligands with hydrogens were prepared into mol2 files using amber99 force field to compute the charges. The zinc ion at the active sites was retained into the receptor files. The receptor files with hydrogens were prepared into a mol2 file and the charges were calculated using gasteiger force field. All the residues and charges were visually inspected to insure consistency and reasonable charges among different ligands and receptors.

DOCK 6.0 calculations- DOCK 6.0 was used to calculate the protein/ligand binding energies. The calculations were performed starting from the X-ray crystal structure. Ligands were extracted from the X-ray structure, and hydrogen atoms were added according to the hydroxamic group deprotonated; partial atomic

charges were calculated using amber99. The ligands were modeled based on X-ray structures that were already minimized against experimental diffraction data. Energy contributions for individual atoms were extracted from DOCK energy output. The grid size was set to 100 x 100 x 100 points with a grid spacing of 0.3 Å centered on the original ligand in crystal structure complex. The grid box included the whole binding site of the proteins and provided enough space for ligand translational and rotational walk. Step sizes of 1.0 Å for translation and the cluster RMSD threshold was set to 2.0 Å. The number of ligands per cluster was set to 100.

Fluorescence Spectroscopy – Binding of #1403 to MMP-9 was assayed through the change of tryptophan emission spectra obtained on a Spex Fluorolog 3-21 fluorometer (Edison, NJ). Recombinant MMP-9 (50 nM) or MMP-9/PEX-2 (50 nM) was added to a cuvette (1.0 mL final volume) containing buffer made of 50 mM Tris-HCl, 60 mM KCl and 0.05% Tween 20, pH 7.4 and gently stirred with a small magnetic stir bar. The sample was excited at 280 nm and emission scans were collected from 290 to 400 nm, using slit widths of 0.3 mm. Three independent emission scans were collected and averaged. Data (λ_{max} wavelengths) were fitted in graphpad to determine the Kd using the following equation: $[Bound] = \frac{Capacity[Free]}{K_d + [Free]}$.

Statistical Analysis- Data is expressed as the mean ± standard error of triplicates. Each experiment was repeated as least 3 times. Student's *t*-test and analysis of variants (ANOVA) were used to assess differences with $p < 0.05$ and $p < 0.01$ considered to be significant.

Reference

1. Lopez-Otin C, Bond JS. Proteases: Multifunctional Enzymes in Life and Disease. Journal of Biological Chemistry 2008; 283: 30433-7.
2. Levene PA. The cleavage products of proteoses. Journal of Biological Chemistry 1905; 1: 45-58.
3. Lopez-Otin C, Matrisian LM. Emerging roles of proteases in tumour suppression. Nat Rev Cancer 2007; 7: 800-8.
4. Sternlicht MD, Werb Z. How matrix metalloproteinases regulate cell behavior. Annu Rev Cell Dev Bi 2001; 17: 463-516.
5. Kessenbrock K, Plaks V, Werb Z. Matrix metalloproteinases: regulators of the tumor microenvironment. Cell 2010; 141: 52-67.
6. Overall CM, Lopez-Otin C. Strategies for MMP inhibition in cancer: innovations for the post-trial era. Nat Rev Cancer 2002; 2: 657-72.
7. Nagase H, Woessner JF, Jr. Matrix metalloproteinases. J Biol Chem 1999; 274: 21491-4.
8. Birkedal-Hansen H, Moore WG, Bodden MK, et al. Matrix metalloproteinases: a review. Crit Rev Oral Biol Med 1993; 4: 197-250.
9. Windsor LJ, Bodden MK, Birkedal-Hansen B, Engler JA, Birkedal-Hansen H. Mutational analysis of residues in and around the active site of human fibroblast-type collagenase. J Biol Chem 1994; 269: 26201-7.
10. Cha H, Kopetzki E, Huber R, Lanzendorfer M, Brandstetter H. Structural basis of the adaptive molecular recognition by MMP9. J Mol Biol 2002; 320: 1065-79.
11. Cao J, Kozarekar P, Pavlaki M, Chiarelli C, Bahou WF, Zucker S. Distinct roles for the catalytic and hemopexin domains of membrane type 1-matrix metalloproteinase in substrate degradation and cell migration. JBiolChem 2004; 279: 14129-39.

12. Visse R, Nagase H. Matrix metalloproteinases and tissue inhibitors of metalloproteinases: structure, function, and biochemistry. Circ Res 2003; 92: 827-39.
13. Van Wart HE, Birkedal-Hansen H. The cysteine switch: a principle of regulation of metalloproteinase activity with potential applicability to the entire matrix metalloproteinase gene family. Proc Natl Acad Sci U S A 1990; 87: 5578-
14. Bjorklund M, Koivunen E. Gelatinase-mediated migration and invasion of cancer cells. Biochim Biophys Acta 2005; 1755: 37-69.
15. Pei D, Weiss SJ. Furin-dependent intracellular activation of the human stromelysin-3 zymogen. Nature 1995; 375: 244-7.
16. Sato H, Kinoshita T, Takino T, Nakayama K, Seiki M. Activation of a recombinant membrane type 1-matrix metalloproteinase (MT1-MMP) by furin and its interaction with tissue inhibitor of metalloproteinases (TIMP)-2. FEBS Lett 1996; 393: 101-4.
17. Yana I, Weiss SJ. Regulation of membrane type-1 matrix metalloproteinase activation by proprotein convertases. Mol Biol Cell 2000; 11: 2387-401.
18. Pei D, Kang T, Qi H. Cysteine array matrix metalloproteinase (CA-MMP)/MMP-23 is a type II transmembrane matrix metalloproteinase regulated by a single cleavage for both secretion and activation. J Biol Chem 2000; 275: 33988-97.
19. Marchenko GN, Strongin AY. MMP-28, a new human matrix metalloproteinase with an unusual cysteine-switch sequence is widely expressed in tumors. Gene 2001; 265: 87-93.
20. Lohi J, Wilson CL, Roby JD, Parks WC. Epilysin, a novel human matrix metalloproteinase (MMP-28) expressed in testis and keratinocytes and in response to injury. J Biol Chem 2001; 276: 10134-44.
21. Butler GS, Butler MJ, Atkinson SJ, et al. The TIMP2 membrane type 1 metalloproteinase "receptor" regulates the concentration and efficient

activation of progelatinase A. A kinetic study. J Biol Chem 1998; 273: 871-80.

22. Strongin AY, Collier I, Bannikov G, Marmer BL, Grant GA, Goldberg GI. Mechanism of cell surface activation of 72-kDa type IV collagenase. Isolation of the activated form of the membrane metalloprotease. J Biol Chem 1995; 270: 5331-8.
23. Morrison CJ, Butler GS, Bigg HF, Roberts CR, Soloway PD, Overall CM. Cellular activation of MMP-2 (gelatinase A) by MT2-MMP occurs via a TIMP-2-independent pathway. J Biol Chem 2001; 276: 47402-10.
24. Takino T, Sato H, Shinagawa A, Seiki M. Identification of the second membrane-type matrix metalloproteinase (MT-MMP-2) gene from a human placenta cDNA library. MT-MMPs form a unique membrane-type subclass in the MMP family. J Biol Chem 1995; 270: 23013-20.
25. Pei D. Identification and characterization of the fifth membrane-type matrix metalloproteinase MT5-MMP. J Biol Chem 1999; 274: 8925-32.
26. Velasco G, Cal S, Merlos-Suarez A, et al. Human MT6-matrix metalloproteinase: identification, progelatinase A activation, and expression in brain tumors. Cancer Res 2000; 60: 877-82.
27. English WR, Puente XS, Freije JM, et al. Membrane type 4 matrix metalloproteinase (MMP17) has tumor necrosis factor-alpha convertase activity but does not activate pro-MMP2. J Biol Chem 2000; 275: 14046-55.
28. Mudgett JS, Hutchinson NI, Chartrain NA, et al. Susceptibility of stromelysin 1-deficient mice to collagen-induced arthritis and cartilage destruction. Arthritis Rheum 1998; 41: 110-21.
29. Itoh T, Ikeda T, Gomi H, Nakao S, Suzuki T, Itohara S. Unaltered secretion of beta-amyloid precursor protein in gelatinase A (matrix metalloproteinase 2)-deficient mice. J Biol Chem 1997; 272: 22389-92.
30. Wilson CL, Heppner KJ, Labosky PA, Hogan BLM, Matrisian LM. Intestinal tumorigenesis is suppressed in mice lacking the metalloproteinase matrilysin. P Natl Acad Sci USA 1997; 94: 1402-7.

31. Shipley JM, Wesselschmidt RL, Kobayashi DK, Ley TJ, Shapiro SD. Metalloelastase is required for macrophage-mediated proteolysis and matrix invasion in mice. P Natl Acad Sci USA 1996; 93: 3942-6.
32. Masson R, Lefebvre O, Noel A, et al. In vivo evidence that the stromelysin-3 metalloproteinase contributes in a paracrine manner to epithelial cell malignancy. Journal of Cell Biology 1998; 140: 1535-41.
33. Vu TH, Shipley JM, Bergers G, et al. MMP-9/gelatinase B is a key regulator of growth plate angiogenesis and apoptosis of hypertrophic chondrocytes. Cell 1998; 93: 411-22.
34. Holmbeck K, Bianco P, Caterina J, et al. MT1-MMP-deficient mice develop dwarfism, osteopenia, arthritis, and connective tissue disease due to inadequate collagen turnover. Cell 1999; 99: 81-92.
35. Zhou Z, Apte SS, Soininen R, et al. Impaired endochondral ossification and angiogenesis in mice deficient in membrane-type matrix metalloproteinase I. Proc Natl Acad Sci U S A 2000; 97: 4052-7.
36. Baker AH, Edwards DR, Murphy G. Metalloproteinase inhibitors: biological actions and therapeutic opportunities. J Cell Sci 2002; 115: 3719-27.
37. Williamson RA, Marston FA, Angal S, et al. Disulphide bond assignment in human tissue inhibitor of metalloproteinases (TIMP). Biochem J 1990; 268: 267-
38. Williamson RA, Carr MD, Frenkiel TA, Feeney J, Freedman RB. Mapping the binding site for matrix metalloproteinase on the N-terminal domain of the tissue inhibitor of metalloproteinases-2 by NMR chemical shift perturbation. Biochemistry 1997; 36: 13882-9.
39. Gomis-Ruth FX, Maskos K, Betz M, et al. Mechanism of inhibition of the human matrix metalloproteinase stromelysin-1 by TIMP-1. Nature 1997; 389: 77-
40. Goldberg GI, Marmer BL, Grant GA, Eisen AZ, Wilhelm S, He CS. Human 72-kilodalton type IV collagenase forms a complex with a tissue inhibitor of metalloproteases designated TIMP-2. Proc Natl Acad Sci U S A 1989; 86: 8207-

41. Morgunova E, Tuuttila A, Bergmann U, Tryggvason K. Structural insight into the complex formation of latent matrix metalloproteinase 2 with tissue inhibitor of metalloproteinase 2. Proc Natl Acad Sci U S A 2002; 99: 7414-9.
42. Dufour A, Sampson NS, Zucker S, Cao J. Role of the hemopexin domain of matrix metalloproteinases in cell migration. J Cell Physiol 2008; 217: 643-51.
43. Woessner JF, Nagase H. Matrix metalloproteinases and TIMPs. Oxford: Oxford University Press; 2000.
44. Gomez DE, Alonso DF, Yoshiji H, Thorgeirsson UP. Tissue inhibitors of metalloproteinases: structure, regulation and biological functions. Eur J Cell Biol 1997; 74: 111-22.
45. Netzer KO, Suzuki K, Itoh Y, Hudson BG, Khalifah RG. Comparative analysis of the noncollagenous NC1 domain of type IV collagen: identification of structural features important for assembly, function, and pathogenesis. Protein Sci 1998; 7: 1340-51.
46. Takahashi C, Sheng Z, Horan TP, et al. Regulation of matrix metalloproteinase-9 and inhibition of tumor invasion by the membrane-anchored glycoprotein RECK. Proc Natl Acad Sci U S A 1998; 95: 13221-6.
47. Liepinsh E, Banyai L, Pintacuda G, Trexler M, Patthy L, Otting G. NMR structure of the netrin-like domain (NTR) of human type I procollagen C-proteinase enhancer defines structural consensus of NTR domains and assesses potential proteinase inhibitory activity and ligand binding. J Biol Chem 2003; 278: 25982-9.
48. Overall CM, Kleifeld O. Towards third generation matrix metalloproteinase inhibitors for cancer therapy. Br J Cancer 2006; 94: 941-6.
49. Kim YM, Jang JW, Lee OH, et al. Endostatin inhibits endothelial and tumor cellular invasion by blocking the activation and catalytic activity of matrix metalloproteinase. Cancer Res 2000; 60: 5410-3.

50. Werb Z. ECM and cell surface proteolysis: regulating cellular ecology. Cell 1997; 91: 439-42.
51. Orian-Rousseau V. CD44, a therapeutic target for metastasising tumours. Eur J Cancer 2010; 46: 1271-7.
52. Pure E, Assoian RK. Rheostatic signaling by CD44 and hyaluronan. Cell Signal 2009; 21: 651-5.
53. Naor D, Sionov RV, Ish-Shalom D. CD44: structure, function, and association with the malignant process. Adv Cancer Res 1997; 71: 241-319.
54. Yu Q, Stamenkovic I. Cell surface-localized matrix metalloproteinase-9 proteolytically activates TGF-beta and promotes tumor invasion and angiogenesis. Genes Dev 2000; 14: 163-76.
55. Yu WH, Woessner JF, Jr., McNeish JD, Stamenkovic I. CD44 anchors the assembly of matrilysin/MMP-7 with heparin-binding epidermal growth factor precursor and ErbB4 and regulates female reproductive organ remodeling. Genes Dev 2002; 16: 307-23.
56. Marrero-Diaz R, Bravo-Cordero JJ, Megias D, et al. Polarized MT1-MMP-CD44 interaction and CD44 cleavage during cell retraction reveal an essential role for MT1-MMP in CD44-mediated invasion. Cell Motil Cytoskeleton 2009; 66: 48-61.
57. Kajita M, Itoh Y, Chiba T, et al. Membrane-type 1 matrix metalloproteinase cleaves CD44 and promotes cell migration. J Cell Biol 2001; 153: 893-904.
58. Janik ME, Litynska A, Vereecken P. Cell migration-the role of integrin glycosylation. Biochim Biophys Acta 2010; 1800: 545-55.
59. Brooks PC, Silletti S, von Schalscha TL, Friedlander M, Cheresh DA. Disruption of angiogenesis by PEX, a noncatalytic metalloproteinase fragment with integrin binding activity. Cell 1998; 92: 391-400.
60. Stricker TP, Dumin JA, Dickeson SK, et al. Structural analysis of the alpha(2) integrin I domain/procollagenase-1 (matrix metalloproteinase-1) interaction. J Biol Chem 2001; 276: 29375-81.

61. Sabeh F, Li XY, Saunders TL, Rowe RG, Weiss SJ. Secreted versus membrane-anchored collagenases: relative roles in fibroblast-dependent collagenolysis and invasion. J Biol Chem 2009; 284: 23001-11.
62. Hotary KB, Allen ED, Brooks PC, Datta NS, Long MW, Weiss SJ. Membrane type I matrix metalloproteinase usurps tumor growth control imposed by the three-dimensional extracellular matrix. Cell 2003; 114: 33-45.
63. Desai B, Ma T, Chellaiah MA. Invadopodia and matrix degradation, a new property of prostate cancer cells during migration and invasion. J Biol Chem 2008; 283: 13856-66.
64. Weber BH, Vogt G, Pruett RC, Stohr H, Felbor U. Mutations in the tissue inhibitor of metalloproteinases-3 (TIMP3) in patients with Sorsby's fundus dystrophy. Nat Genet 1994; 8: 352-6.
65. Gilles C, Polette M, Coraux C, et al. Contribution of MT1-MMP and of human laminin-5 gamma2 chain degradation to mammary epithelial cell migration. J Cell Sci 2001; 114: 2967-76.
66. Koshikawa N, Schenk S, Moeckel G, et al. Proteolytic processing of laminin-5 by MT1-MMP in tissues and its effects on epithelial cell morphology. FASEB J 2004; 18: 364-6.
67. Noe V, Fingleton B, Jacobs K, et al. Release of an invasion promoter E-cadherin fragment by matrilysin and stromelysin-1. J Cell Sci 2001; 114: 111-8.
68. McGuire JK, Li Q, Parks WC. Matrilysin (matrix metalloproteinase-7) mediates E-cadherin ectodomain shedding in injured lung epithelium. Am J Pathol 2003; 162: 1831-43.
69. Deryugina EI, Quigley JP. Matrix metalloproteinases and tumor metastasis. Cancer Metastasis Rev 2006; 25: 9-34.
70. Agarwal D, Goodison S, Nicholson B, Tarin D, Urquidi V. Expression of matrix metalloproteinase 8 (MMP-8) and tyrosinase-related protein-1 (TYRP-1) correlates with the absence of metastasis in an isogenic human breast cancer model. Differentiation 2003; 71: 114-25.

71. Orlichenko LS, Radisky DC. Matrix metalloproteinases stimulate epithelial-mesenchymal transition during tumor development. Clin Exp Metastasis 2008; 25: 593-600.
72. Lochter A, Galosy S, Muschler J, Freedman N, Werb Z, Bissell MJ. Matrix metalloproteinase stromelysin-1 triggers a cascade of molecular alterations that leads to stable epithelial-to-mesenchymal conversion and a premalignant phenotype in mammary epithelial cells. J Cell Biol 1997; 139: 1861-72.
73. Bergers G, Brekken R, McMahon G, et al. Matrix metalloproteinase-9 triggers the angiogenic switch during carcinogenesis. Nat Cell Biol 2000; 2: 737-
74. Kaplan RN, Riba RD, Zacharoulis S, et al. VEGFR1-positive haematopoietic bone marrow progenitors initiate the pre-metastatic niche. Nature 2005; 438: 820-7.
75. Kaplan RN, Rafii S, Lyden D. Preparing the "soil": the premetastatic niche. Cancer Res 2006; 66: 11089-93.
76. Hiratsuka S, Watanabe A, Aburatani H, Maru Y. Tumour-mediated upregulation of chemoattractants and recruitment of myeloid cells predetermines lung metastasis. Nat Cell Biol 2006; 8: 1369-75.
77. Kraling BM, Wiederschain DG, Boehm T, Rehn M, Mulliken JB, Moses MA. The role of matrix metalloproteinase activity in the maturation of human capillary endothelial cells in vitro. J Cell Sci 1999; 112 (Pt 10): 1599-609.
78. Du R, Lu KV, Petritsch C, et al. HIF1alpha induces the recruitment of bone marrow-derived vascular modulatory cells to regulate tumor angiogenesis and invasion. Cancer Cell 2008; 13: 206-20.
79. Lee S, Jilani SM, Nikolova GV, Carpizo D, Iruela-Arispe ML. Processing of VEGF-A by matrix metalloproteinases regulates bioavailability and vascular patterning in tumors. J Cell Biol 2005; 169: 681-91.

80. O'Reilly MS, Wiederschain D, Stetler-Stevenson WG, Folkman J, Moses MA. Regulation of angiostatin production by matrix metalloproteinase-2 in a model of concomitant resistance. J Biol Chem 1999; 274: 29568-71.
81. Maeshima Y, Colorado PC, Kalluri R. Two RGD-independent alpha vbeta 3 integrin binding sites on tumstatin regulate distinct anti-tumor properties. J Biol Chem 2000; 275: 23745-50.
82. Coussens LM, Tinkle CL, Hanahan D, Werb Z. MMP-9 supplied by bone marrow-derived cells contributes to skin carcinogenesis. Cell 2000; 103: 481-90.
83. Galvez BG, Matias-Roman S, Albar JP, Sanchez-Madrid F, Arroyo AG. Membrane type 1-matrix metalloproteinase is activated during migration of human endothelial cells and modulates endothelial motility and matrix remodeling. J Biol Chem 2001; 276: 37491-500.
84. Devy L, Huang L, Naa L, et al. Selective inhibition of matrix metalloproteinase-14 blocks tumor growth, invasion, and angiogenesis. Cancer Res 2009; 69: 1517-26.
85. Opdenakker G, Van den Steen PE, Van Damme J. Gelatinase B: a tuner and amplifier of immune functions. Trends Immunol 2001; 22: 571-9.
86. Van Den Steen PE, Proost P, Grillet B, et al. Cleavage of denatured natural collagen type II by neutrophil gelatinase B reveals enzyme specificity, post-translational modifications in the substrate, and the formation of remnant epitopes in rheumatoid arthritis. Faseb Journal 2002; 16: -.
87. Hamada T, Arima N, Shindo M, Sugama K, Sasaguri Y. Suppression of adjuvant arthritis of rats by a novel matrix metalloproteinase-inhibitor. Brit J Pharmacol 2000; 131: 1513-20.
88. Lauffenburger DA, Horwitz AF. Cell migration: A physically integrated molecular process. Cell 1996; 84: 359-69.
89. Yu Q, Stamenkovic I. Localization of matrix metalloproteinase 9 to the cell surface provides a mechanism for CD44-mediated tumor invasion. Genes Dev 1999; 13: 35-48.

90. Sanceau J, Truchet S, Bauvois B. Matrix metalloproteinase-9 silencing by RNA interference triggers the migratory-adhesive switch in Ewing's sarcoma cells. J Biol Chem 2003; 278: 36537-46.
91. Friedl P, Wolf K. Tumour-cell invasion and migration: Diversity and escape mechanisms. Nature Reviews Cancer 2003; 3: 362-74.
92. Wolf K, Mazo I, Leung H, et al. Compensation mechanism in tumor cell migration: mesenchymal-amoeboid transition after blocking of pericellular proteolysis. Journal of Cell Biology 2003; 160: 267-77.
93. D'haese A, Wuyts A, Dillen C, et al. In vivo neutrophil recruitment by granulocyte chemotactic protein-2 is assisted by gelatinase B/MMP-9 in the mouse. J Interf Cytok Res 2000; 20: 667-74.
94. Wang X, Fu X, Brown PD, Crimmin MJ, Hoffman RM. Matrix Metalloproteinase Inhibitor Bb-94 (Batimastat) Inhibits Human Colon-Tumor Growth and Spread in a Patient-Like Orthotopic Model in Nude-Mice. Cancer Research 1994; 54: 4726-8.
95. Bergers G, Javaherian K, Lo KM, Folkman J, Hanahan D. Effects of angiogenesis inhibitors on multistage carcinogenesis in mice. Science 1999; 284: 808-12.
96. Pavlaki M, Zucker S. Matrix metalloproteinase inhibitors (MMPIs): the beginning of phase I or the termination of phase III clinical trials. Cancer Metastasis Rev 2003; 22: 177-203.
97. Sorsa T, Ramamurthy NS, Vernillo AT, et al. Functional sites of chemically modified tetracyclines: inhibition of the oxidative activation of human neutrophil and chicken osteoclast pro-matrix metalloproteinases. J Rheumatol 1998; 25: 975-82.
98. Cianfrocca M, Cooley TP, Lee JY, et al. Matrix metalloproteinase inhibitor COL-3 in the treatment of AIDS-related Kaposi's sarcoma: a phase I AIDS malignancy consortium study. J Clin Oncol 2002; 20: 153-9.
99. Wynn RL. Latest FDA approvals for dentistry. Gen Dent 1999; 47: 19-22.
100. Galardy RE, Cassabonne ME, Giese C, et al. Low molecular weight inhibitors in corneal ulceration. Ann Ny Acad Sci 1994; 732: 315-23.

101. Whittaker M, Floyd CD, Brown P, Gearing AJ. Design and therapeutic application of matrix metalloproteinase inhibitors. Chem Rev 1999; 99: 2735-76.
102. Zucker S, Cao J, Chen WT. Critical appraisal of the use of matrix metalloproteinase inhibitors in cancer treatment. Oncogene 2000; 19: 6642-50.
103. Lee M, Fridman R, Mobashery S. Extracellular proteases as targets for treatment of cancer metastases. Chem Soc Rev 2004; 33: 401-9.
104. Van den Steen PE, Van Aelst I, Hvidberg V, et al. The hemopexin and O-glycosylated domains tune gelatinase B/MMP-9 bioavailability via inhibition and binding to cargo receptors. J Biol Chem 2006; 281: 18626-37.
105. Burg-Roderfeld M, Roderfeld M, Wagner S, Henkel C, Grotzinger J, Roeb E. MMP-9-hemopexin domain hampers adhesion and migration of colorectal cancer cells. Int J Oncol 2007; 30: 985-92.
106. Egeblad M, Werb Z. New functions for the matrix metalloproteinases in cancer progression. Nat Rev Cancer 2002; 2: 161-74.
107. Opdenakker G, Van Damme J. Chemokines and proteinases in autoimmune diseases and cancer. Verh K Acad Geneeskd Belg 2002; 64: 105-36.
108. Cao J, Rehemtulla A, Pavlaki M, Kozarekar P, Chiarelli C. Furin directly cleaves proMMP-2 in the trans-Golgi network resulting in a nonfunctioning proteinase. J Biol Chem 2005; 280: 10974-80.
109. Knight CG, Willenbrock F, Murphy G. A novel coumarin-labelled peptide for sensitive continuous assays of the matrix metalloproteinases. FEBS Lett 1992; 296: 263-6.
110. Cao J, Drews M, Lee HM, Conner C, Bahou WF, Zucker S. The propeptide domain of membrane type 1 matrix metalloproteinase is required for binding of tissue inhibitor of metalloproteinases and for activation of pro-gelatinase A. J Biol Chem 1998; 273: 34745-52.

111. Olson MW, Bernardo MM, Pietila M, et al. Characterization of the monomeric and dimeric forms of latent and active matrix metalloproteinase-9. Differential rates for activation by stromelysin 1. J Biol Chem 2000; 275: 2661-8.
112. Jozic D, Bourenkov G, Lim NH, et al. X-ray structure of human proMMP-1: new insights into procollagenase activation and collagen binding. J Biol Chem 2005; 280: 9578-85.
113. Goldberg GI, Strongin A, Collier IE, Genrich LT, Marmer BL. Interaction of 92-kDa type IV collagenase with the tissue inhibitor of metalloproteinases prevents dimerization, complex formation with interstitial collagenase, and activation of the proenzyme with stromelysin. J Biol Chem 1992; 267: 4583-91.
114. Dudley DT, Pang L, Decker SJ, Bridges AJ, Saltiel AR. A Synthetic Inhibitor of the Mitogen-Activated Protein-Kinase Cascade. Proc of the National Academy of Sciences of the United States of America 1995; 92: 7686-9.
115. Vlahos CJ, Matter WF, Hui KY, Brown RF. A Specific Inhibitor of Phosphatidylnositol 3-Kinase, 2-(4-Morpholinyl)-8-Phenyl-4h-1-Benzopyran-4-One (Ly294002). Journal of Biological Chemistry 1994; 269: 5241-8.
116. Bennett BL, Sasaki DT, Murray BW, et al. SP600125, an anthrapyrazolone inhibitor of Jun N-terminal kinase. Proc of the National Academy of Sciences of the United States of America 2001; 98: 13681-6.
117. Chijiwa T, Mishima A, Hagiwara M, et al. Inhibition of Forskolin-Induced Neurite Outgrowth and Protein-Phosphorylation by a Newly Synthesized Selective Inhibitor of Cyclic Amp-Dependent Protein-Kinase, N-[2-(P-Bromocinnamylamino)Ethyl]-5-Isoquinolinesulfonamide (H-89), of Pc12d Pheochromocytoma Cells. J Biol Chem 1990; 265: 5267-72.
118. Chitaley K, Wingard CJ, Webb RC, et al. Antagonism of Rho-kinase stimulates rat penile erection via a nitric oxide-independent pathway. Nat Med 2001; 7: 119-22.

119. Ridley AJ, Schwartz MA, Burridge K, et al. Cell migration: integrating signals from front to back. Science 2003; 302: 1704-9.
120. Rosenblum G, Van den Steen PE, Cohen SR, et al. Insights into the structure and domain flexibility of full-length pro-matrix metalloproteinase-9/gelatinase B. Structure 2007; 15: 1227-36.
121. Nagase H, Visse R, Murphy G. Structure and function of matrix metalloproteinases and TIMPs. Cardiovasc Res 2006; 69: 562-73.
122. Schulz R. Intracellular targets of matrix metalloproteinase-2 in cardiac disease: rationale and therapeutic approaches. Annu Rev Pharmacol Toxicol 2007; 47: 211-42.
123. Hu Y, Ivashkiv LB. Costimulation of chemokine receptor signaling by matrix metalloproteinase-9 mediates enhanced migration of IFN-alpha dendritic cells. J Immunol 2006; 176: 6022-33.
124. Monferran S, Paupert J, Dauvillier S, Salles B, Muller C. The membrane form of the DNA repair protein Ku interacts at the cell surface with metalloproteinase 9. EMBO J 2004; 23: 3758-68.
125. Zucker S, Hymowitz M, Conner C, et al. Measurement of matrix metalloproteinases and tissue inhibitors of metalloproteinases in blood and tissues. Clinical and experimental applications. Ann Ny Acad Sci 1999; 878: 212-27.
126. Tian YC, Chen YC, Chang CT, et al. Epidermal growth factor and transforming growth factor-beta1 enhance HK-2 cell migration through a synergistic increase of matrix metalloproteinase and sustained activation of ERK signaling pathway. Exp Cell Res 2007; 313: 2367-77.
127. Dufour A, Zucker S, Sampson NS, Kuscu C, Cao J. Role of matrix metalloproteinase-9 (MMP-9) dimers in cell migration: design of inhibitory peptides. J Biol Chem 2010.
128. Redondo-Munoz J, Ugarte-Berzal E, Garcia-Marco JA, et al. Alpha4beta1 integrin and 190-kDa CD44v constitute a cell surface docking complex for gelatinase B/MMP-9 in chronic leukemic but not in normal B cells. Blood 2008; 112: 169-78.

129. Kim Y, Lee YS, Choe J, Lee H, Kim YM, Jeoung D. CD44-epidermal growth factor receptor interaction mediates hyaluronic acid-promoted cell motility by activating protein kinase C signaling involving Akt, Rac1, Phox, reactive oxygen species, focal adhesion kinase, and MMP-2. J Biol Chem 2008; 283: 22513-28.
130. Tsukita S, Oishi K, Sato N, Sagara J, Kawai A. ERM family members as molecular linkers between the cell surface glycoprotein CD44 and actin-based cytoskeletons. J Cell Biol 1994; 126: 391-401.
131. Bourguignon LY, Gilad E, Brightman A, Diedrich F, Singleton P. Hyaluronan-CD44 interaction with leukemia-associated RhoGEF and epidermal growth factor receptor promotes Rho/Ras co-activation, phospholipase C epsilon-Ca2+ signaling, and cytoskeleton modification in head and neck squamous cell carcinoma cells. J Biol Chem 2006; 281: 14026-40.
132. Murai T, Miyauchi T, Yanagida T, Sako Y. Epidermal growth factor-regulated activation of Rac GTPase enhances CD44 cleavage by metalloproteinase disintegrin ADAM10. Biochem J 2006; 395: 65-71.
133. Massova I, Kotra LP, Fridman R, Mobashery S. Matrix metalloproteinases: structures, evolution, and diversification. FASEB J 1998; 12: 1075-95.
134. Davis BG. Biochemistry. Mimicking posttranslational modifications of proteins. Science 2004; 303: 480-2.
135. Cao J, Rehemtulla A, Bahou W, Zucker S. Membrane type matrix metalloproteinase 1 activates pro-gelatinase A without furin cleavage of the N-terminal domain. J Biol Chem 1996; 271: 30174-80.
136. Acharya PS, Majumdar S, Jacob M, et al. Fibroblast migration is mediated by CD44-dependent TGF beta activation. J Cell Sci 2008; 121: 1393-402.
137. Partridge JJ, Madsen MA, Ardi VC, et al. Functional analysis of matrix metalloproteinases and tissue inhibitors of metalloproteinases differentially expressed by variants of human HT-1080 fibrosarcoma exhibiting high and low levels of intravasation and metastasis. J Biol Chem 2007; 282: 35964-77.

138. Rolli M, Fransvea E, Pilch J, Saven A, Felding-Habermann B. Activated integrin alpha v beta 3 cooperates with metalloproteinase MMP-9 in regulating migration of metastatic breast cancer cells. Proc of the National Academy of Sciences of the United States of America 2003; 100: 9482-7.
139. Stefanidakis M, Karjalainen K, Jaalouk DE, et al. Role of leukemia cell invadosome in extramedullary infiltration. Blood 2009; 114: 3008-17.
140. Ogata Y, Itoh Y, Nagase H. Steps Involved in Activation of the Pro-Matrix Metalloproteinase-9 (Progelatinase-B)-Tissue Inhibitor of Metalloproteinases-1 Complex by 4-Aminophenylmercuric Acetate and Proteinases. J Biol Chem 1995; 270: 18506-11.
141. Roderfeld M, Graf J, Giese B, et al. Latent MMP-9 is bound to TIMP-1 before secretion. Biol Chem 2007; 388: 1227-34.
142. Toth M, Gervasi DC, Fridman R. Phorbol ester-induced cell surface association of matrix metalloproteinase-9 in human MCF1OA breast epithelial cells. Cancer Research 1997; 57: 3159-67.
143. Owen CA, Hu ZM, Barrick B, Shapiro SD. Inducible expression of tissue inhibitor of metalloproteinases-resistant matrix metalloproteinase-9 on the cell surface of neutrophils. Am J Resp Cell Mol 2003; 29: 283-94.
144. Olson MW, Toth M, Gervasi DC, Sado Y, Ninomiya Y, Fridman R. High affinity binding of latent matrix metalloproteinase-9 to the alpha2(IV) chain of collagen IV. J Biol Chem 1998; 273: 10672-81.
145. Collier IE, Saffarian S, Marmer BL, Elson EL, Goldberg G. Substrate recognition by gelatinase A: the C-terminal domain facilitates surface diffusion. Biophys J 2001; 81: 2370-7.
146. Ellerbroek SM, Halbleib JM, Benavidez M, et al. Phosphatidylinositol 3-kinase activity in epidermal growth factor-stimulated matrix metalloproteinase-9 production and cell surface association. Cancer Res 2001; 61: 1855-61.
147. Yao JS, Chen Y, Zhai W, Xu K, Young WL, Yang GY. Minocycline exerts multiple inhibitory effects on vascular endothelial growth factor-induced

smooth muscle cell migration: the role of ERK1/2, PI3K, and matrix metalloproteinases. Circ Res 2004; 95: 364-71.

148. Samanna V, Ma T, Mak TW, Rogers M, Chellaiah MA. Actin polymerization modulates CD44 surface expression, MMP-9 activation, and osteoclast function. J Cell Physiol 2007; 213: 710-20.
149. Coussens LM, Fingleton B, Matrisian LM. Matrix metalloproteinase inhibitors and cancer: trials and tribulations. Science 2002; 295: 2387-92.
150. Mantuano E, Inoue G, Li X, et al. The hemopexin domain of matrix metalloproteinase-9 activates cell signaling and promotes migration of schwann cells by binding to low-density lipoprotein receptor-related protein. J Neurosci 2008; 28: 11571-82.
151. Ezhilarasan R, Jadhav U, Mohanam I, Rao JS, Gujrati M, Mohanam S. The hemopexin domain of MMP-9 inhibits angiogenesis and retards the growth of intracranial glioblastoma xenograft in nude mice. Int J Cancer 2009; 124: 306-15.
152. Bjorklund M, Heikkila P, Koivunen E. Peptide inhibition of catalytic and noncatalytic activities of matrix metalloproteinase-9 blocks tumor cell migration and invasion. J Biol Chem 2004; 279: 29589-97.
153. Hidalgo M, Eckhardt SG. Development of matrix metalloproteinase inhibitors in cancer therapy. J Natl Cancer Inst 2001; 93: 178-93.
154. Bannikov GA, Karelina TV, Collier IE, Marmer BL, Goldberg GI. Substrate binding of gelatinase B induces its enzymatic activity in the presence of intact propeptide. J Biol Chem 2002; 277: 16022-7.
155. Allan JA, Docherty AJ, Barker PJ, Huskisson NS, Reynolds JJ, Murphy G. Binding of gelatinases A and B to type-I collagen and other matrix components. Biochem J 1995; 309 (Pt 1): 299-306.
156. Doman TN, McGovern SL, Witherbee BJ, et al. Molecular docking and high-throughput screening for novel inhibitors of protein tyrosine phosphatase-1B. J Med Chem 2002; 45: 2213-21.

157. Charifson PS, Corkery JJ, Murcko MA, Walters WP. Consensus scoring: A method for obtaining improved hit rates from docking databases of three-dimensional structures into proteins. J Med Chem 1999; 42: 5100-9.
158. Kuntz ID, Meng EC, Shoichet BK. Structure-Based Molecular Design. Accounts Chem Res 1994; 27: 117-23.
159. Irwin JJ, Shoichet BK. ZINC--a free database of commercially available compounds for virtual screening. J Chem Inf Model 2005; 45: 177-82.
160. Kontoyianni M, McClellan LM, Sokol GS. Evaluation of docking performance: comparative data on docking algorithms. J Med Chem 2004; 47: 558-65.
161. Harkcom WT, Bevan DR. Molecular docking of inhibitors into monoamine oxidase B. Biochem Biophys Res Commun 2007; 360: 401-6.
162. Steinkellner G, Rader R, Thallinger GG, Kratky C, Gruber K. VASCo: computation and visualization of annotated protein surface contacts. Bmc Bioinformatics 2009; 10: 1-11.
163. Rowsell S, Hawtin P, Minshull CA, et al. Crystal structure of human MMP9 in complex with a reverse hydroxamate inhibitor. J Mol Biol 2002; 319: 173-81.
164. Baffy G, Miyashita T, Williamson JR, Reed JC. Apoptosis Induced by Withdrawal of Interleukin-3 (Il-3) from an Il-3-Dependent Hematopoietic-Cell Line Is Associated with Repartitioning of Intracellular Calcium and Is Blocked by Enforced Bcl-2 Oncoprotein Production. J Biol Chem 1993; 268: 6511-9.
165. James NG, Byrne SL, Steere AN, Smith VC, MacGillivray RT, Mason AB. Inequivalent contribution of the five tryptophan residues in the C-lobe of human serum transferrin to the fluorescence increase when iron is released. Biochemistry 2009; 48: 2858-67.
166. James NG, Berger CL, Byrne SL, Smith VC, MacGillivray RT, Mason AB. Intrinsic fluorescence reports a global conformational change in the N-lobe of human serum transferrin following iron release. Biochemistry 2007; 46: 10603-11.

167. Kakehi K, Oda Y, Kinoshita M. Fluorescence polarization: analysis of carbohydrate-protein interaction. Anal Biochem 2001; 297: 111-6.
168. Ardi VC, Kupriyanova TA, Deryugina EI, Quigley JP. Human neutrophils uniquely release TIMP-free MMP-9 to provide a potent catalytic stimulator of angiogenesis. Proc of the National Academy of Sciences of the United States of America 2007; 104: 20262-7.
169. Mantuano E, Inoue G, Li XQ, et al. The Hemopexin Domain of Matrix Metalloproteinase-9 Activates Cell Signaling and Promotes Migration of Schwann Cells by Binding to Low-Density Lipoprotein Receptor-Related Protein. J Neurosci 2008; 28: 11571-82.
170. Ezhilarasan R, Jadhav U, Mohanam I, Rao JS, Gujrati M, Mohanam S. The hemopexin domain of MMP-9 inhibits angiogenesis and retards the growth of intracranial glioblastoma xenograft in nude mice. Int J Cancer 2009; 124: 306-15.
171. Bjorklund M, Heikkila P, Koivunen E. Peptide inhibition of catalytic and noncatalytic activities of matrix metalloproteinase-9 blocks tumor cell migration and invasion. J Biol Chem 2004; 279: 29589-97.
172. Zucker S, Lysik RM, Zarrabi MH, Moll U. M(r) 92,000 type IV collagenase is increased in plasma of patients with colon cancer and breast cancer. Cancer Res 1993; 53: 140-6.
173. Cao J, Chiarelli C, Richman O, Zarrabi K, Kozarekar P, Zucker S. Membrane type 1 matrix metalloproteinase induces epithelial-to-mesenchymal transition in prostate cancer. J Biol Chem 2008; 283: 6232-40.
174. Zucker S, Wieman JM, Lysik RM, et al. Enrichment of Collagen and Gelatin Degrading Activities in the Plasma-Membranes of Human Cancer-Cells. Cancer Res 1987; 47: 1608-14.
175. Albrecht-Buehler G. The phagokinetic tracks of 3T3 cells. Cell 1977; 11: 395-404.

176. Zucker S, Conner C, DiMassmo BI, et al. Thrombin induces the activation of progelatinase A in vascular endothelial cells. Physiologic regulation of angiogenesis. J Biol Chem 1995; 270: 23730-8.
177. Imai K, Okada Y. Purification of matrix metalloproteinases by column chromatography. Nat Protoc 2008; 3: 1111-24.
178. Natchus MG, Bookland RG, Laufersweiler MJ, et al. Development of new carboxylic acid-based MMP inhibitors derived from functionalized propargylglycines. J Med Chem 2001; 44: 1060-71.
179. Hu X, Shelver WH. Docking studies of matrix metalloproteinase inhibitors: zinc parameter optimization to improve the binding free energy prediction. J Mol Graph Model 2003; 22: 115-26.

Appendix

Plasmid:

Plasmid Name MMP-9 wild type

Creator Rafael Fridman

Base Vector/Company: pcDNA™3.1/*myc-His(-)* C

Resistant Gene (antibiotic) : Ampicillin

Insert:

Insert Size: 2121 Base Pairs **Cloning Sites 5': *EcoRI* ; 3': *HindIII***

PCR primer 1 : #1315 **PCR primer 2 :** #1359

Sequenced: **Yes**

Functional Assays:

1) gelatin zymogram

2) western Blot

3)_____

Plasmid Map:

CMV promoter: bases 209-863
T7 promoter/priming site: bases 863-882
Multiple cloning site: bases 895-1006
myc epitope: bases 1007-1036
Polyhistidine tag: bases 1052-1069
BGH reverse priming site: bases 1113-1130
BGH polyadenylation signal: bases 1116-1343
f1 origin: bases 1389-1817
SV40 promoter and origin: bases 1844-2152
Neomycin resistance gene: bases 2227-3021
SV40 polyadenylation signal: bases 3195-3325
pUC origin: bases 3708-4381
Ampicillin resistance gene: bases 4526-5386
(complementary strand)

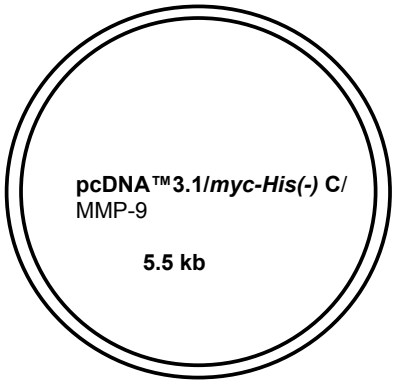

Plasmid:

Plasmid Name MMP-9ΔPEX

Creator Antoine Dufour

Base Vector/Company: pcDNA™3.1/*myc-His(-)* C

Resistant Gene (antibiotic) : Ampicillin

Insert:

Insert Size: 1539 Base Pairs **Cloning Sites 5': *EcoRI* ; 3': *HindIII***

PCR primer 1 : #1315 **PCR primer 2 :** #1342

Sequenced: **Yes**

Functional Assays:

1) gelatin zymogram

2) western Blot

3)_____

Plasmid Map:

CMV promoter: bases 209-863
T7 promoter/priming site: bases 863-882
Multiple cloning site: bases 895-1006
myc epitope: bases 1007-1036
Polyhistidine tag: bases 1052-1069
BGH reverse priming site: bases 1113-1130
BGH polyadenylation signal: bases 1116-1343
f1 origin: bases 1389-1817
SV40 promoter and origin: bases 1844-2152
Neomycin resistance gene: bases 2227-3021
SV40 polyadenylation signal: bases 3195-3325
pUC origin: bases 3708-4381
Ampicillin resistance gene: bases 4526-5386
(complementary strand)

Plasmid:

Plasmid Name MMP-9/MMP-1_{PEX}

Creator Antoine Dufour

Base Vector/Company: pcDNA™3.1/*myc-His(-)* C

Resistant Gene (antibiotic) : Ampicillin

Insert:

Insert Size: 2120 Base Pairs **Cloning Sites 5': *EcoRI* ; 3': *HindIII***

PCR primer 1 : #1315 **PCR primer 2 :** #1318

Sequenced: **Yes**

Functional Assays:

1) gelatin zymogram

2) western Blot

3) _____

Plasmid Map:

CMV promoter: bases 209-863
T7 promoter/priming site: bases 863-882
Multiple cloning site: bases 895-1006
myc epitope: bases 1007-1036
Polyhistidine tag: bases 1052-1069
BGH reverse priming site: bases 1113-1130
BGH polyadenylation signal: bases 1116-1343
f1 origin: bases 1389-1817
SV40 promoter and origin: bases 1844-2152
Neomycin resistance gene: bases 2227-3021
SV40 polyadenylation signal: bases 3195-3325
pUC origin: bases 3708-4381
Ampicillin resistance gene: bases 4526-5386
(complementary strand)

Plasmid:

Plasmid Name MMP-9E^{230}→A

Creator Antoine Dufour

Base Vector/Company: pcDNA™3.1/*myc-His(-)* C

Resistant Gene (antibiotic) : Ampicillin

Insert:

Insert Size: 2121 Base Pairs **Cloning Sites 5': *EcoRI* ; 3': *HindIII***

PCR primer 1 : #2523 **PCR primer 2 :** #2524

Sequenced: **Yes**

Functional Assays:

1) gelatin zymogram

2) western Blot

3)_____

Plasmid Map:

CMV promoter: bases 209-863
T7 promoter/priming site: bases 863-882
Multiple cloning site: bases 895-1006
myc epitope: bases 1007-1036
Polyhistidine tag: bases 1052-1069
BGH reverse priming site: bases 1113-1130
BGH polyadenylation signal: bases 1116-1343
f1 origin: bases 1389-1817
SV40 promoter and origin: bases 1844-2152
Neomycin resistance gene: bases 2227-3021
SV40 polyadenylation signal: bases 3195-3325
pUC origin: bases 3708-4381
Ampicillin resistance gene: bases 4526-5386 (complementary strand)

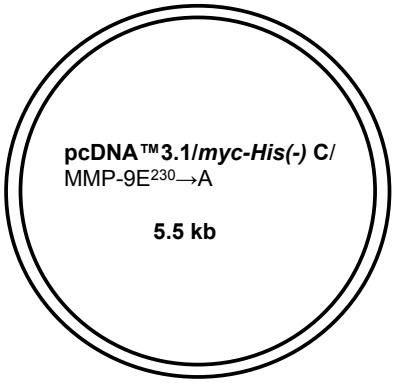

Plasmid:

Plasmid Name MMP-9ΔOG

Creator Antoine Dufour

Base Vector/Company: pcDNA™3.1/*myc-His(-)* C

Resistant Gene (antibiotic) : Ampicillin

Insert:

Insert Size: 1915 Base Pairs **Cloning Sites 5': *EcoRI* ; 3': *HindIII***

PCR primer 1 : #1357 **PCR primer 2 :** #1358

Sequenced: **Yes**

Functional Assays:

1) gelatin zymogram

2) western Blot

3)_____

Plasmid Map:

CMV promoter: bases 209-863
T7 promoter/priming site: bases 863-882
Multiple cloning site: bases 895-1006
myc epitope: bases 1007-1036
Polyhistidine tag: bases 1052-1069
BGH reverse priming site: bases 1113-1130
BGH polyadenylation signal: bases 1116-1343
f1 origin: bases 1389-1817
SV40 promoter and origin: bases 1844-2152
Neomycin resistance gene: bases 2227-3021
SV40 polyadenylation signal: bases 3195-3325
pUC origin: bases 3708-4381
Ampicillin resistance gene: bases 4526-5386
(complementary strand)

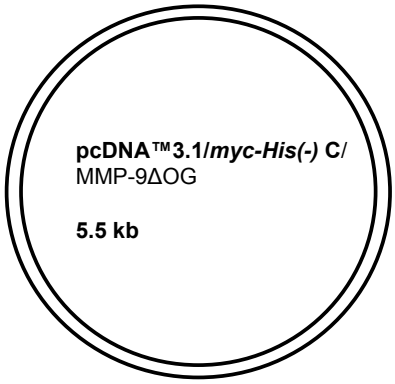

Plasmid:

Plasmid Name MMP-9/Myc

Creator Antoine Dufour

Base Vector/Company: pcDNA™3.1/*myc-His(-)* C

Resistant Gene (antibiotic) : Ampicillin

Insert:

Insert Size: 2159 Base Pairs **Cloning Sites 5': *EcoRI* ; 3': *HindIII***

PCR primer 1 : #1315 **PCR primer 2 :** #2507

Sequenced: **Yes**

Functional Assays:

1) gelatin zymogram

2) western Blot

3)_____

Plasmid Map:

CMV promoter: bases 209-863
T7 promoter/priming site: bases 863-882
Multiple cloning site: bases 895-1006
myc epitope: bases 1007-1036
Polyhistidine tag: bases 1052-1069
BGH reverse priming site: bases 1113-1130
BGH polyadenylation signal: bases 1116-1343
f1 origin: bases 1389-1817
SV40 promoter and origin: bases 1844-2152
Neomycin resistance gene: bases 2227-3021
SV40 polyadenylation signal: bases 3195-3325
pUC origin: bases 3708-4381
Ampicillin resistance gene: bases 4526-5386
(complementary strand)

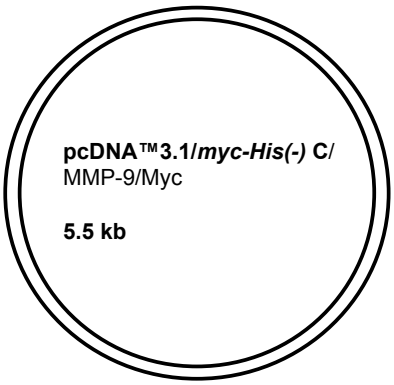

Plasmid:

Plasmid Name MMP-9/HA

Creator Antoine Dufour

Base Vector/Company: pcDNA™3.1/*myc-His(-)* C

Resistant Gene (antibiotic) : Ampicillin

Insert:

Insert Size: 2148 Base Pairs **Cloning Sites 5': *EcoRI* ; 3': *HindIII***

PCR primer 1 : #2512 **PCR primer 2 :** #2513

Sequenced: **Yes**

Functional Assays:

1) gelatin zymogram

2) western Blot

3)_____

Plasmid Map:

CMV promoter: bases 209-863
T7 promoter/priming site: bases 863-882
Multiple cloning site: bases 895-1006
myc epitope: bases 1007-1036
Polyhistidine tag: bases 1052-1069
BGH reverse priming site: bases 1113-1130
BGH polyadenylation signal: bases 1116-1343
f1 origin: bases 1389-1817
SV40 promoter and origin: bases 1844-2152
Neomycin resistance gene: bases 2227-3021
SV40 polyadenylation signal: bases 3195-3325
pUC origin: bases 3708-4381
Ampicillin resistance gene: bases 4526-5386
(complementary strand)

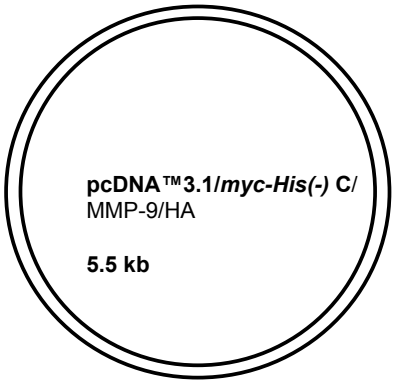

Plasmid:

Plasmid Name MMP-9/MMP-2PEX/Myc

Creator Antoine Dufour

Base Vector/Company: pcDNA™3.1/*myc-His(-)* C

Resistant Gene (antibiotic) : Ampicillin

Insert:

Insert Size: 2090 Base Pairs **Cloning Sites 5': *EcoRI* ; 3': *HindIII***

PCR primer 1 : #1315 and #2534 **PCR primer 2 :** #1356 and #2535

Sequenced: **Yes**

Functional Assays:

1) gelatin zymogram
2) western Blot
3) _____

Plasmid Map:

CMV promoter: bases 209-863
T7 promoter/priming site: bases 863-882
Multiple cloning site: bases 895-1006
myc epitope: bases 1007-1036
Polyhistidine tag: bases 1052-1069
BGH reverse priming site: bases 1113-1130
BGH polyadenylation signal: bases 1116-1343
f1 origin: bases 1389-1817
SV40 promoter and origin: bases 1844-2152
Neomycin resistance gene: bases 2227-3021
SV40 polyadenylation signal: bases 3195-3325
pUC origin: bases 3708-4381
Ampicillin resistance gene: bases 4526-5386
(complementary strand)

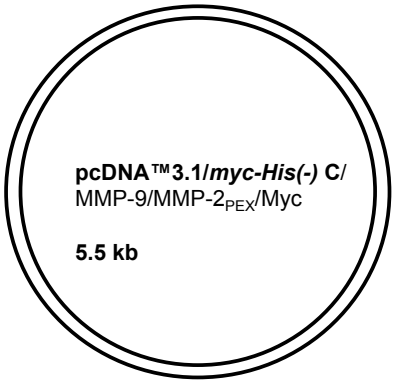

Plasmid:

Plasmid Name MMP-9/Blade I

Creator Antoine Dufour

Base Vector/Company: pcDNA™3.1/*myc-His(-)* C

Resistant Gene (antibiotic): Ampicillin

Insert:

Insert Size: 2090 Base Pairs **Cloning Sites 5': *EcoRI* ; 3': *HindIII***

PCR primer 1 : #1315 and #2557 **PCR primer 2 :** #2558 and #2507

Sequenced: **Yes**

Functional Assays:

1) gelatin zymogram

2) western Blot

3)_____

Plasmid Map:

CMV promoter: bases 209-863
T7 promoter/priming site: bases 863-882
Multiple cloning site: bases 895-1006
myc epitope: bases 1007-1036
Polyhistidine tag: bases 1052-1069
BGH reverse priming site: bases 1113-1130
BGH polyadenylation signal: bases 1116-1343
f1 origin: bases 1389-1817
SV40 promoter and origin: bases 1844-2152
Neomycin resistance gene: bases 2227-3021
SV40 polyadenylation signal: bases 3195-3325
pUC origin: bases 3708-4381
Ampicillin resistance gene: bases 4526-5386
(complementary strand)

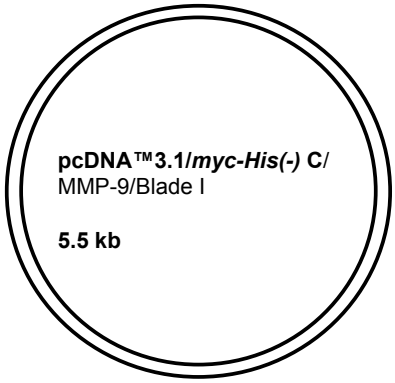

Plasmid:

Plasmid Name MMP-9/Blade II

Creator Antoine Dufour

Base Vector/Company: pcDNA™3.1/*myc-His(-)* C

Resistant Gene (antibiotic): Ampicillin

Insert:

Insert Size: 2090 Base Pairs **Cloning Sites 5': *EcoRI* ; 3': *HindIII***

PCR primer 1 : #1315 and #2596 **PCR primer 2 :** #2507 and #2597

Sequenced: **Yes**

Functional Assays:

1) gelatin zymogram
2) western Blot
3) _____

Plasmid Map:

CMV promoter: bases 209-863
T7 promoter/priming site: bases 863-882
Multiple cloning site: bases 895-1006
myc epitope: bases 1007-1036
Polyhistidine tag: bases 1052-1069
BGH reverse priming site: bases 1113-1130
BGH polyadenylation signal: bases 1116-1343
f1 origin: bases 1389-1817
SV40 promoter and origin: bases 1844-2152
Neomycin resistance gene: bases 2227-3021
SV40 polyadenylation signal: bases 3195-3325
pUC origin: bases 3708-4381
Ampicillin resistance gene: bases 4526-5386
(complementary strand)

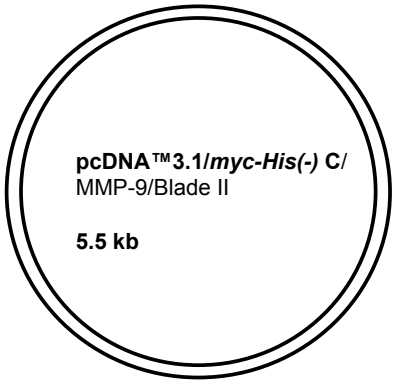

Plasmid:

Plasmid Name MMP-9/Blade III

Creator Antoine Dufour

Base Vector/Company: pcDNA™3.1/*myc-His(-)* C

Resistant Gene (antibiotic): Ampicillin

Insert:

Insert Size: 2090 Base Pairs **Cloning Sites 5': *EcoRI* ; 3': *HindIII***

PCR primer 1 : #1315 and #2540 **PCR primer 2 :** #2507 and #2541

Sequenced: **Yes**

Functional Assays:

1) gelatin zymogram

2) western Blot

3)_____

Plasmid Map:

CMV promoter: bases 209-863
T7 promoter/priming site: bases 863-882
Multiple cloning site: bases 895-1006
myc epitope: bases 1007-1036
Polyhistidine tag: bases 1052-1069
BGH reverse priming site: bases 1113-1130
BGH polyadenylation signal: bases 1116-1343
f1 origin: bases 1389-1817
SV40 promoter and origin: bases 1844-2152
Neomycin resistance gene: bases 2227-3021
SV40 polyadenylation signal: bases 3195-3325
pUC origin: bases 3708-4381
Ampicillin resistance gene: bases 4526-5386
(complementary strand)

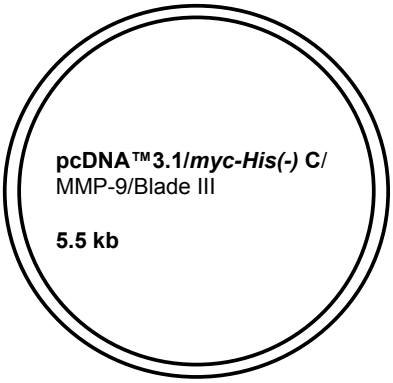

Plasmid:

Plasmid Name MMP-9/Blade IV

Creator Antoine Dufour

Base Vector/Company: pcDNA™3.1/*myc-His(-)* C

Resistant Gene (antibiotic) : Ampicillin

Insert:

Insert Size: 2090 Base Pairs **Cloning Sites 5': *EcoRI* ; 3': *HindIII***

PCR primer 1 : #1315 and #2538 **PCR primer 2 :** #2507 and #2539

Sequenced: **Yes**

Functional Assays:

1) gelatin zymogram

2) western Blot

3)_____

Plasmid Map:

CMV promoter: bases 209-863
T7 promoter/priming site: bases 863-882
Multiple cloning site: bases 895-1006
myc epitope: bases 1007-1036
Polyhistidine tag: bases 1052-1069
BGH reverse priming site: bases 1113-1130
BGH polyadenylation signal: bases 1116-1343
f1 origin: bases 1389-1817
SV40 promoter and origin: bases 1844-2152
Neomycin resistance gene: bases 2227-3021
SV40 polyadenylation signal: bases 3195-3325
pUC origin: bases 3708-4381
Ampicillin resistance gene: bases 4526-5386
(complementary strand)